Regulation of organelle pH by glycosphingolipids

Seléne van der Poel

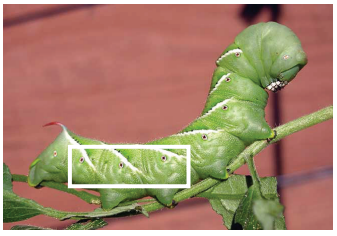

Cover design: enlargement of boxed area. Picture of the caterpillar *Manduca sexta* courtesy of Helen M. Roman (http://www.hmrprint.com)

Paranimfen:
Joep van den Dikkenberg
Ruud Cox

ISBN: 978-94-610-8069-1
Printed by: Gildeprint Drukkerijen - Enschede

The research described in this thesis was performed at the Researchgroup Membrane Enzymology, Utrecht University, The Netherlands with financial support from the Dutch Organisation of Sciences (NWO-Echo)

Printing of this thesis was financially supported by:
J.E. Jurriaanse Stichting, Rotterdam, The Netherlands

Regulation of organelle pH by glycosphingolipids

Regulatie van de zuurgraad in organellen door glycosfingolipiden

(met een samenvatting in het Nederlands)

Proefschrift

ter verkrijging van de graad van doctor aan de Universiteit Utrecht
op gezag van de rector magnificus, prof. dr. J.C. Stoof,
in gevolge het besluit van het college voor promoties
in het openbaar te verdedigen op
woensdag 8 september 2010 des ochtends te 10.30 uur

door

Seléne van der Poel

geboren op 28 juli 1981 te Gorinchem

Promotor: prof. dr. G.F.B.P. van Meer

Table of Contents

Abbreviations

BSA	bovine serum albumin
CCCP	carbonyl cyanide m-chlorophenylhydrazone
Cer	ceramide
CHAPS	3-[(3-cholamidopropyl)dimethyl-ammonio]-1-propanesulfonate
Chol	cholesterol
CHS	Chediak-Higashi syndrome
ConcA	concanamycin A
CPE	ceramide-phosphoethanolamine
ER	endoplasmic reticulum
FITC	fluorescein isothiocyanate
FLIM	fluorescence lifetime imaging microscopy
GCS	glucosylceramide synthase
GlcCer	glucosylceramide
GlcSph	glucosylsphingosine
GLTP	glycolipid transfer protein
GM3	glycolipid monosialoganglioside (NeuAcα2-3Galβ1-4Glcβ1-1Cer)
GSL	glycosphingolipids
HA	haemagglutinin
Hepes	4-(2-hydroxyethyl)-1-piperazineethanesulfonic acid
HPS	Hermansky-Pudlak syndrome
LacCer	lactosylceramide
LAMP	lysosome-associated membrane protein
LXR	liver-x receptors
MeOH	methanol
Mitf	microphthalmia-associated transcription factor
Oca2	oculocutaneous albinism type 2
OA	ocular albinism
PC	phosphatidylcholine
PDMP	D-*threo*-1-phenyl-2-decanoylamino-3-morpholino-1-propanol
PE	phosphatidylethanolamine
PM	plasma membrane
PNS	post nuclear supernatant
SaliA	salicylihalimide A
SM	sphingomyelin
TGN	*trans*-Golgi network
TLC	thin layer chromatography
V-ATPase	vacuolar-type H^+-translocating ATPase

Chapter 1

Pigment-producing melanocytes for studying the important physiological parameters protein sorting, pH and glycosphingolipids

Seléne van der Poel and Gerrit van Meer

Membrane Enzymology, Bijvoet Center and Institute of Membranes, Utrecht University, Utrecht, The Netherlands

Abstract

Pigmentation of melanocytes depends on the assembly and maturation of the pigment bodies, the melanosomes. It heavily relies on protein sorting, but also pH and glycosphingolipids play a role in pigmentation. Although pigmentation has been extensively studied, the role of pH and glycosphingolipids remains unresolved. Understanding the pigmentation process may not only help to improve skin treatments or cosmetics, but also to cure pigmentation disorders, and maybe even malignant melanoma. This review aims to provide an insight in the role of pH and glycosphingolipids in the pigmentation process. Moreover, melanocytes provide an excellent biological environment to study the connection between these general physiological parameters.

Melanocytes are pigment-producing cells

We get a tan from sunbathing because specialised cells, the melanocytes, are stimulated to make extra pigment in response to exposure to UV light (Tadokoro et al., 2005). This tan not only has an aesthetic appeal, but also provides protection as pigment in the upper dermis protects the lower dermis against DNA damage and facilitates apoptosis (Yamaguchi et al., 2006). Pigmentation is needed in skin, eye retina and hair. Melanocytes synthesise pigment or melanin in designated organelles, the melanosomes, and deal with pigmentation in different ways. In the eye and hair, pigment is stored in the place of synthesis, the melanosomes. In the skin, the pigment-carrying melanosomes are transported along actin towards the plasma membrane (Hume et al., 2007). There, the organelles are transferred from the melanocyte to surrounding keratinocytes by an unknown mechanism. Keratinocytes then carry the pigment throughout the epidermis (Van den Bossche et al., 2006).

Melanosomes are organelles related to lysosomes. They belong to the "secretory lysosomes" (Blott and Griffiths, 2002). Evidence has been piling up that the contents of the melanosomes travel through the endosomal system. Raposo and Marks (2007) recently proposed that premelanosomes are derived from vacuolar membranes of early endosomes and that maturation requires protein delivery from tubular endosomal domains. One example of a protein that is delivered via the endosomal system is the structural component of melanosomes, the protein PMEL17. PMEL17 is cleaved in endosomes by proprotein convertase prior to initiation of melanosome formation (Berson et al., 2001; 2003; Theos et al., 2005).

Formation of melanosomes

After initiation of melanosome formation, the premelanosomes mature through four distinct stages. During the first stages, the melanosomes are structurally established by the build-up of an intrinsic network of one protein, PMEL17, resulting in elongated protein striations or fibrils, which leads to an elliptic shaped organelle. PMEL17 is cleaved into two fragments, one 'sticky' lumenal fragment, Mα, and a smaller cytosolic fragment Mβ (Berson et al., 2001; 2003). The first maturation stages I and II are distinguished by the degree of fibril formation and later maturation stages III and IV by the amount of pigment deposited on the fibrils (reviewed by Marks and Seabra, 2001; Raposo and Marks, 2007). Cleavage of PMEL17 also requires MART1, a melanosome-specific transmembrane protein (Hoashi et al., 2005). PMEL17 is found to also form fibrils *in vitro* (Fowler et al., 2006) and when transfected into non-melanocytic cells (Berson et al., 2001). Without PMEL17, premelanosomes stay round and never mature into proper melanosomes (Theos et al., 2005). Therefore, PMEL17 is enough to form the structural basis of melanosomes.

When the fibrils are fully formed in stage II, other enzymes are transported towards the melanosomes for melanin production. Tyrosinase (Tyr), tyrosinase related protein-1 (TYRP1) and DOPAchrome tautomerase (also known as TRP-2) are sorted to the melanosome and found there in stage III and stage IV (Raposo et al., 2001; Kushimoto et al., 2001; Theos et al., 2005). The protein components of melanin synthesis are listed in Table I.

Melanin synthesis

The first and rate-limiting step in melanin synthesis is the conversion of the amino acid L-tyrosine to L-DOPA by the enzyme tyrosinase. The L-DOPA is attached to the fibrils probably by polymerization and further processed to form melanins. Melanins are DOPA-based reactive indols (Orlow et al., 1992) that are generated by several oxidation and hydroxylation reactions mediated by tyrosinase in part but mainly TYRP1 and TRP-2 (Kobayashi et al., 1994). The melanosome protects the cell from contact with the highly reactive indols. Red and yellow melanins, or pheomelanins, are synthesized under different conditions with reduction reactions using cysteine. Pheomelanins differ from the more commonly known eumelanins, the black or brown pigments, and have been studied in less detail (Jimbow et al., 1979; Kobayashi et al., 1995). Research into pigmentation disorders has identified other factors besides the proteins required for melanosome formation and melanin synthesis to be important for pigmentation. Melanin synthesis is schematically represented in Figure 1.

Table I. Melanocyte-specific protein components of melanin synthesis. Table adapted from Raposo and Marks (2007).

Protein	Other names	Function	Localisation
MART1		Regulation fibril formation (1)	Melanosomes/late endosomes
OCA2	Pink-eyed dilution, P-protein	Putative anion transporter (2)	Likely in melanosomes
OCA4	SLC45A2, MATP, underwhite	Putative membrane transporter (3)	Likely in melanosomes
OA1	GPR143	Putative G-protein coupled receptor (4)	Melanosomes and lysosomes
PMEL17	Gp100, ME20, silver	Fibrils (5)	Full: Endosomes Cleaved: Melanosomes
SLC45A5		Putative cation exchanger (6)	Likely melanosomes
Tyrosinase		Initiation melanin synthesis; catalysis oxidation L-tyrosine to L-DOPA (7)	Melanosomes stage III and IV
TRP-2	DOPAchrome tautomerase	Catalysis late step eumelanin synthesis (8)	Melanosomes stage III and IV
TYRP1	TRP-1, gp75	Putative catalytic activity or modulation tyrosinase activity (9)	Melanosomes stage III and IV

(1) Hoashi et al., 2005 (2) Lee et al., 1994; Brilliant et al., 2001 (3) Newton et al., 2001 (4) Giordano et al., 2009; Palmisano et al., 2008 (5) Berson et al., 2003 (6) Lamason et al., 2005 (7) Hearing, 1999 (8) Costin et al., 2005 (9) Kobayashi et al., 1994

Pigmentation disorders

Disorders in pigmentation are common and are found in all kinds of forms and severities. The knowledge gathered on these diseases originated mainly from mouse coat colour mutants or immortalised cell lines from mice or human patients. There are hypo- and hyper-pigmentation diseases, which concern the loss and gain of pigmentation, respectively. In this review we will focus on the hypopigmentation diseases as these are most common and best investigated. The hypopigmentation diseases are listed in Table II. A loss of pigmentation can occur when either the melanocytes are not present at all or melanin is not produced in intact melanocytes. In Piebaldism, Waardenburg syndrome and Tietz syndrome, there is a defect in development and

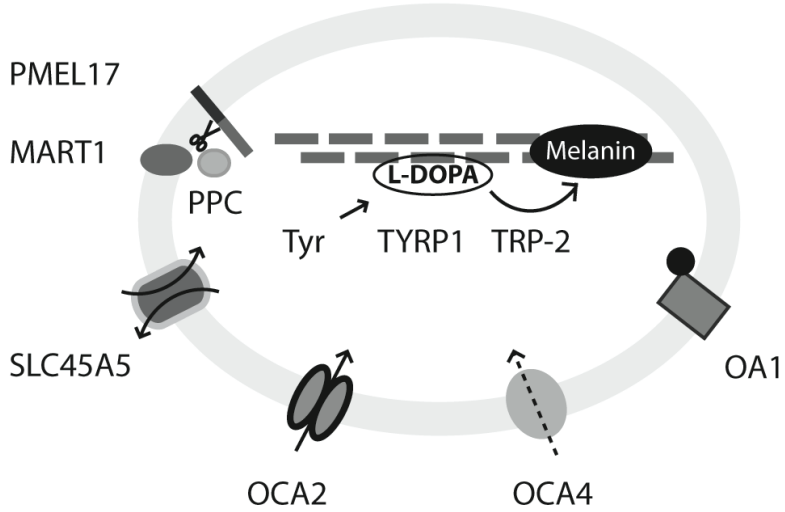

Figure 1. Melanin synthesis in melanosome from melanocyte in the eye. First, PMEL17 is cleaved by a calcium-dependent proprotein convertase (PPC) assisted by the transmembrane protein MART1 to produce a 'sticky' lumenal fragment that forms fibrils. The SLC45A5 is a pH-dependent sodium/calcium symporter that delivers the calcium for cleavage of PMEL17. OCA2 is a putative chloride channel that presumably plays a role in pH. OCA4 is a putative transmembrane transporter with unknown cargo. OA1 is a putative G-protein coupled receptor. When fibril formation is completed at the end of stage II, enzymes for pigment synthesis are found in the melanosome. Tyrosinase (Tyr) catalyses the first step to convert L-tyrosine to L-DOPA, possibly modulated by TYRP1. L-DOPA polymerises onto the fibril of PMEL17 fragments and is further converted to melanin by TYRP1 and the DOPAchrome tautomerase (TRP-2), which catalyses the last step of synthesis of melanin.

migration of the melanoblast, the origin of melanocytes during embryonic development, resulting in the lack of melanocytes. Genes involved in stem cell growth and/or development are affected and listed in Table II (reviewed by Dessinioti et al., 2009). Because a lack of melanocytes cannot help us in the quest to understand the process of melanogenesis, we will not discuss these diseases further.

Hypopigmentation in humans that is caused by a malfunction of melanin synthesis in melanocytes includes ocular and oculocutaneous albinism, which affect mainly the eyes and both skin and eyes, respectively. Ocular albinism (OA) is mainly found in one type, namely type I, and is caused by mutations in the OA1 locus. This locus codes for the OA1 protein, a 7-transmembrane protein homologous to G-protein coupled receptors. It is not yet clear why mutations cause eye specific defects (Lopez et al., 2008; Palmisano et al., 2008; Giordano et al., 2009).

Oculocutaneous albinism (OCA) is mainly found in four different types,

I-IV, but types I and II are most common. Oculocutaneous albinism types I and III are caused by mutations in enzymes involved in melanin synthesis, tyrosinase and TYRP1, respectively (King et al., 1985; Boissy et al., 1996). These mutations cause partial or total loss of function of these enzymes and in some cases lead to their retention in the ER (Toyofuku et al., 2001). The most common hypopigmentation disease among Caucasians, oculocutaneous albinism type II (OCA2), is caused by mutations in the pink-eyed dilution protein or OCA2 protein (Lee et al., 1994; Brilliant et al., 2001). The function of OCA2 is still unknown although there are indications that point to an anion transporter (Rinchik et al., 1993; Staleva et al., 2002). OCA4 is caused by mutations in the SLC45A2 protein, also known as MATP, that result in the underwhite phenotype in mice. The protein is homologous to sucrose/proton symporters in plants (Newton et al., 2001). OCA4 mutations are the major cause of oculocutaneous albinism in the Japanese population (Konno et al., 2009).

Oculocutaneous albinism is also found as a consequence of the rare autosomal recessive disorders Hermansky-Pudlak syndrome (HPS) and Chediak-Higashi syndrome (CHS), which cause increased mortality. HPS patients display bleeding defects due to platelet dysfunction, lung disease, inflammatory bowel disease, cardiomyopathy and renal disease. The patients with Chediak-Higashi syndrome are susceptible to infection and can develop lymphofollicular malignancy. Mutations causing HPS and CHS are not in melanocyte-specific proteins: in HPS they are mainly mutations in BLOC-1, -2 and -3 (BLOC stands for biogenesis of lysosome-related organelle complex) and the adaptor protein AP-3 (Wei et al., 2006; Raposo and Marks, 2007). Both BLOC and adaptor proteins play a role in cargo recognition for sorting from the endosomes to the melanosomes (Kantheti et al., 1998; Dell'Angelica et al., 1999; Theos et al., 2005). CHS is caused by mutations in the lysosomal trafficking regulator gene, LYST, which also affect structure and function of the "secretory lysosomes" including the melanosomes (Kaplan et al., 2008).

In Griscelli syndrome, another rare autosomal recessive disorder, melanocytes display defects in the transport of melanosomes to the cell periphery and to neighbouring cells (van Gele et al., 2009). Depending on the protein that is mutated, myosin 5A, Rab27A, and melanophilin in type 1, 2 and 3, respectively, the patients display additional neuronal and immunological defects (not type 3 which only displays pigmentary abnormalities).

The role of protein sorting in pigmentation

OCA1-4

The most common phenotype found in mouse models and cell lines with a pigmen-

Table II. Diseases that cause hypopigmentation.

Disease	Gene/Protein	Characteristics
Piebaldism	c-Kit, Stem cell growth factor (SCF), SLUG (1)	Lack of melanocytes
Waardenburg syndrome	Endothelin 3 (EDN3), EDNR8, PAX3, MITF, SLUG, SOX10 (1)	Lack of melanocytes
Tietz syndrome	Microphthalmia transcription factor (MITF) (1)	Lack of melanocytes
OA1 type 1	OA1 (2)	Eye-specific defects, cause unkown
OCA1	Tyrosinase (3)	Loss-of-function tyrosinase / ER retention
OCA2	P-protein/OCA2 (4)	Tyrosinase and TYRP1 mis-sorting
OCA3	TYRP1 (2)	Loss-of-function TYRP1 / ER retention
OCA4	SLC45A2/MATP (5)	Tyrosinase and TYRP1 mis-sorting
Hermansky-Pudlack syndrome type 1-8	AP-3, Bloc-1, -2 or -3 (6)	Tyrosinase or TYRP1 mislocalisation or ER retention
Chediak-Higashi syndrome	LYST (lysosomal trafficking regulator gene) (7)	Aberrant structure and function of secretory lysosomes
Griscelli type 1-3	Myosin 5A, Rab27A, melanophilin (8)	Aberrant transport of melanosomes

(1) Dessiniotti et al., 2009 (2) Lopez et al., 2008; Palmisano et al., 2008; Giordano et al., 2009 (3) King et al., 1985; Boissy et al., 1996; Toyofuku et al., 2001 (4) Lee et al., 1994; Brilliant et al., 2001; Manga et al., 2001 (5) Newton et al., 2001 (6) Wei et al., 2006; Raposo and Marks, 2007 (7) Kaplan et al., 2008 (8) van Gele et al., 2009

tation disorder, is a defect in the sorting of melanosomal proteins to melanosomes, which is required for melanin synthesis. The causes of the aberrant sorting of melanosomal proteins are diverse. The proteins themselves can be mutated, as it is in the case of OCA1 and OCA3 for tyrosinase and TYRP1, respectively. Mutations in the enzymes produce partial or total loss of function in the more severe disease forms, which in some cases involves retention of the enzymes in the ER rendering OCA1 and OCA3 as ER retention diseases (Toyofuku et al., 2001).

In OCA2, the OCA2 or P-protein is affected, which leads to a block of tyrosinase sorting in a perinuclear area resembling the Golgi (Chen et al., 2002). Manga et al. (2001) found that also TYRP1 is differently localised and found TYRP1 in smaller granules in OCA2-deficient cells compared to the wild-type melanoma cells on a sucrose gradient. The localisation of both tyrosinase and TYRP1 was restored upon retransfection with OCA2 (Chen et al., 2002). However, Puri et al. (2000) found no effect on TYRP1 localisation. Similar antibodies were used for both studies but the use of different cell lines may have caused this discrepancy. Whether OCA2 participates directly or indirectly in protein sorting remains unresolved. There are indications that OCA2 is in fact an anion transporter as the protein resembles citrate and arsenic anion transporters and expression of the OCA2 protein in *Saccharomyces cerevisiae* further sensitised the yeast cells for arsenicals (Rinchik et al., 1993; Staleva et al., 2002). Therefore, it is likely that OCA2 has an indirect effect on protein sorting by creating the right environment for protein sorting and pigment production.

In OCA4, localisation of tyrosinase and TYRP1 are affected, in this case because of a mutation in the SLC45A2/MATP protein (Costin et al., 2003). Because SLC45A2 is thought to function as a transporter protein (it resembles the sucrose/proton transporter in plants), it is probably also indirectly involved in protein sorting.

HPS and CHS

The oculocutaneous albinism in Hermansky-Pudlak syndrome (HPS) and Chediak-Higashi syndrome (CHS) is due to the fact that these disorders are caused by mutations in proteins directly involved in protein sorting. Mouse models for HPS and CHS were instrumental in identifying factors involved in the sorting pathways and their function (Raposo and Marks, 2007).

Adaptor protein complexes (APs) play a role in linking transmembrane proteins to coated buds on post-Golgi membranes, and thereby selecting cargo for specific transport pathways (reviewed by Bonifacino et al., 2003; Peden et al., 2004; Theos et al., 2005). In HPS type 2, mutations in AP-3 cause retention of tyrosinase in the endosomes, but not TYRP1 (Huizing et al., 2001). Therefore, sorting of melanosomal proteins is likely to be mediated via several pathways. TYRP1 contains a different cytoplasmic sorting signal that binds AP-1 and not AP-3 and is therefore not affected by a defect in AP-3 (Theos et al., 2005).

The mutations that cause most types of HPS are in proteins that are part of the Biogenesis of Lysosome-related Organelle Complex (BLOC) proteins. The proteins BLOC-1 and -2 have been shown to function in transport from endosome towards the lysosome-related organelles, such as the melanosome (Di Pietro et al., 2006; Setty et al., 2007). Mutations in BLOC-1, in subunits HSP7 and 8 to be precise, cause TYRP1 mislocalisation to early endosomes and the cell surface (Setty et al., 2007). Because

BLOC-1 and AP-3 affect different melanosomal proteins, it is likely these constitute two separate pathways for sorting. Interestingly, it was found that BLOC-1 interacts with BLOC-2 and AP-3 (Di Pietro et al., 2006), and when BLOC-1 is absent, different proteins are sorted via AP-3 (Salazar et al., 2006). BLOC-1 and AP-3 localise to early endosomes, but BLOC-1 concentrates in tubules and less in AP-3 containing buds (Di Pietro et al., 2006).

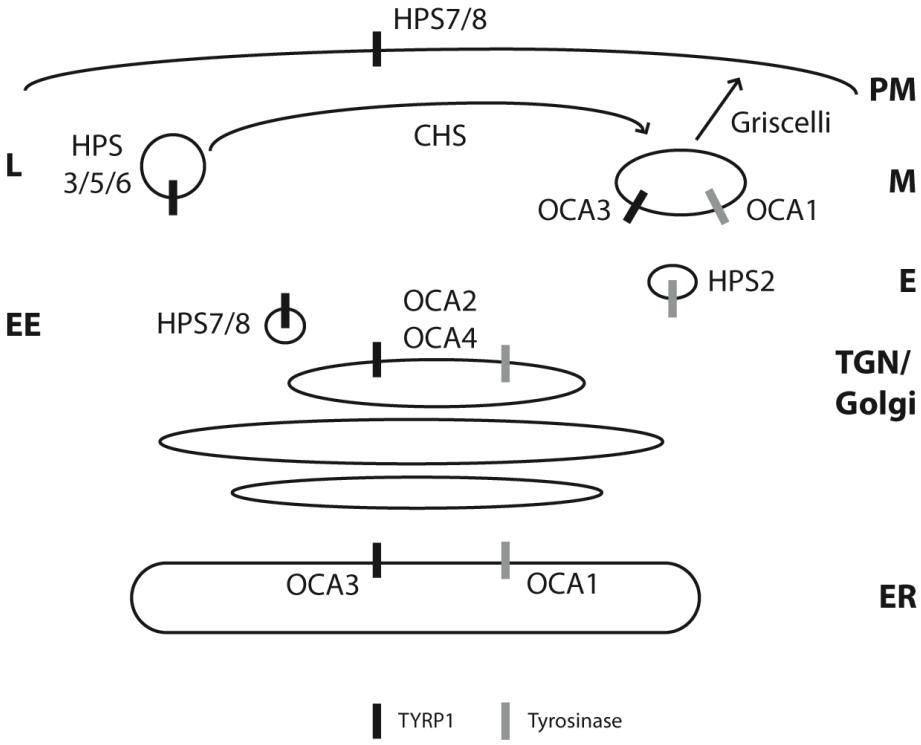

Figure 2. Hypopigmentation diseases and protein sorting. Oculocutaneous albinism (OCA) causing diseases, OCA1 and OCA3 lead to loss-of-function and, in some cases, ER retention of tyrosinase and TYRP1 respectively. OCA2 results in tyrosinase and possibly TYRP1 missorting and in the case of OCA4, both tyrosinase and TYRP1 are missorted. Hermansky-Pudlack syndrome (HSP) is a malfunction of the general sorting machinery due to mutations in AP-3 and BLOC 1, 2 and 3 proteins. HPS2 is a malfunction of AP-3 leading to tyrosinase sorting to endosomes (E), in HPS8/7, BLOC1 is affected leading to TYRP1 sorting to early endosomes (EE) and the cell surface (PM). Finally HPS3/5/6 are a malfunction of BLOC2 and consequently, TYRP1 is degraded, probably in lysosomes (L). HPS1/4 are caused by BLOC3 malfunction with unknown consequences. Chediak-Higashi syndrome (CHS) is a disease that leads to a general aberrant function and structure of secretory lysosomes such as melanosomes. In Griscelli disease, melanosomes are not transported to the plasma membrane (PM) or transferred to neighbouring cells.

BLOC-2 consists of three subunits HPS3, HPS5 and HPS6, which can carry known disease-related mutations (Di Pietro et al., 2004). When BLOC-2 is affected, TYRP1 is subsequently targeted for degradation. This suggests that BLOC-2 is involved in a different part of the sorting pathway (Di Pietro et al., 2006; Helip-Wooley et al., 2007). HPS 1 and 4 are subunits of BLOC-3, the function of which has not been elucidated (Di Pietro et al., 2005; Wei et al., 2006). In non-pigmented cells BLOC-3 plays a role in the motility and distribution of the late endosome and lysosome (Falcón-Pérez et al., 2005). In Figure 2, the affected sorting pathways are indicated.

The role of pH in pigmentation

Although melanosomes are derived from lysosomes, the pH needed for melanin production is still under debate. It has been published that the melanosomes have a low pH (Bhatnagar et al., 1993). Puri and coworkers (2000) used DAMP, a dye that accumulates in acidic compartments, and observed that it colocalised with the melanosomal protein TYRP1 in wild-type cells confirming the low pH in melanosomes. No colocalisation was observed in OCA2-deficient cells. However, the conclusion that the melanosomes became less acidic in OCA2-deficient cells is not compelling because TYRP1 was shown to be mislocalised in OCA2-deficient cells (Manga et al., 2001). TYRP1 was found in concentrated patches near the plasma membrane (Chen et al. 2002) as opposed to the presence of TYRP1 in punctate structures as reported by Puri and coworkers (2000). Similar antibodies were used for both studies but the use of different cell lines may have caused this discrepancy.

It has been observed that ammonium chloride and inhibitors of the proton pump (vacuolar-type H^+-translocating ATPase or V-ATPase) result in pigmented OCA2-deficient cells (Ni-Komatsu and Orlow, 2006), which fuelled the notion that melanosomes have an alkaline pH. However, an electron microscopy study showed that cells treated with ammonium chloride indeed had pigmented bodies, but these appeared pigmented lysosomes and not properly assembled melanosomes (Groux-Degroote et al., 2008). This suggests that the rescue of pigmentation in OCA2 mutant cells would be due to activation of tyrosinase missorted to lysosomes by pH neutralisation. Independently, a complete neutralisation of the lumenal pH of intracellular compartments appears to release tyrosinase under conditions where it is stuck in the ER (Watabe et al., 2004). Actually, it has been argued that a low pH inhibits tyrosinase, and that a melanosomal proton-sodium antiporter (Basrur et al., 2003) activates tyrosinase by reducing the acidity in the melanosomes (Smith et al., 2004). Alternatively, via such antiporters the putative Ca^{2+}/Na^+ exchanger SLC25A5, identified as a protein required for pigmentation, may drive Ca^{2+} import (Lamason et al., 2005), which

may be required for proper melanosome assembly via the Ca^{2+}-dependent cleavage of PMEL17 by furin (reviewed by Thomas et al., 2002). Furthermore, as a putative anion transporter, OCA2 may affect the pH in the melanosomes, as influx of anions in the lumen abolishes the inhibiting membrane potential built-up by the proton pump. The proton pump is able to pump in more protons and further acidify the lumen.

The concentration of the various ions, one of them being the proton, affects not only protein conformation and receptor-ligand interactions, but also the affinity of protein-protein interactions and thus oligomerisation. In various cases, the change in proton concentration encountered after endocytosis has been shown to act as a conformational switch. Examples are iron release by transferrin (Dautry-Varsat, 1986) and the fusogenicity of viral spike proteins (Doms et al., 1985).

Whether or not melanosomes prove to be alkaline or acidic, pH does seem to play a role in melanin production. Melanocytes provide an excellent biological environment to investigate the role of this important fundamental parameter in protein sorting of melanosomal proteins.

The role of glycosphingolipids in pigmentation

Sprong and coworkers (2001) described that a lack of glycosphingolipids in a B-16 mouse melanoma mutant cell line, GM95, causes hypopigmentation. The glycosphingolipid-deficient mutant GM95 cells lack the first enzyme required for glycosphingolipid synthesis, glucosylceramide synthase (GCS; Ichikawa et al., 1994). Tyrosinase sorting and pigmentation was restored upon transfection of GCS and proper melanosomes were visualised by electron microscopy (EM; Groux-Degroote et al., 2008). GM95 cells do not have properly formed melanosomes and tyrosinase was mislocalised to the perinuclear Golgi area. A tyrosinase construct with an elongated transmembrane domain escaped the sorting block in the Golgi area and restored pigmentation. This suggested that glycosphingolipids play a role in protein sorting and when the tyrosinase is allowed to go past the sorting block in the Golgi, pigmentation is restored. However, Groux-Degroote et al. (2008) found with electron microscopy of the cells that no melanosomes were formed but pigmentation was restored because of the presence of blackened lysosomes. Correction of tyrosinase sorting was not sufficient to restore melanosome formation and the cells had somehow bypassed the need for the organelles. Therefore, glycosphingolipids seem to fulfil an additional role in melanosome biogenesis, possibly in melanosome formation.

Although it is known that adaptor protein complexes recognise and bind a di-leucine motif located on the cytoplasmic side of the protein cargo (Höning et al., 1998; Calvo et al., 1999), Groux-Degroote et al. (2008) found that the sorting informa-

tion that discriminates melanosomal from lysosomal proteins is located in the lumenal domain. In wild-type MEB4 melanocytes, proteins destined for the melanosomes took the selective intracellular pathway while lysosomal proteins took the non-selective pathway via the plasma membrane. In the absence of glycosphingolipids these sorting events were reversed. The proteins may need to oligomerise to be recognised as cargo for AP-3, similar to AP-2 (Grass et al., 2004). Glycosphingolipids can possibly provide the correct conditions for oligomerisation, for example the correct membrane environment or lumenal condition, to be followed by AP-3 binding to the di-leucine motif on the cytoplasmic domain. The correct packaging of melanosomal cargo thus requires two separate signals. Notably, also sorting of PMEL17 has been reported to depend on the lumenal domain (Theos et al., 2005). Therefore, glycosphingolipids seem to play a dual role; in melanosome biogenesis in an unknown fashion, and in protein sorting via protein oligomerisation. The role of glycosphingolipids and pH are schematically represented in Figure 3.

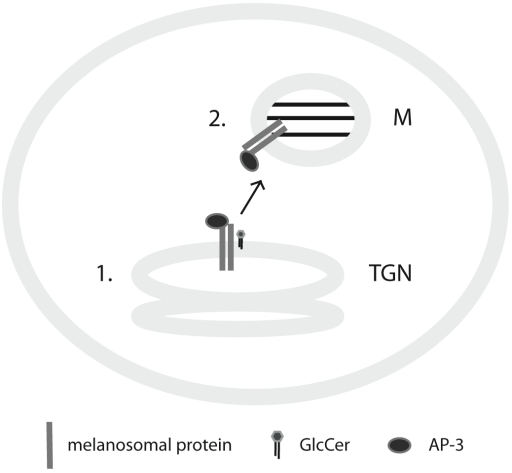

Figure 3. Role of glycosphingolipids and pH in pigmentation. (1) Glycosphingolipids, represented by glucosylceramide on the cytosolic leaflet, or the lumenal pH in the TGN can both play a role in oligomerisation of proteins for selection by AP-3 for sorting to the melanosome (M). (2) The lumenal pH presumably plays a role in formation of melanosomes, via de cleavage of PMEL17 and the activity of tyrosinase.

Perspectives

The ability to make pigment is a cellular specialisation of melanocytes, and separate lysosome-related organelles, the melanosomes, are generated for this purpose. As it

is a specialisation, processes that play a role in pigmentation can be researched in a biological setting without the need of turning off vital processes. However, it proves to be difficult to trace the common phenotype of protein mislocalisation back to the factors that are the actual cause of the mishap in protein sorting. The Hermansky-Pudlak and Chediak-Higashi mouse models provide an excellent environment to look at protein sorting on a broader scale. Mouse coat color mutants have elucidated a number of melanocyte-specific sorting features. The example of the glycosphingolipid-deficient cell line shows that the sorting of melanosomal proteins is interwoven with general physiological parameters at the molecular level. Pigmentation proves to be a complex process wherein protein sorting, pH and glycosphingolipids appear essential. We aim to understand the fundamentals of pigmentation and pigment synthesis that we get an insight in the interplay between these three basic biologically vital functions. Specialised cells like the melanocytes give us the opportunity to investigate fundamental parameters in a physiologically relevant biological setting.

Scope of this thesis

Glycosphingolipids are essential for eukaryotic life, and we set out to investigate the function of these lipids in glycosphingolipid-deficient GM95 cells. These lipids play a role in melanosome biogenesis and protein sorting, which depends on the lumenal domain (**Chapter 1**). In **Chapter 2** we describe that one lumenal parameter, the lumenal pH, in the TGN and lysosomes depends on glycosphingolipids. In our search to find the affected pH determinant, we stumbled upon two factors that were affected in GM95 cells, namely the transcription of the melanocyte-specific putative anion channel Oca2 and the *in vitro* activity of the proton pump V-ATPase in isolated total membranes. In **Chapter 3** we explored the activity of the V-ATPase further and found that glycosphingolipids may compete with two inhibitors for binding the V-ATPase. This suggests there is a direct effect of the lipids on the V-ATPase and in order to investigate this, we developed a reconstitution procedure of the insect V-ATPase from *Manduca sexta* in **Chapter 4**. The V-ATPase was, for the first time, successfully reconstituted in a broad variety of liposomes. We addressed the question whether there is a direct lipid-protein interaction with photoactivatable and clickable lipid analogues in **Chapter 5**. The lipid analogue of glucosylceramide (GlcCer), the precursor for higher glycosphingolipids, preferentially binds subunit c in the transmembrane V_o domain of the V-ATPase. This is in agreement with the binding site of the two inhibitors of the V-ATPase. In **Chapter 6**, the major findings are presented and it is discussed how GlcCer may regulate lumenal pH.

References

Basrur V, Yang F, Kushimoto T, et al. Proteomic analysis of early melanosomes: identification of novel melanosomal proteins. *J Proteome Res* 2003;2:69-79.

Berson JF, Harper DC, Tenza D, Raposo G, Marks MS. Pmel17 initiates premelanosome morphogenesis within multivesicular bodies. *Mol Biol Cell* 2001;12:3451-64.

Berson JF, Theos AC, Harper DC, Tenza D, Raposo G, Marks MS. Proprotein convertase cleavage liberates a fibrillogenic fragment of a resident glycoprotein to initiate melanosome biogenesis. *J Cell Biol* 2003;161:521-33.

Bhatnagar V, Anjaiah S, Puri N, Darshanam BN, Ramaiah A. pH of melanosomes of B16 murine melanoma is acidic: its physiological importance in the regulation of melanin biosynthesis. *Arch Biochem Biophys* 1993;307:183-92.

Blott EJ, Griffiths GM. Secretory lysosomes. *Nat Rev Mol Cell Biol* 2002;3:122-31.

Boissy RE, Zhao H, Oetting WS, et al. Mutation in and lack of expression of tyrosinase-related protein-1 (TRP-1) in melanocytes from an individual with brown oculocutaneous albinism: a new subtype of albinism classified as "OCA3". *Am J Hum Genet* 1996;58:1145-56.

Bonifacino JS, Traub LM. Signals for sorting of transmembrane proteins to endosomes and lysosomes. *Annu Rev Biochem* 2003;72:395-447.

Brilliant M, Gardner J. Melanosomal pH, pink locus protein and their roles in melanogenesis. *J Invest Dermatol* 2001;117:386-7.

Brilliant MH. The mouse p (pink-eyed dilution) and human P genes, oculocutaneous albinism type 2 (OCA2), and melanosomal pH. *Pigment Cell Res* 2001;14:86-93.

Calvo PA, Frank DW, Bieler BM, Berson JF, Marks MS. A cytoplasmic sequence in human tyrosinase defines a second class of di-leucine-based sorting signals for late endosomal and lysosomal delivery. *J Biol Chem* 1999;274:12780-9.

Chen K, Manga P, Orlow SJ. Pink-eyed dilution protein controls the processing of tyrosinase. *Mol Biol Cell* 2002;13:1953-64.

Costin GE, Valencia JC, Vieira WD, Lamoreux ML, Hearing VJ. Tyrosinase processing and intracellular trafficking is disrupted in mouse primary melanocytes carrying the underwhite (uw) mutation. A model for oculocutaneous albinism (OCA) type 4. *J Cell Sci* 2003;116:3203-12.

Costin GE, Valencia JC, Wakamatsu K, et al. Mutations in dopachrome tautomerase (Dct) affect eumelanin/pheomelanin synthesis, but do not affect intracellular trafficking of the mutant protein. *Biochem J* 2005;391:249-59.

Dautry-Varsat A. Receptor-mediated endocytosis: the intracellular journey of transferrin and its receptor. *Biochimie* 1986;68:375-81.

Dell'Angelica EC, Shotelersuk V, Aguilar RC, Gahl WA, Bonifacino JS. Altered trafficking of lysosomal proteins in Hermansky-Pudlak syndrome due to mutations in the beta 3A subunit of the AP-3 adaptor. *Mol Cell* 1999;3:11-21.

Dessinioti C, Stratigos AJ, Rigopoulos D, Katsambas AD. A review of genetic disorders of

hypopigmentation: lessons learned from the biology of melanocytes. *Exp Dermatol* 2009;18:741-9.

Di Pietro SM, Dell'Angelica EC. The cell biology of Hermansky-Pudlak syndrome: recent advances. *Traffic* 2005;6:525-33.

Di Pietro SM, Falcon-Perez JM, Dell'Angelica EC. Characterization of BLOC-2, a complex containing the Hermansky-Pudlak syndrome proteins HPS3, HPS5 and HPS6. *Traffic* 2004;5:276-83.

Di Pietro SM, Falcon-Perez JM, Tenza D, et al. BLOC-1 interacts with BLOC-2 and the AP-3 complex to facilitate protein trafficking on endosomes. *Mol Biol Cell* 2006;17:4027-38.

Doms RW, Helenius A, White J. Membrane fusion activity of the influenza virus hemagglutinin. The low pH-induced conformational change. *J Biol Chem* 1985;260:2973-81.

Falcón-Pérez JM, Nazarian R, Sabatti C, Dell'Angelica EC. Distribution and dynamics of Lamp1-containing endocytic organelles in fibroblasts deficient in BLOC-3. *J Cell Sci* 2005;118:5243-55.

Fowler DM, Koulov AV, Alory-Jost C, Marks MS, Balch WE, Kelly JW. Functional amyloid formation within mammalian tissue. *PLoS Biol* 2006;4:e6.

Giordano F, Bonetti C, Surace EM, Marigo V, Raposo G. The ocular albinism type 1 (OA1) G-protein-coupled receptor functions with MART-1 at early stages of melanogenesis to control melanosome identity and composition. *Hum Mol Genet* 2009;18:4530-45.

Grass I, Thiel S, Honing S, Haucke V. Recognition of a basic AP-2 binding motif within the C2B domain of synaptotagmin is dependent on multimerization. *J Biol Chem* 2004;279:54872-80.

Groux-Degroote S, van Dijk SM, Wolthoorn J, et al. Glycolipid-dependent sorting of melanosomal from lysosomal membrane proteins by lumenal determinants. *Traffic* 2008;9:951-63.

Hearing VJ. Biochemical control of melanogenesis and melanosomal organization. *J Investig Dermatol Symp Proc* 1999;4:24-8.

Helip-Wooley A, Westbroek W, Dorward HM, et al. Improper trafficking of melanocyte-specific proteins in Hermansky-Pudlak syndrome type-5. *J Invest Dermatol* 2007;127:1471-8.

Hoashi T, Watabe H, Muller J, Yamaguchi Y, Vieira WD, Hearing VJ. MART-1 is required for the function of the melanosomal matrix protein PMEL17/GP100 and the maturation of melanosomes. *J Biol Chem* 2005;280:14006-16.

Höning S, Sandoval IV, von Figura K. A di-leucine-based motif in the cytoplasmic tail of LIMP-II and tyrosinase mediates selective binding of AP-3. *EMBO J* 1998;17:1304-14.

Huizing M, Anikster Y, Gahl WA. Hermansky-Pudlak syndrome and Chediak-Higashi syndrome: disorders of vesicle formation and trafficking. *Thromb Haemost* 2001;86:233-45.

Hume AN, Ushakov DS, Tarafder AK, Ferenczi MA, Seabra MC. Rab27a and MyoVa are the primary Mlph interactors regulating melanosome transport in melanocytes. *J Cell Sci* 2007;120:3111-22.

Ichikawa S, Nakajo N, Sakiyama H, Hirabayashi Y. A mouse B16 melanoma mutant deficient in glycolipids. *Proc Natl Acad Sci U S A* 1994;91:2703-7.

Jimbow K, Oikawa O, Sugiyama S, Takeuchi T. Comparison of eumelanogenesis and pheomelanogenesis in retinal and follicular melanocytes; role of vesiculo-globular bodies in melano-some differentiation. *J Invest Dermatol* 1979;73:278-84.

Kantheti P, Qiao X, Diaz ME, et al. Mutation in AP-3 delta in the mocha mouse links en-

dosomal transport to storage deficiency in platelets, melanosomes, and synaptic vesicles. *Neuron* 1998;21:111-22.

Kaplan J, De Domenico I, Ward DM. Chediak-Higashi syndrome. *Curr Opin Hematol* 2008;15:22-9.

King RA, Olds DP. Hairbulb tyrosinase activity in oculocutaneous albinism: suggestions for pathway control and block location. *Am J Med Genet* 1985;20:49-55.

Kobayashi T, Urabe K, Winder A, et al. DHICA oxidase activity of TRP1 and interactions with other melanogenic enzymes. *Pigment Cell Res* 1994;7:227-34.

Kobayashi T, Vieira WD, Potterf B, Sakai C, Imokawa G, Hearing VJ. Modulation of melanogenic protein expression during the switch from eu- to pheomelanogenesis. *J Cell Sci* 1995;108 (Pt 6):2301-9.

Konno T, Abe Y, Kawaguchi M, Kondo T, Tomita Y, Suzuki T. Functional analysis of OCA4mutant sequences using under white mouse melanocytes. *Pigment Cell Melanoma Res* 2009;22:235-7.

Kushimoto T, Basrur V, Valencia J, et al. A model for melanosome biogenesis based on the purification and analysis of early melanosomes. *Proc Natl Acad Sci U S A* 2001;98:10698-703.

Lamason RL, Mohideen MA, Mest JR, et al. SLC24A5, a putative cation exchanger, affects pigmentation in zebrafish and humans. *Science* 2005;310:1782-6.

Lee ST, Nicholls RD, Schnur RE, et al. Diverse mutations of the P gene among African-Americans with type II (tyrosinase-positive) oculocutaneous albinism (OCA2). *Hum Mol Genet* 1994;3:2047-51.

Lopez VM, Decatur CL, Stamer WD, Lynch RM, McKay BS. L-DOPA is an endogenous ligand for OA1. *PLoS Biol* 2008;6:e236.

Manga P, Boissy RE, Pifko-Hirst S, Zhou BK, Orlow SJ. Mislocalization of melanosomal proteins in melanocytes from mice with oculocutaneous albinism type 2. *Exp Eye Res* 2001;72:695-710.

Marks MS, Seabra MC. The melanosome: membrane dynamics in black and white. *Nat Rev Mol Cell Biol* 2001;2:738-48.

Newton JM, Cohen-Barak O, Hagiwara N, et al. Mutations in the human orthologue of the mouse underwhite gene (uw) underlie a new form of oculocutaneous albinism, OCA4. *Am J Hum Genet* 2001;69:981-8.

Ni-Komatsu L, Orlow SJ. Heterologous expression of tyrosinase recapitulates the misprocessing and mistrafficking in oculocutaneous albinism type 2: effects of altering intracellular pH and pink-eyed dilution gene expression. *Exp Eye Res* 2006;82:519-28.

Orlow SJ, Osber MP, Pawelek JM. Synthesis and characterization of melanins from dihydroxyindole-2-carboxylic acid and dihydroxyindole. *Pigment Cell Res* 1992;5:113-21.

Palmisano I, Bagnato P, Palmigiano A, et al. The ocular albinism type 1 protein, an intracellular G protein-coupled receptor, regulates melanosome transport in pigment cells. *Hum Mol Genet* 2008;17:3487-501.

Peden AA, Oorschot V, Hesser BA, Austin CD, Scheller RH, Klumperman J. Localization of the AP-3 adaptor complex defines a novel endosomal exit site for lysosomal membrane proteins. *J Cell Biol* 2004;164:1065-76.

Puri N, Gardner JM, Brilliant MH. Aberrant pH of melanosomes in pink-eyed dilution (p) mutant melanocytes. *J Invest Dermatol* 2000;115:607-13.

Ralston GB. Temperature and pH dependence of the self-association of human spectrin. *Biochemistry* 1991;30:4179-86.

Raposo G, Marks MS. Melanosomes--dark organelles enlighten endosomal membrane transport. *Nat Rev Mol Cell Biol* 2007;8:786-97.

Raposo G, Tenza D, Murphy DM, Berson JF, Marks MS. Distinct protein sorting and localization to premelanosomes, melanosomes, and lysosomes in pigmented melanocytic cells. *J Cell Biol* 2001;152:809-24.

Rinchik EM, Bultman SJ, Horsthemke B, et al. A gene for the mouse pink-eyed dilution locus and for human type II oculocutaneous albinism. *Nature* 1993;361:72-6.

Salazar G, Craige B, Styers ML, et al. BLOC-1 complex deficiency alters the targeting of adaptor protein complex-3 cargoes. *Mol Biol Cell* 2006;17:4014-26.

Setty SR, Tenza D, Truschel ST, et al. BLOC-1 is required for cargo-specific sorting from vacuolar early endosomes toward lysosome-related organelles. *Mol Biol Cell* 2007;18:768-80.

Smith DR, Spaulding DT, Glenn HM, Fuller BB. The relationship between Na(+)/H(+) exchanger expression and tyrosinase activity in human melanocytes. *Exp Cell Res* 2004;298:521-34.

Sprong H, Degroote S, Claessens T, et al. Glycosphingolipids are required for sorting melanosomal proteins in the Golgi complex. *J Cell Biol* 2001;155:369-80.

Staleva L, Manga P, Orlow SJ. Pink-eyed dilution protein modulates arsenic sensitivity and intracellular glutathione metabolism. *Mol Biol Cell* 2002;13:4206-20.

Tadokoro T, Yamaguchi Y, Batzer J, et al. Mechanisms of skin tanning in different racial/ethnic groups in response to ultraviolet radiation. *J Invest Dermatol* 2005;124:1326-32.

Theos AC, Truschel ST, Raposo G, Marks MS. The Silver locus product Pmel17/gp100/Silv/ME20: controversial in name and in function. *Pigment Cell Res* 2005;18:322-36.

Thomas G. Furin at the cutting edge: from protein traffic to embryogenesis and disease. *Nat Rev Mol Cell Biol* 2002;3:753-66.

Toyofuku K, Wada I, Valencia JC, Kushimoto T, Ferrans VJ, Hearing VJ. Oculocutaneous albinism types 1 and 3 are ER retention diseases: mutation of tyrosinase or Tyrp1 can affect the processing of both mutant and wild-type proteins. *FASEB J* 2001;15:2149-61.

Van Den Bossche K, Naeyaert JM, Lambert J. The quest for the mechanism of melanin transfer. *Traffic* 2006;7:769-78.

Van Gele M, Dynoodt P, Lambert J. Griscelli syndrome: a model system to study vesicular trafficking. *Pigment Cell Melanoma Res* 2009;22:268-82.

Van Meer G, Voelker DR, Feigenson GW. Membrane lipids: where they are and how they behave. *Nat Rev Mol Cell Biol* 2008;9:112-24.

Wakamatsu K, Ito S. Advanced chemical methods in melanin determination. *Pigment Cell Res* 2002;15:174-83.

Watabe H, Valencia JC, Yasumoto K, et al. Regulation of tyrosinase processing and trafficking by organellar pH and by proteasome activity. *J Biol Chem* 2004;279:7971-81.

Wei ML. Hermansky-Pudlak syndrome: a disease of protein trafficking and organelle function. *Pigment Cell Res* 2006;19:19-42.

Yamaguchi Y, Takahashi K, Zmudzka BZ, et al. Human skin responses to UV radiation: pigment in the upper epidermis protects against DNA damage in the lower epidermis and facilitates apoptosis. *FASEB J* 2006;20:1486-8.

Yamashita T, Wada R, Sasaki T, et al. A vital role for glycosphingolipid synthesis during development and differentiation. *Proc Natl Acad Sci U S A* 1999;96:9142-7.

Chapter 2

Melanocyte pigmentation requires lowering of organelle pH via glycosphingolipid-dependent expression of Oca2

Seléne van der Poel[1], Jasja Wolthoorn[3], Dave van den Heuvel[2], Joep van den Dikkenberg[1], Maarten Egmond[1], Hans Gerritsen[2], Hein Sprong[4] and Gerrit van Meer[1]

[1] Membrane Enzymology, Bijvoet Center and Institute of Membranes, Utrecht University, Utrecht, The Netherlands

[2] Molecular Biophysics, Utrecht University, Utrecht, The Netherlands

[3] Present address: TNO Quality of Life, Zeist, The Netherlands

[4] Present address: National Institute of Public Health and Environment (RIVM), Bilthoven, The Netherlands

Abstract

GM95 mutant melanocytes are unable to synthesise pigment due to the inactivation of glycolipid synthesis. Using pH-sensitive fluorescent probes and fluorescence lifetime imaging microscopy (FLIM), we found that the pH in the TGN and lysosomes is less acidic than wild-type MEB4 melanocytes. Whereas the pH in the TGN and lysosomes in MEB4 cells was as low as 5 and 4, respectively, this was >1 pH unit higher in GM95 cells, similar to HeLa cells and fibroblasts. The cytosolic pH was 7.5 in all cells. When glycosphingolipid synthesis in MEB4 cells was inhibited, the lysosomal pH became less acidic. We measured a similar increase in pH in the lysosomes of melanocytes expressing oculocutaneous albinism due to a mutation in the melanocyte-specific protein Oca2, and indeed GM95 cells do not express Oca2. Oca2 expression depended on glycolipid synthesis as its expression was restored by retransfection of GM95 with the missing glucosylceramide transferase. Our data indicate that Oca2 transcription is regulated via a novel lipid-mediated transcription pathway, possibly via liver X receptors (LXR). Still, transfection of Oca2 into GM95 cells did not restore pigmentation. Thus besides Oca2 expression, glycosphingolipids are required for one other step in proper melanosome function.

Introduction

Glycosphingolipids are essential for mammalian life as a lack of these lipids has been shown to be embryonically lethal in mice (Yamashita et al., 1999). It all starts with the synthesis of glucosylceramide (GlcCer), the simplest of the glycosphingolipids, from ceramide and UDP-glucose by glucosylceramide synthase (GCS) (Ichikawa et al., 1996) which is thereby one of the enzymes regulating the pool of pro-apoptotic ceramide (Futerman and Hannun, 2004). Part of the GlcCer is converted to lactosylceramide, precursor for complex glycosphingolipids. From their site of synthesis in the Golgi lumen, these complex glycosphingolipids reach the cell surface where they function as receptors and receptor activity regulators (Hakomori, 2002; 2004). On the lumenal surface of the Golgi and endosomes, glycosphingolipids and cholesterol are thought to form microdomains that are important for sorting membrane proteins (van Meer, 1989; Sharma et al., 2003). In epithelial cells such domains are directed towards the apical surface (Simons and van Meer, 1988).

Although glycosphingolipids are essential for mammalian embryonic development, the mouse melanocyte mutant cell line GM95 does not have an active GCS and survives without glycosphingolipids (Ichikawa et al., 1994). However, GM95 cells do not assemble pigmented melanosomes. As a possible cause we observed

defective sorting of melanosomal and lysosomal proteins from the Golgi to their destination (Sprong et al., 2001; Groux-Degroote et al., 2008). Transfection with the GCS restored protein sorting and melanosome formation, whereby the activity of the lactosylceramide synthase to synthesise higher glycosphingolipids was not required. The defects were not corrected by exogenous GlcCer but they were corrected by glucosylsphingosine. Both reached the Golgi lumen as GlcCer, because both were converted to a complex glycosphingolipid, but while exogenous GlcCer reached the Golgi lumen by recycling on the lumenal surface of transport vesicles, glucosylsphingosine was most likely first acylated to GlcCer on the cytosolic surface. The suggestion that a cytosolic pool of GlcCer is required for melanosomal protein sorting is compatible with the fact that the synthesis of new GlcCer by GCS occurs on the cytosolic side of the Golgi (Coste et al., 1986; Futerman and Pagano, 1991; Jeckel et al., 1992) and maybe the ER (Kohyama-Koganeya et al., 2004).

Unexpectedly, the glycosphingolipid–dependent sorting signal in the melanosomal proteins is localised in their lumenal domain, which brought up the question how this lumenal information can be translated in the inclusion of these proteins into a budding transport vesicle destined for the melanosomes. We have suggested that the lumenal conditions in the sorting compartment may lead to oligomerisation of specifically the melanosomal proteins, resulting in recognition by the cognate adaptor proteins (Groux-Degroote et al., 2008). Here we describe one lumenal parameter, the pH, that differs between the melanoma mutant GM95 and wild-type MEB4 cell line. Interestingly, the protein mutated in the most common form of human albinism, oculocutaneous albinism type II, may be involved in the generation of a low pH (Puri et al., 2000). It is the melanocyte-specific OCA2/P-protein (Oca2/p-protein in mice). We now report that a pigmentation phenotype-inducing mutation in Oca2 results in a higher pH in the lysosomes, and that Oca2 is not expressed by the glycosphingolipid-deficient GM95 cells, unless induced by transfection with the GCS. Finally, transfection with Oca2 did not fully restore GM95 pigmentation, which suggests that GlcCer, besides restoring Oca2 expression, has a second function in melanosome assembly.

Results

MEB4 cells have a much lower pH in TGN and lysosomes than GM95 cells

In order to investigate the pH in the *trans* Golgi Network (TGN) and lysosomes, we used the retrograde transport of proteins via the plasma membrane to the TGN and the endocytotic transport to the lysosomes to bring pH-sensitive probes into the lumen of these organelles. At the plasma membrane, these proteins were labelled with

specific antibodies coupled to pH-sensitive fluorescent probes. The pH-sensitive fluorescent antibodies were taken up and recycled through the TGN, or accumulated in the lysosomes.

For pH measurements in the TGN, a chimera construct of the TGN-resident protein TGN38 with the lumenal domain of the plasma membrane protein CD25 was used as described earlier by Demaurex et al. (1998). The protein was targeted with fluorescein-labeled (FITC) anti-CD25 antibodies. As shown in Figure 1A, the construct was found in a similar compartment in MEB4 and GM95 cells. The fluorescein staining partially overlapped with the *trans* Golgi protein α-2,6-sialyltransferase as was expected for a protein in the TGN when compared to a *trans* Golgi localised protein. In HeLa cells, the anti-CD25-FITC antibodies in addition gave a punctate staining throughout the cell. This has been found previously (Demaurex et al., 1998). The pH was determined by measuring the fluorescence lifetime of fluorescein with Fluorescence Lifetime Imaging Microscopy (FLIM). The principle of this technique is explained in Supplemental Figure S1. The lifetime of fluorescein was pH-sensitive over a range of 2 pH units as shown in Supplemental Figure S2. Calibration curves were made in living cells using the K^+/H^+ exchanger nigericin and high potassium buffers (Thomas et al., 1979). The calibration in living cells and the probe in buffer were similar therefore only one curve is shown (Supplemental Figure S2).

The pH in the TGN in the wild-type MEB4 cells was far lower (5.1 ± 0.3) than in the glycosphingolipid-deficient GM95 cells (6.5 ± 0.3), see Figure 1B. When GM95 cells were retransfected with the glucosylceramide synthase (GCS) thus restoring the ability to produce glycosphingolipids resulting in the GM95-GCS cell line, the pH in the TGN was similar to that of the wild-type MEB4 cells (5.0 ± 0.3). This suggests that glycosphingolipids regulate pH in the TGN. The pH in the TGN of HeLa cells (6.6 ± 0.2) was similar to that found in GM95 cells, which shows that wild-type melanocytic MEB4 cells have an exceptionally low pH in the TGN.

In order to judge whether this glycosphingolipid effect on the pH was limited to the TGN, the pH was also measured in lysosomes. The lysosomal protein LAMP-1, which recycles over the plasma membrane, was targeted with anti-LAMP-1 coupled to Oregon Green (OG). MEB4 and GM95 cells, with mouse fibroblasts (MF) as a control, were incubated with OG-anti-LAMP-1 antibodies and the endocytosed antibodies showed complete co-localisation with the endogenous lysosomal protein LAMP-2 (Figure 2A). The lifetimes measured in lysosomes of MEB4, GM95, GM95-GCS and MF cells were converted into pH values using the calibration curve from Supplemental Figure S2. The calibration curve was obtained in a similar manner as in the TGN. Figure 2B shows that the lysosomal pH in MEB4 cells was again substantially lower (4.1 ± 0.1) than in GM95 cells (5.4 ± 0.2). Restoration of the ability to produce glycophingolipids by transfection of GCS in the GM95-GCS cells, lowered the lysosomal pH even below

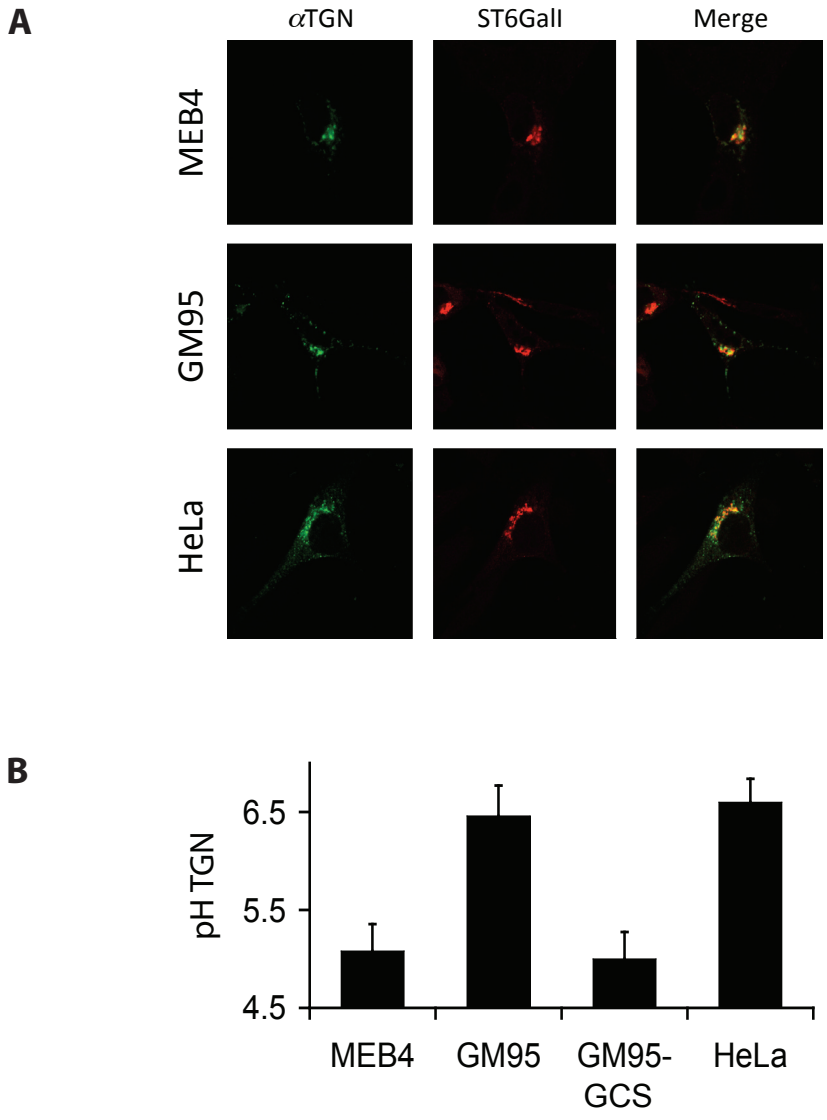

Figure 1. The pH in the melanocyte TGN depends on glycosphingolipids. (A) Localisation of endocytosed anti-CD25-FITC in the Golgi area. Cells expressing CD25-TGN38 were incubated with rat anti-CD25-FITC antibody (αTGN) overnight, fixed, permeabillised, and co-labelled with mouse anti-myc-α2,6 sialyltransferase (ST6GalI), visualised with Texas-red anti-mouse. (B) pH in the TGN. Average lifetime values for anti-CD25-FITC in MEB4, GM95, GM95-Res and Hela cells, ± S.D. with n=23, n=23, n=13 and n=18 cells, respectively, were measured and the average pH value of the TGN in these cells was calculated from the pH calibration curve (Supplemental Figure S2).

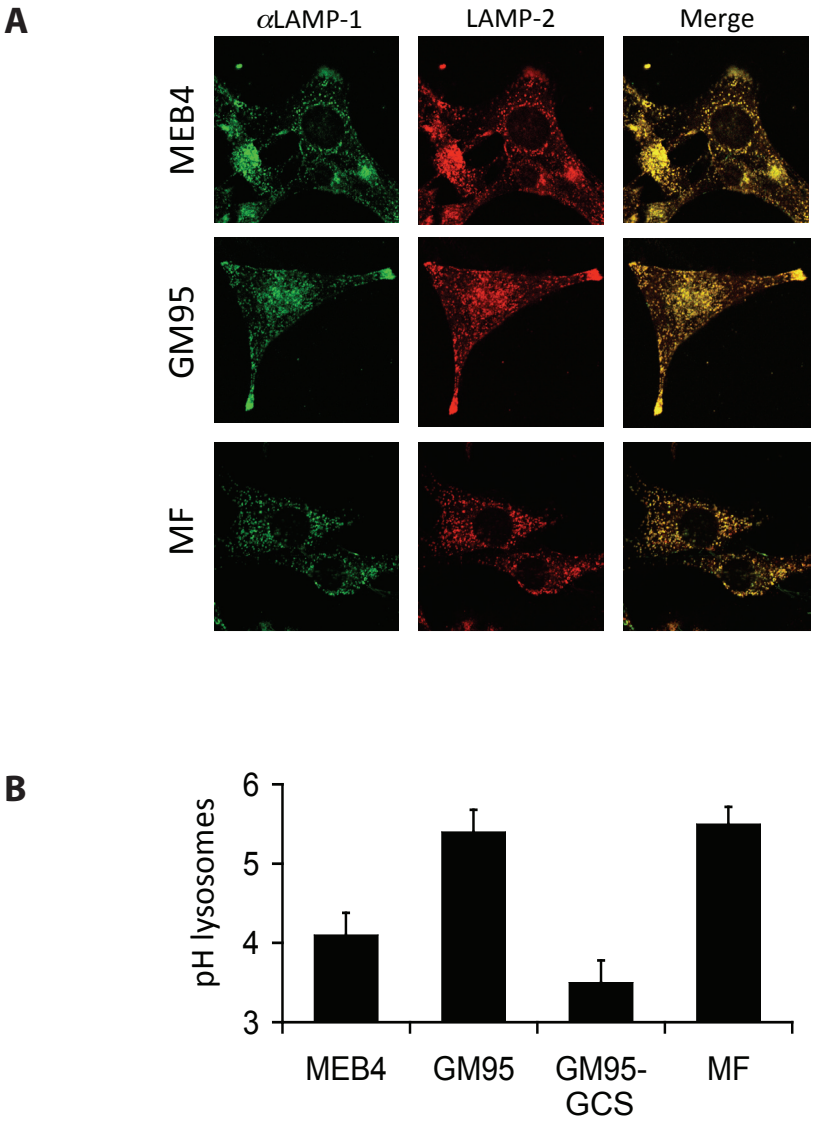

Figure 2. Glycosphingolipids also lower the pH in lysosomes. (A) Intracellular localisation of endocytosed oregon green (OG)-labelled anti-LAMP-1 in lysosomes. MEB4, GM95, GM95-Res cells and mouse fibroblasts (MF) were incubated with OG-anti-LAMP-1 for 5 h, fixed and permeabilised, and co-labelled with mouse anti-LAMP-2 and visualised with Texas-red anti-mouse. (B) Lysosomal pH. Average lifetime values for OG-anti-LAMP-1 in MEB4, GM95, GM95-Res and MF cells, with n=18, n=18, n=10 and n=6 cells, respectively, were measured and the average pH of the lysosomes was calculated from the pH calibration curve (Supplemental Figure S2).

the pH found in the wild-type MEB4 cells (3.5 ± 0.1). This indicates that also the pH in lysosomes is regulated by glycosphingolipids. The fact that the control (MF) again displayed a pH similar to the GM95 cells is indicative of an unusually low pH in MEB4 lysosomes.

The exceptionally low pH in MEB4 cells in both the TGN and lysosomes can be caused by a lower pH in the cytosol. Therefore, the cytosolic pH was tested using cell permeant carboxy SNAFL-diacetate, which becomes fluorescent and trapped in the cytosol when cleaved by cytosolic esterases. The carboxy SNAFL-diacetate has been applied before as a pH-sensitive probe suitable for FLIM (Sanders et al., 1995; Lin et al., 2003). As shown in Figure 3A, after allowing SNAFL uptake, a cytosolic pattern was observed in MEB4, GM95 and HeLa cells with the probe prominently localised in the nucleus. Calibration curves in Supplemental Figure S2 showed that the probe was

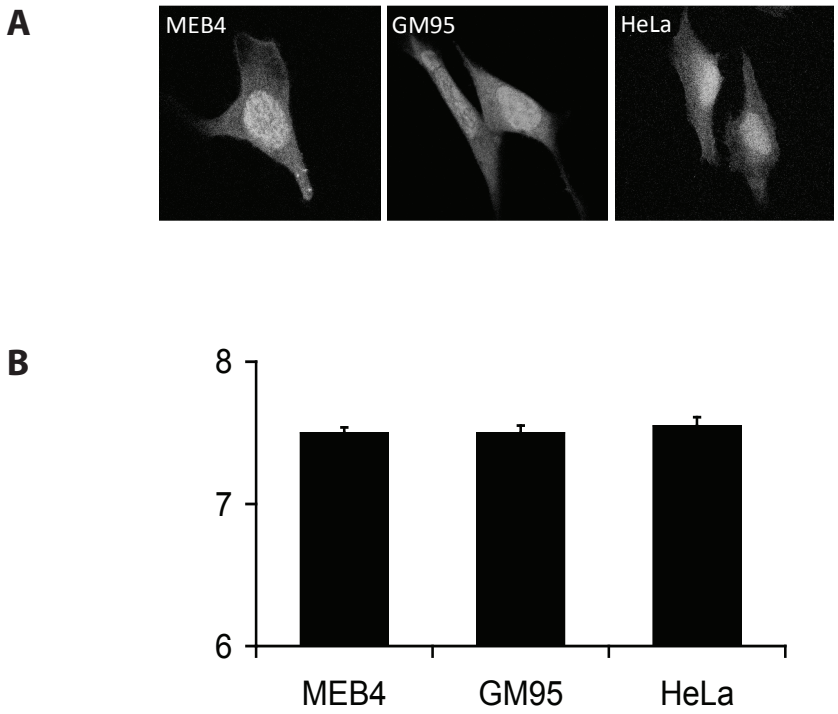

Figure 3. The cytosolic pH is independent of glycosphingolipids. (A) Intracellular localisation of the cytosolic pH probe SNAFL after 10 min uptake of the non-fluorescent SNAFL-diacetate. (B) The pH in the cytosol. Average lifetime values for SNAFL in MEB4, GM95 and HeLa cells, with n=7, n=4 and n=7 cells, respectively, were determined and converted to the average pH values of the cytosol in these cells using the corresponding pH calibration curve (Supplemental Figure S2).

pH-sensitive over a small range and somewhat different calibration curves were recorded for different cell lines. However, using the appropriate calibration for each cell line, the pH in the cytosol was similar in MEB4 and GM95 cells (7.5 ± 0.1) and HeLa cells (7.6 ± 0.1). Lifetime values for the probe localised in the nucleus did not significantly differ from measurements in the cytosol (results not shown).

The lysosomal pH in MEB4 cells depends on glycosphingolipid synthesis but not on V-ATPase activity

When glycosphingolipid synthesis was inhibited by addition of 10 μM D-*threo*-1-phenyl-2-decanoylamino-3-morpholino-1-propanol (PDMP) for 12 h, the lysosomal pH in MEB4 cells shifted up towards the lysosomal pH in GM95 cells (Figure 4A). The inhibitor did not affect the pH in GM95 cells, which do not synthesise glycosphingolipids in the first place. The treatment of living cells with PDMP indeed dramatically decreased the content of the simplest glycosphingolipid, glucosylceramide (GlcCer), in a total cell lipid extract and in time also decreased the more complex glycolipid monosialoganglioside GM3 (NeuAcα2-3Galβ1-4Glcβ1-1Cer) as shown by acidic orcinol staining of glycosphingolipids (Brückner, 1955) in Figure 4B. The pH values calculated from the calibration curve indicated in Figure 4A were different as was found earlier (Figure 2A), as the lifetime values measured in this data set were much lower for both MEB4 and GM95 cells. Although the pH of melanosomes, an organelle derived from lysosomes, can be as low as 3 (Bhatnagar et al., 1993), as far as we know there has been no evidence

> Figure 4. Glycosphingolipid synthesis is required for correct lysosomal pH. (A) Gaussian distribution of lifetime values of OG-anti-LAMP-1 in lysosomes of MEB4 and GM95 cells. Cells were incubated with 10 μM PDMP for 12 h prior to OG-anti-LAMP-1 uptake for 5 h. Gaussians were fitted to histograms (bin size 0.01 ns) of lifetime values, obtained in 3 independent experiments. The measurements for MEB4 cells, – and + PDMP, and GM95 cells, – and + PDMP, were from 21, 18, 19 and 19 cells, with the average number of 416, 318, 191 and 114 pixels per cell, respectively. The bin with the highest occurrence (amount of pixels) was set at 100% and the histogram was expressed in relative occurrence (%). (B) Glycosphingolipid levels after PDMP treatment. Cells were treated with PDMP, and lipids were extracted and with orcinol/H_2SO_4 (left) and iodine (right) as described in Materials and Methods. (C) PDMP incubation did not affect *in vitro* V-ATPase activity. Total membranes from GM95 and MEB4 were isolated and the V-ATPase activity assay was performed as described in Materials and Methods. The activity of the V-ATPase in the presence of 2 mM NaN_3 and 0.1 mM vanadate is defined as the difference between the ATPase activity in the absence and that in the presence of 200 nM concanamycin A, which is the concanamycin-sensitive ATPase activity. The V-ATPase activity is expressed in nmol P_i per mg protein per min. Values represent the average of 2 independent experiments in triplicate in the presence of 10 μM CCCP. (D) Equal amounts of V-ATPase were present in the activity assay. Aliquots of the total membranes, input of the assay, were boiled in SDS sample buffer and the proteins were separated on 17% SDS PAGE gel. The blot was decorated with rabbit anti-subunit B of the V-ATPase and mouse anti-p23, as described in Materials and Methods.

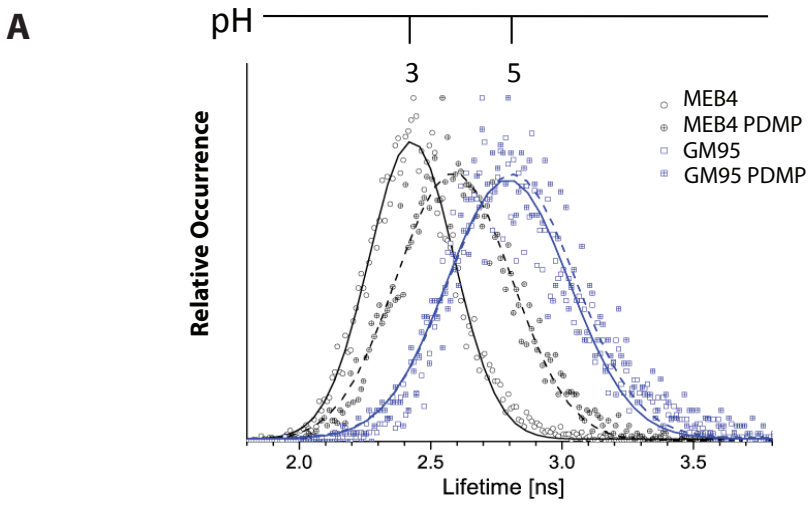
A
pH
3
5
Relative Occurrence
MEB4
MEB4 PDMP
GM95
GM95 PDMP
2.0
2.5
3.0
3.5
Lifetime [ns]

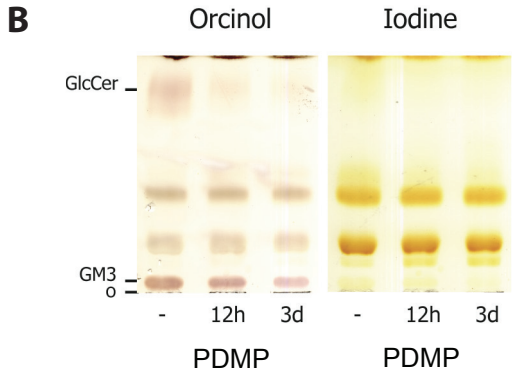
B
Orcinol
Iodine
GlcCer
GM3
-
12h
3d
-
12h
3d
PDMP
PDMP

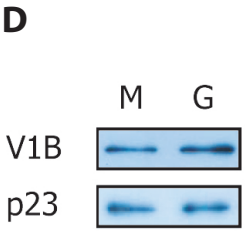
D
M
G
V1B
p23

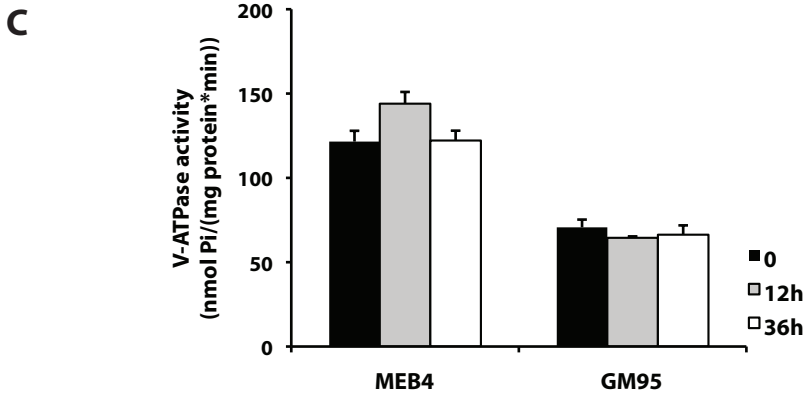
C
V-ATPase activity
(nmol Pi/(mg protein*min))
200
150
100
50
0
MEB4
GM95
0
12h
36h

in literature that lysosomes can achieve that kind of pH value.

In order to investigate the mechanism by which glycosphingolipids lower the lumenal pH, we studied the proton pump or vacuolar-type H^+-translocating ATPase (V-ATPase), which generates low pH in the lumen. The V-ATPase is a transmembrane protein complex that acidifies a range of different organelles in the cell. The activity of the proton pump was investigated by looking at its ATP hydrolysis activity. The amount of inorganic phosphate (P_i), generated by hydrolysis of ATP into ADP and P_i, was determined in a colorimetric assay in the presence of 5 mM Mg^+ and 1 mM ATP, which is 10 and 5–fold higher respectively than the K_ms of the V-ATPase (David and Barron, 1994). The background in the assay of mitochondrial and transport ATPases was lowered by addition of inhibitors, 2 mM azide and 0.1 mM vanadate. The V-ATPase activity was defined as the difference in signal in the absence and presence of a specific inhibitor of the V-ATPase, concanamycin A (Woo et al., 1992; Dröse et al., 1993). The maximum V-ATPase activity was determined in the presence of the protonophore carbonyl cyanide m-chlorophenylhydrazone (CCCP), which dissipates the inhibitory proton gradient and membrane potential built up by proton pumping (Skulachev et al., 1967; Steen et al., 1993).

The activity of the proton pump probed by its ATPase activity was insensitive to PDMP (Figure 4C). Therefore, the V-ATPase does not have a role in increasing the lysosomal pH in MEB4 cells by PDMP. Strikingly, the V-ATPase activity in GM95 cells was two-fold lower in total cellular membranes compared to MEB4 cells, while both cell lines had the same amount of V-ATPase as shown by western blotting (Figure 4D). The difference was independent of the proton gradient and membrane potential as these measurements were performed in the presence of the protonophore CCCP. This suggests that the V-ATPase activity depends on glycosphingolipids and this feature will be explored further in Chapter 3 of this booklet.

The melanocytic specific protein Oca2 plays a role in lysosomal pH

It has been reported that the melanocyte-specific membrane protein Oca2/p-protein is required for acidification of melanosomes (Puri et al., 2000). Oculocutaneous Albinism type II (OCA2) is the most common pigmentation disease among Caucasians and is caused by mutations in the pink-eyed dilution protein, p-protein, also known as OCA2 (human; Oca2 in mouse; Ramsay et al., 1992; Durham-Pierre et al., 1994; Lee et al., 1994). The lysosomal pH was investigated in cell lines that lack Oca2. The wild-type mouse melanoma cell line Melan-a and mutant cell lines that lacked Oca2, Melan-p5 and -p7 (Sviderskaya et al., 1997), were incubated with OG-anti-LAMP-1 after which the lysosomal pH was measured by FLIM. The wild-type cells had a significantly lower pH in the lysosomes than both mutant cell lines Melan-p5 and -p7 (Figure 5A). Melan-a cells indeed expressed Oca2 while both mutant cell lines did not have any

Oca2 mRNA, as determined by reverse transcriptase (RT) PCR (Figure 5B). This suggests that Oca2 plays a role in the regulation of lysosomal pH.

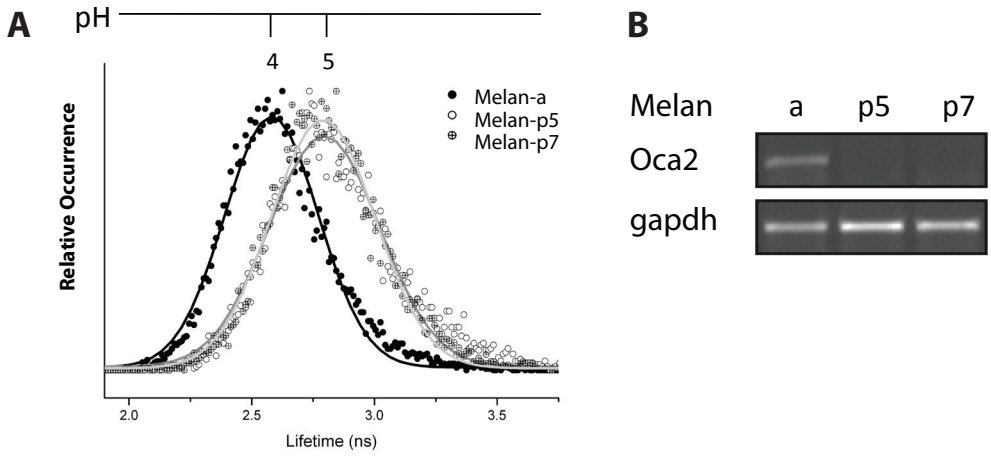

Figure 5. Oca2 influences lysosomal pH. (A) Lysosomal pH is elevated in the absence of Oca2. Gaussian distribution of lifetime values of OG-αLAMP-1 in lysosomes of wild-type Melan-a cells and knock-out Melan-p5 and -p7 cells. Cells were allowed to endocytose OG-αLAMP-1 for 5 h and lysosomal pH was determined by fluorescence lifetime imaging microscopy (FLIM). The lifetime values were obtained from 3 independent experiments, measuring on average 14 cells per experiment. The measurements for Melan-a cells (black solid circles), Melan-p5 cells (open circles) and Melan-p7 cells (crossed circles) were from n (# cells), n = 43, n = 41, n = 39, respectively. The circles represent histograms (bin size 0.01 ns) of all pixels of measured lifetimes of OG-αLAMP-1 in lysosomes and Gaussians were fitted, represented by the black, dark grey and light grey lines for Melan-a, Melan-p5 and Melan–p7, respectively. The bin with the highest occurence (amount of pixels) was set at 100% and the histogram was expressed in relative occurence (%). (B) Melan-p cells do not express Oca2. Total RNA was isolated from Melan-a (left column), Melan-p5 (middle column) and Melan-p7 (right column) and semi quantitative reverse transcriptase-polymerase chain reaction (RT-PCR) was performed with the appropriate primers as described in Materials and Methods, on mouse Oca2 (first row) and gapdh (second row). Fragments were amplified with polymerase chain reaction (PCR) using the appropriate primers and resolved on a 1% agarose gel.

Transcription of Oca2 depends on glycosphingolipids

The presence of Oca2 in MEB4 and GM95 cells was investigated using RT-PCR. The pigment producing wild-type cell line MEB4 had Oca2, while the glycosphingolipid-deficient GM95 cells did not have Oca2 mRNA (Figure 6A) and did not produce pigment as was described earlier by Sprong et al. (2001). When the GM95 cells were retransfected with GCS to synthesise glycosphingolipids, not only pigmentation was

largely restored but also the Oca2 transcripts were recovered with RT-PCR. Thus, transcription of Oca2 depended on the presence of an active GCS.

When the cells were treated with PDMP, and its analog D-*threo*-1-(3',4'-ethylenedioxy)phenyl-2-palmitoylamino-3-pyrrolidino-1-propanol (P4; Lee et al., 1999), Oca2 expression was not affected (Figure 6B). Even when the GlcCer content and the content of the more complex glycolipid GM3 were almost brought to trace amounts, undetectable by orcinol staining, Oca2 transcripts were unaffected. Therefore, Oca2 transcription depended on the presence of GCS, however the inhibitors PDMP or P4 did not affect transcription.

Several lipid-mediated signalling pathways have been identified that play a role in pigmentation. Some of these were targeted using signalling activators to investigate whether they are involved in the induction of Oca2 transcription. Known endogenous signalling agents are fatty acids that induce the nuclear receptors peroxisome proliferator-activated receptors (PPAR) (Janowski et al., 1996; Michalik et al., 2007).

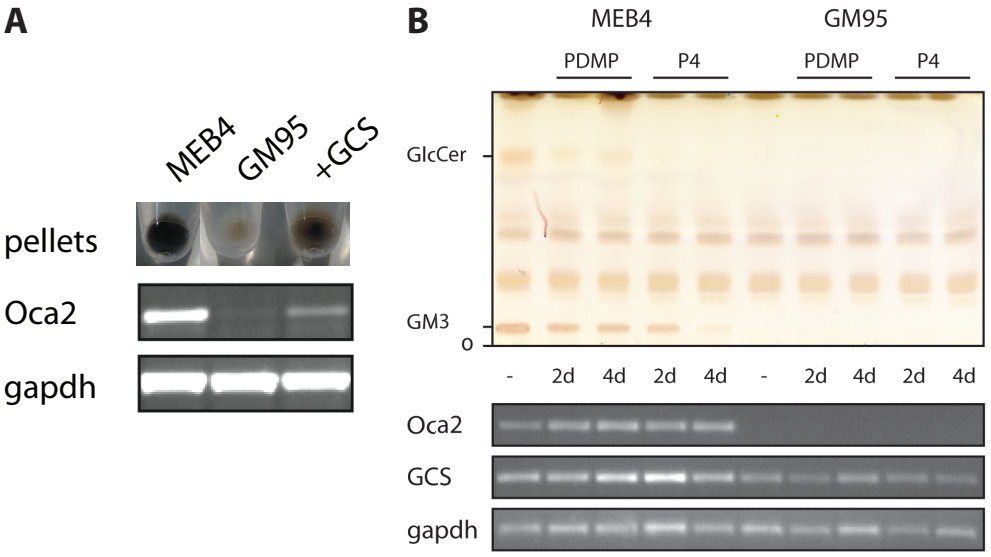

Figure 6. Transcription of Oca2 depends on glycosphingolipids. (A) Oca2 mRNA is restored upon synthesis of glycosphingolipids. Total RNA was isolated with MEB4, GM95 mock-transfected with pCB7 (GM95) and GM95 retransfected with pCB7-GCS-KKVK (+GCS). RT-PCR was performed on Oca2 (first row) and gapdh (second row) as described. (B) Removal of glycosphingolipids does not reduce Oca2 transcripts. Cells were treated with 10 µM PDMP for 12 h or 3 d. RNA isolation and RT-PCR procedures were as described.

It has also been reported that the sphingolipids ceramide-phosphoethanolamine (CPE) or sphingosylphosphocholine (lysosphingomyelin) signal microphthalmia-associated transcription factor (Mitf) (Higuchi et al., 2003; Saha et al., 2009). Pigmentation was also induced by an increase in intracellular cAMP (Ma et al., 2006; Sato et al., 2009). Addition of the panactivator of PPARs, linoleic acid, and dimethylethanolamine, a precursor for CPE to induce Mitf, did not induce Oca2 transcription in GM95 cells (results not shown). Addition of 3-isobutyl-1-methylxanthine (IBMX), which increases intracellular cAMP levels, did increase pigment production, however did not induce Oca2 transcription (results not shown). This suggests that the transcription of Oca2 is regulated via a novel glycosphingolipid-mediated signalling pathway.

GM95 cells do not have an Oca2 phenotype

When GM95 cells were stably transfected with constructs coding for human HA-tagged OCA2 and a mutant OCA2 (OCA2 mut) that is mislocalised to the plasma membrane, OCA2 was transcribed in both cases although not to the extent of MEB4 cells (Figure 7A; Sitaram et al., 2009). Transfection of OCA2 in GM95 cells had no effect on the V-ATPase activity in total membranes compared to GM95 cells while the amount of enzyme was the same in these membrane preparations according to western blot of subunit B of the V-ATPase (Figure 7B). The transcription of the glucosylceramide synthase (GCS) was increased after transfection of OCA2 (Figure 7A), however, did not lead to an active enzyme as no GlcCer or the more complex glycosphingolipid GM3 were detected on TLC with acidic orcinol staining (Figure 7C). The HA-tagged OCA2 and OCA2mut proteins had a lysosomal/melanosomal and mostly plasma membrane localisation respectively as described before (Figure 7D; Sitaram et al., 2009).

When Oca2-deficient mouse melanoma cell lines were treated with the precursor of melanin, L-tyrosine, the hypopigmentation phenotype was restored (Sviderskaya et al., 1997; Rosemblat et al., 1998). The block in the development of melanosomes and tyrosinase sorting is removed and pigmentation is restored. However, in the case of GM95, the hypopigmentation phenotype could not be restored with L-tyrosine while the same treatment did completely restore pigmentation in Melan-p7 cells (Figure 8A). Furthermore, the transfection of OCA2 did not correct tyrosinase missorting in GM95 cells as tyrosinase was mostly found in the Golgi or Golgi-associated structures (Figure 8B). The phenotype observed in GM95 cannot be the result of the lack of Oca2 alone and glycosphingolipids are needed to correct the phenotype completely.

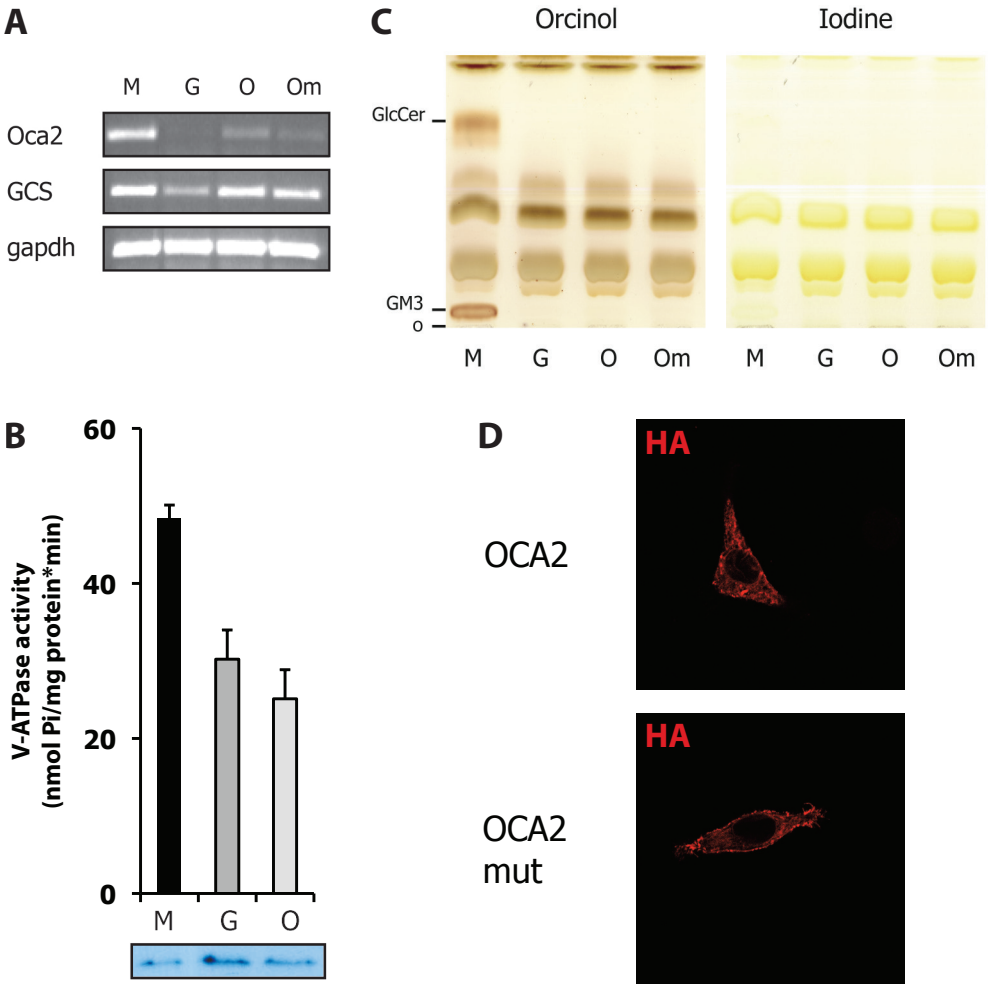

Figure 7. OCA2 does not completely repair the GSL-deficient phenotype. (A) Transfection of OCA2 in GM95 cells leads to OCA2 transcription. GM95 cells were transfected with OCA2 and mutated OCA2, which is mislocalised to the plasma membrane. MEB4 (M), GM95 (G), GM95-OCA2 (O) and GM95-OCA2mut (Om) were grown on 10 cm dishes and were tested by RT-PCR for expression of Oca2, GCS and gapdh as described. (B) Oca2 does not influence V-ATPase activity. Membranes from MEB4 (M), GM95 (G), GM95-OCA2 (O) and GM95-OCA2mut (Om) were assayed for V-ATPase activity as described in Materials and Methods. Below, a western blot of the subunit B of the V-ATPase shows a similar amount of protein present during the assay. (D) Oca2 does not induce glycosphingolipid synthesis. Lipids were extracted from MEB4 (M), GM95 (G), GM95-Oca2 (O) and GM95-Oca2mut (Om). The same amount of phospholipids was analysed on TLC. (E) Localisation of the Oca2 contructs. GM95 cells stably expressing OCA2 and OCA2mut were grown on coverslips for 2d. Cells were fixed, permeabilised as described in Materials and Methods. OCA2 and OCA2mut were targeted with mouse αHA and visualised using mouse Alexa-488. Pictures were taken with the confocal microscope.

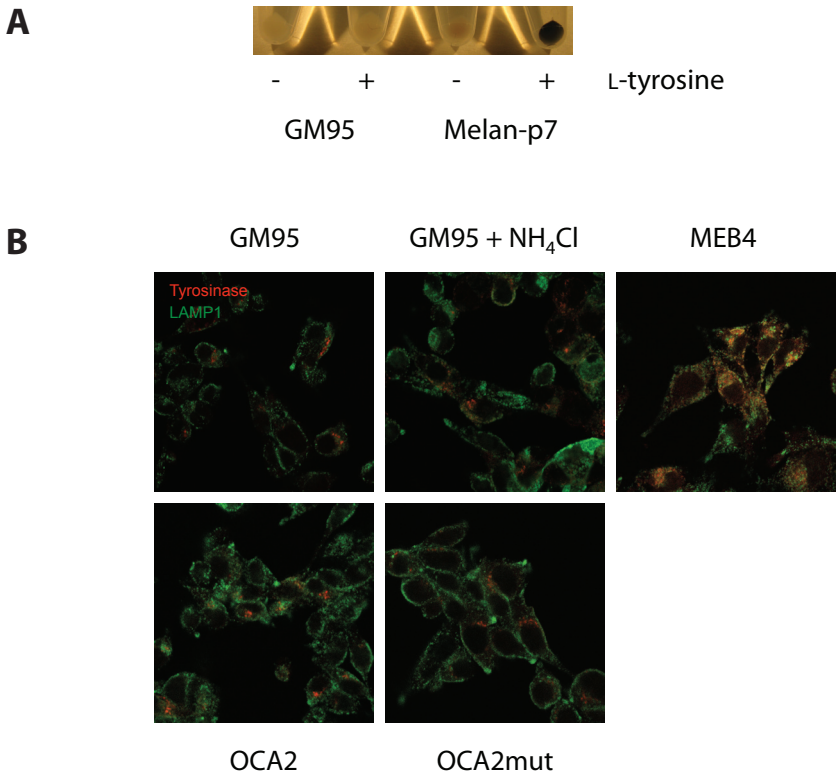

Figure 8. GM95 cells do not have the Oca2 phenotype. (A) Addition of L-tyrosine restores hypopigmentation phenotype in Melan-p7, but not in GM95 cells. Cells on dishes were incubated with 5 mM L-tyrosine for 7d, then harvested using trypsin/EDTA and pelleted in PBS. (B) Oca2 does not restore tyrosinase mislocalisation in GM95 cells. Cells were grown on coverslips for two days and GM95 cells were treated with 10 mM NH_4Cl for 2 h prior to fixation as described. Tyrosinase (red) and LAMP-1 (green) were targeted with rabbit anti-pep7 and rat anti-1D4B respectively and visualised using rabbit Alexa-610 and rat FITC.

Discussion

Here we report that the pH in the lumen of TGN and lysosomes of melanoma cells is much lower than in a mutant lacking an active GCS. Retransfection lowered and GlcCer synthase inhibition increased lysosomal pH. Melanocytes lacking the membrane protein Oca2 also displayed an increased lysosomal pH, and indeed the mutant lacking GCS activity did not express Oca2 either. Transcription of Oca2 depended on an active GCS, however retransfection of OCA2 in this mutant did not restore pigmentation suggesting that GCS is required for pigmentation.

Determinants of lumenal pH

The existence of a gradient of pH along the secretory and endocytic pathway is in agreement with our findings that lysosomes have a lower pH than the TGN (Weisz, 2003). Unexpectedly, the GM95 cells had a normal pH compared to fibroblasts and the wild-type melanoma cells were different with an exceptionally low pH in both TGN and lysosomes. This is the first report that melanocytes have a lower lumenal pH in secretory and endocytotic organelles compared to fibroblasts. Melanosomes are lysosome-related organelles, which are acidic (Puri et al., 2000; Raposo and Marks, 2007). It has been reported that the melanosomal pH can be as low as 3 (Bhatnagar et al., 1993), similar to what we measured for melanocytic lysosomes in some of our experiments. The pH in TGN and lysosomes in MEB4 cells is much lower compared to glycospingolipid-deficient cells. There are three major determinants for maintaining the low lumenal pH of cellular organelles: (1) proton pumping by the V-ATPase, (2) proton leak and (3) ion channels contributing to lumenal ion concentrations (Grabe and Oster, 2001).

The activity of the V-ATPase is two-fold higher in wild-type MEB4 cells compared to the glycosphingolipid-deficient GM95 cells and this difference is independent of the proton gradient and membrane potential as was determined by addition of the protonophore CCCP during the activity assay (Figure 4). This suggests that the activity of the proton pump is glycosphingolipid-dependent.

Whether the proton leak is altered in glycosphingolipid-deficient cells remains to be determined. Glycosphingolipids are known to play a role in the barrier function in the apical membrane of epithelial cells (Simons and Van Meer, 1988). The lack of these lipids can cause increased permeablility to protons, resulting in a lower proton gradient and render the lumen less acidic. This would stimulate the V-ATPase because it would pump against a lower proton gradient. The facts that intact membranes from GM95 cells have a lower V-ATPase activity than those from wild-type MEB4 cells and that the difference was maintained after addition of the protonophore CCCP, argue against an increase of proton leak in glycosphingolipid-deficient GM95 cells.

Pumping protons into the lumen builds up a proton gradient and membrane potential (Mitchell, 1961). Channelling anions into the lumen, which counteract the charge build-up by protons, enables the proton pump to pump more protons into the lumen thereby further acidifying the organelle. This channelling function in melanocytes is possibly fulfilled by Oca2.

Oca2 as a putative anion channel

Oca2 is a melanocyte-specific protein with 12 predicted transmembrane domains and is homologous to citrate and arsenite transmembrane transporters (Rinchik et

al., 1993; Staleva et al., 2002). In fact, Staleva and coworkers (2002) found that transfection of Oca2 in *Saccharomyces cerevisiae* sensitised the yeast cells to arsenicals. This renders Oca2 a prime candidate for an anion conductor that helps melanoma cells to achieve an exceptionally low lumenal pH in their compartments.

Lysosomal pH measurements with Melan cells agree with the notion that Oca2 may be an anion conductance channel. When Oca2 is absent, the pH is increased in the lysosomes. Anions are not channelled into the lumen, therefore a membrane potential is built up inhibiting the V-ATPase and this results in a less acidic pH. The role of Oca2 in regulating pH has been controversial, the fact that V-ATPase inhibitors and addition of ammonium chloride can restore pigmentation would argue for a neutral pH in the working melanosome (Ni-Komatsu and Orlow, 2006) and it has been suggested that Oca2 neutralises pH (Ancans et al., 2001). However, electron microscopy studies of the ammonium chloride treated cells showed blackened lysosomes (Groux-Degroote et al., 2008) thereby suggesting that a neutral pH induces a situation that is not relevant for melanosome biogenesis under physiological conditions. Data presented here suggests that Oca2 does play a role and lowers the pH in the lysosomes.

Transfection of OCA2 in the glycosphingolipid deficient cell line GM95 did not alter the V-ATPase activity in total membranes (Figure 7). This argues against OCA2 being a possible ion conductance channel. However, the transcription of OCA2 was considerably lower compared to MEB4 cells. Furthermore, as total membranes consist mainly of ER and Golgi, the V-ATPase in endosomes/lysosomes, where OCA2-HA is localised (Figure 8), will have a minor contribution to the total V-ATPase activity. Separation of organelles before activity assays may prove beneficial to investigate a possible role of OCA2 as an anion channel in V-ATPase activity. However, the difference in V-ATPase activity between GM95 and MEB4 membranes was independent of the proton and electrochemical gradient as determined with the protonophore CCCP. As Oca2 will not channel anions in the absence of gradients, the lack of Oca2 in GM95 cells does not solely cause loss of V-ATPase activity. The effects of glycosphingolipids on the V-ATPase is further explored in Chapter 3.

Oca2 and glycosphingolipids

Pigmentation in Oca2-deficient Melan-p cells could be restored by incubation with L-tyrosine, a precursor of melanin, ER-retention of tyrosinase was relieved (Halaban et al., 2001) and mature melanosomes were observed (Rosemblat et al., 1998). Incubation of GM95 cells with L-tyrosine did not induce pigment production. Moreover, transfection of Oca2 in the GM95 cells did not restore pigmentation or tyrosinase sorting (Figure 7 and 8). Therefore, the phenotype in GM95 cells is not caused solely by lack of Oca2, and glycosphingolipids are required to restore the phenotype.

Besides influencing transcription levels, glycosphingolipids perhaps also

modulate Oca2 function. Oca2 channel function could be lipid-dependent, similar to the channel function of the bacterial potassium (KcsA) channel, which is dependent on negatively charged lipids (Valiyaveetil et al., 2002). Structurally, glycosphingolipids provide a more ordered membrane environment, which can benefit protein function. The V-ATPase for instance was found preferably in detergent resistant membranes (Dermine et al., 2001; Gkantiragas et al., 2001; Yoshinaka et al., 2004), which are enriched in cholesterol and sphingolipids, however this is not known for the Oca2 protein.

Inhibition of glycosphingolipid synthesis

The inhibitor of glycosphingolipid synthesis, PDMP, caused a less acidic pH in lysosomes of MEB4 cells. Glycosphingolipids were substantially lowered, but pH determinants such as the V-ATPase and Oca2 were not affected, even when glycosphingolipids were undetectable on TLC after incubation with P4 (Figure 6). A remnant pool of GlcCer or higher glycolipids, undetected by orcinol staining, is possibly sufficient for V-ATPase activation and sustained Oca2 expression. The Oca2 mRNA transcripts can also be highly stable. However, as mRNAs typically have a half-life of minutes to hours (Hollams et al., 2002), a stability of 4 days seems to be extremely long. Alternatively, expression can be lowered independent of mRNA transcript levels. We could not study the Oca2 protein level because of a lack of tools directed against the endogenous Oca2 protein. Therefore, how PDMP exactly increases pH in MEB4 lysosomes remains to be determined.

A novel glycosphingolipid-mediated transcription pathway

Interestingly, we found that transcription of Oca2 is absent from glycosphingolipid-deficient GM95 cells and is restored upon transfection of an active GCS. Therefore, a product of the synthase is a prime candidate for a molecule that either directly or indirectly influences a transcription factor. There are multiple examples of lipid signalling in literature, with fatty acids and sterols as endogenous signalling agents that bind to transcription factors (Janowski et al., 1996; Michalik et al., 2007). There are also some reports on sphingolipids, such as ceramide-phosphoethanolamine (CPE) or sphingosylphosphocholine (lysosphingomyelin) as the signalling molecules (Higuchi et al., 2003; Saha et al., 2009).

Because conversion to LacCer and GM3 was not required for correcting the GM95 phenotype (Sprong et al., 2001; Groux-Degroote et al., 2008), GlcCer is the prime candidate for the signalling agent affecting the level of Oca2 mRNA and protein. GlcCer is synthesised on the cytosolic surface of the GlcCer is synthesised on the cytosolic surface of the Golgi and therefore has direct access to cytosolic proteins like transcription factors. However, when we decreased the GlcCer levels with PDMP by

about 60% or almost abolished GlcCer with P4 according to orcinol staining, no effect on Oca2 mRNA level was observed. Other candidates for being the GCS produced signalling lipid are possible by-products of the GCS. In fact, the synthase has been reported to also be able to synthesise sterylglucoside (Hillig et al., 2003). Although sterylglucoside is the main glycolipid in plants, it has been reported that cholesteryl-glucoside is made in human fibroblasts, upon heat shock stress (Kunimoto et al., 2000; 2002).

The inhibitor NB-DGJ (N-butyldeoxygalactonojirimycin), which resembles glucose, could be used to inhibit the synthesis of glucosylceramide and cholesteryl-glucoside as opposed to the ceramide-resembling inhibitors PDMP and P4. NB-DGJ also affected the lysosomal pH in MEB4 compared to GM95 cells although the effect was less convincing than PDMP (data not shown). Interestingly, sterylglucoside has been shown to influence pH by increasing the activity of the tonoplast V-ATPase proton pump in plants (Yamaguchi and Kasamo, 2001).

The transcription pathway via the liver X receptors (LXR) is known to be induced by oxysterols. These nuclear receptors are located in the liver to react on nutrients and play a role in fatty acid metabolism (Janowski et al., 1996; Peet et al., 1998; Schultz et al., 2000). Only recently, these receptors were also found in melanoma cells (Kumar et al., 2010). Interestingly, it has been reported that these receptors are activated by soluble glucose (Mitro et al., 2007). The apparent contradiction of participation of a hydrophilic glucose in a hydrophobic receptor-ligand interaction (Lazar and Wilson, 2007), can be solved by a lipophilic glucosylceramide, -sphingosine or -sterol as potential endogenous (co)activators, which are all products of GCS.

Materials and Methods

Materials

Chemicals, unless stated otherwise, were from Sigma-Aldrich (St. Louis, Missouri) and used in the highest purity available. Cell culture media, reagents, antibiotics and fetal bovine serum (FBS "GOLD") were from PAA laboratories (Pasching, Austria). Cell culture plastics were from Costar (Cambridge, MA). All lipids and lipid standards were from Matreya (Pleasant Gap, PA), and were stored as stock solutions in $CHCl_3$/MeOH at -20°C. Phosphatidylcholine (PC) in $CHCl_3$, isolated from egg yolk (Grade I), was from LipidProds (Surrey, England). Concanamycin A was from Wako Pure Chemical Industries, Ltd. (Osaka).

DNA

The CD25-TGN38-pCDM8.1 construct, encoding the lumenal domain of human CD25 and the transmembrane and cytosolic domain of TGN38, was a gift from F. Maxfield (Cornell University, New York).

Myc-tagged α2,6-sialyltransferase-pCB7 and GCS-KKVK-pCB7 were made as described previously (Sprong et al., 2001). GLTP-pQE-9 was a kind gift from P. Mattjus (Åbo Akademi University, Turku, Finland). The constructs encoding the HA-tagged wild-type human OCA2 and mutant OCA2, mislocalised to the plasma membrane, pCR3/OCA2-HA (OCA2 WT) and pCR3/OCA2-HA/AA123 (OCA2 mut) respectively, were kind gifts from M. Marks (University of Pennsylvania School of Medicine, Philadelphia, PA).

Cell culture and transfection

GCS-deficient GM95 and their parental MEB4 cells were from RIKEN Cell Bank (Tsukuba, Japan) and were grown in high glucose Dulbecco's modified Eagle's medium (DMEM) containing 10% FBS at 37°C with 5% CO_2. HeLa cells (G. Warren, London) and mouse fibroblasts WT1.2 cells (MF; J. Wijnholts, The Netherlands Cancer Institute) were grown under the same conditions as GM95 and MEB4 cells. Melan-a, Melan-p5 and Melan-p7 cells were kind gifts from D. Bennett (University of London, London, UK) and were grown in RPMI-1640 medium (Sigma, Zwijndrecht, The Netherlands) with 10% FBS, 200 nM tetradecanol phorbol acetate (TPA) and penicillin/streptomycin. GM95 cells were stably transfected with GCS-KKVK-pCB7 using the Amaxa electroporation system in buffer (15 mM NaH_2PO_4, 35 mM Na_2HPO_4, 5 mM KCl, 10 mM $MgCl_2$, 100 mM NaCl, 20 mM Hepes, 159 mM NaOH, pH 7.2). Selection was done with hygromycin B (0.6 mg/ml) and individual clones were selected using limiting dilution subcloning. Stable transfectants were screened for pigmentation. GM95 cells were transfected with plasmids encoding the OCA2 WT or OCA2 mut using Amaxa as described above. Stable transfectants were selected with G418 (1 mg/ml). For pH measurements in the TGN, cells were grown on 3 cm glass bottom dishes (Mattek Corporation, Ashland, MA) and transiently transfected with CD25-TGN38-pCDM8.1 using Lipofectamine 2000 (Invitrogen Corporation, Carlsbad, CA). After 5 h, transfection medium was changed to normal growth medium with anti-CD25-FITC (5 nM) and the incubation continued for 16 h. For pH measurements in lysosomes, anti-LAMP-1-OG was added to untransfected cells and incubated for 5 h in the presence of 10 µg/ml leupeptin. For pH measurements in the cytosol, cells were incubated with for 20 min with 5 µM carboxy SNAFL-diacetate in HBSS, pH 7.4. For fluorescence lifetime imaging microscopy, cells were incubated with DMEM high glucose, without phenol red, 25 mM Hepes pH 7.4 with 10% FBS and replaced with DMEM/Hepes without FBS just prior to measurements and in HBSS pH 7.4 for measurements of cytosolic pH.

Antibodies and immunofluorescence

The rat conjugated anti-CD25-FITC antibody against human CD25 was from Serotec (Oxford, UK). The polyclonal rabbit anti-human CD25 antiserum was a gift from M. Marks (University of Pennsylvania School of Medicine, Philadelphia, PA). The monoclonal anti-c-myc 9E10 antibody, the rat 1D4B antibody against LAMP-1 and mouse monoclonal anti-HA were from Santa Cruz Biotechnology (Santa Cruz, CA). The monoclonal anti-LAMP-2 antibody ABL-93 was from Developmental Studies Hybridoma Bank (Iowa City, IA). Oregon Green-514 carboxylic acid succinimidyl ester and 5(and 6-)-carboxy SNAFL-1 diacetate were from Molecular Probes (Eugene, OR). Oregon Green (OG) was

coupled to anti-LAMP-1 antibody (1D4B) following the instructions by Molecular Probes. The rabbit polyclonal antibody recognising subunit B of the V-ATPase was a kind gift from M. Forgac (Boston, MA) and the mouse monoclonal anti-p23 (JJ3) antibody was from Abcam (Cambridge, UK). Horseradish peroxidase (HRP)-conjugated secondary goat anti rabbit and mouse IgGs were from Dako (Glostrup, Denmark). The secondary antibody rat-FITC was from Santa Cruz, other secondary antibodies for immunofluorescence were Alexa-conjugated from Molecular Probes. The immunofluorescence procedure was done as described earlier (Sprong et al., 2001).

Reverse-transcriptase polymerase chain reaction

Cells grown on 10 cm dishes were washed with PBS, harvested using trypsin/EDTA and pelleted in PBS. RNA was isolated from cell pellets stored at -80°C using the RNAII isolation kit from Machery-Nagel (Bioké, Leiden, The Netherlands). A cDNA library was constructed using oligo dT and Reverse Transcriptase III from Invitrogen. Transcripts of interest were enhanced by the addition of specific reverse primers during cDNA construction. Fragments were amplified using polymerase chain reaction (PCR) with Taq-Polymerase from Fermentas (St. Leon-Rot, Germany) and the appropriate primers and resolved on a 1% agarose gel.

Lipid analysis

Cells were treated with 10 µM D-*threo*-1-phenyl-2-decanoylamino-3-morpholino-1-propanol (PDMP) or D-*threo*-1-(3',4'-ethylenedioxy)phenyl-2-palmitoylamino-3-pyrrolidino-1-propanol (P4) either for 12 h or 3 d in DMEM and 10% FBS. Cells were washed with PBS, harvested using trypsin/EDTA, subsequently taken up in PBS and pelleted. The pellet was taken up in PBS and the lipids were extracted using the method described by Bligh and Dyer (1959). In short, 3.2 volumes of methanol:chloroform (2.2:1) was added and left at room temperature for 30 min with occasional vortexing. For phase separation, 1 volume of 120 mM KCl with 10 mM acetic acid and 1 volume of chloroform were added and centrifuged at 3,000 x g in a Beckman Coulter for 10 min at room temperature. The bottom organic phase was isolated and dried under N_2. An additional chloroform wash of the aqueous phase was performed and the organic phases were pooled. An equal amount of phospholipids, as determined by the lipid phosphate determination according to Rouser (1970), was spotted on a Thin Layer Chromatography (TLC) plate and separated using acidic running solvent (chloroform/acetone/methanol/acetic acid/H_2O = 50/20/10/10/5 v/v). All lipids were visualised using iodine vapour to ensure equal loading and the glycosphingolipids were visualised using H_2SO_4/orcinol stain (0.2% in 5 M H_2SO_4) and incubation in a 100°C oven.

pH calibrations

Calibration curves of the fluorescence lifetime of the various probes versus the pH were generated using the high potassium/nigericin method (Thomas et al., 1979). For measurements in the TGN, cells were washed twice in calibration buffer (100 mM KOAc, 50 mM KCl, 1 mM $MgCl_2$, 5 mM glucose)

set at a pH value ranging from 5.0 to 7.0, followed by the addition of nigericin (13 µM final concentration). After 5 min, the fluorescence lifetime was measured in at least three different cells. Lysosomes were calibrated in the same calibration buffer with pH values ranging from 3.5 to 5.5. Calibration in the cytosol was done in phosphate buffer (100 mM K_2HPO_4/KH_2PO_4, 50 mM KCl, 5 mM $MgCl_2$, 5 mM glucose) ranging from pH 6.8 to pH 7.8. Average lifetimes were plotted against pH. Error bars represent the sample standard deviation (SD).

Fluorescence Lifetime Imaging Microscopy and Statistical Analysis

Lifetime measurements were performed using a confocal laser scanning microscope (CLSM, Nikon PCM2000). For excitation, 460 nm pulsed light was used. Therefore, the CLSM was equipped with a Tsunami Titanium:Sapphire laser (Spectra-physics, Newport Corporation, Mountain View, CA) that produced 2 ps light pulses at 920 nm with a repetition rate of 82 MHz. For our purposes every 10th pulse was picked with a pulsepicker and the 920 nm was frequency-doubled to 460 nm using a LBO-crystal. The emitted fluorescence, selected with appropriate chromatic filters, was detected using fast GaAsP photon-counting PMT (Hamamatsu, H7421-40, with a 450 ps transient time spread). The output pulses from the PMT were coupled to a four time-gated lifetime module, with four time-gates (de Grauw and Gerritsen, 2001). The four time-gate widths were set to 2 ns each without delay between the time-gates. The start of the first time-gate was delayed until the intensity of a fast decaying dye in the first time-gate was reduced to 10% of the maximal obtainable signal (Rose Bengal, τ = 90 ps, Sigma, Zwijndrecht, The Netherlands; Rodgers, 1981). In order to collect a stack of 4 time-gated intensity images of 160 x 160 pixels, cells were scanned at dwell times of 3 ms per pixel using the 50 µm pinhole of the CLSM and a 60x water immersion objective (Nikon, PlanApo, NA 1.2). The fluorescence lifetime (τ) per pixel was determined by fitting the 4 time-gated intensities (I(t)) per pixel, corrected for the background, with a single-exponential decay function: $I(t)=I(0)\cdot e^{-t/\tau}$. These lifetimes were depicted in a lifetime image (Supplementary Figure S1). The regions with the highest fluorescence intensity were selected by an intensity-threshold. The intensity cut-off was set at the point where the fluorescence resembled a compact signal for the TGN and a punctate signal for lysosomes. The average lifetime of the fluorescence in these pixels was determined from a Gaussian fit of the lifetime histogram. No significant differences in average lifetimes were found when lifetimes of each pixel were weighted or unweighted with their pixel-intensities, therefore we omitted this weighing factor from our calculations. The data was either represented (1) in bar diagrams, where the average is the average when all lifetime histograms are individually fitted to a Gaussian and the standard deviation was determined in these average values or (2) in a lifetime histogram, with bin size 0.01, where the calculated lifetimes of all experiments are taken together and fitted to a Gaussian. For pH calculations, the pH calibration curve was used to determine the pH value corresponding to the average lifetime value. For each cell line lifetimes were measured on at least two independent experimental days. No statistically significant differences between days were found.

Membrane Preparation for ATPase Assays

Cells were grown to 70% confluency on 15 cm dishes and treated with 10 µM PDMP for either 12h or 3d. Cells were washed, scraped and homogenised through a 23 Gauge needle in buffer (0.25 M sucrose, 20 mM Hepes-KOH, 1 mM EDTA, pH 7.4 with protease inhibitors (1 µg/ml aprotinin, 1 µg/ml leupeptin, 1 µg/ml pepstatin, 5 µg/ml antipain, 1 mM benzamidine)). Debris and whole cells were removed with a 1,000 x g spin for 5 min at 4°C. Total membranes were isolated from the post-nuclear supernatant (PNS) using 20,000 x g for 30 min at 4°C. The pellet was taken up in 150 µl buffer (20 mM Hepes-KOH, 150 mM K^+-glutamic acid, 5 mM $MgSO_4$, pH 7.4 with protease inhibitors) and protein content was determined with Amidoblack using BSA as a standard (Schaffner & Weissmann, 1973). The samples were diluted to 0.1 µg/µl.

ATPase assay

The method used has been described in Wieczorek et al. (1990) and Huss et al. (2002). Briefly, V-ATPase activity was determined of 4 µg total protein in 20 mM Hepes-KOH pH 7.4, 60 mM K^+-glutamic acid, 2 mM $MgCl^2$, 6.25% DMSO, 2 mM NaN3 and 0.1 mM vanadate (final concentrations). Addition of 1 mM ATP started the reaction, the sample was incubated for 15 min at 37°C and frozen in liquid N_2 to stop the reaction. The amount of inorganic phosphate (P_i) generated was determined using the malachite green-molybdate-phosphate complex. For the phosphate determination, protein was first precipitated with 5% trichloroacidic acid (TCA) and centrifuged 20,000 x g for 1 min. Approximately one third of supernatant was mixed with 24% H_2SO_4:200 mM Na-molybdate:H_2O (1:3:6 v/v) to final concentrations of 1.5% H_2SO_4 and 37.5 mM Na-molybdate. Then, 1% polyvinyl alcohol with 0.074% malachite green was added and finally 7.8% H_2SO_4. Final concentrations were 4.6% H_2SO_4, 15 mM Na-molybdate, 0.08 % polyvinyl alcohol and 0.006% malachite green. The absorbance was read after 90 min at 625 nm and quantified with a calibration curve of NaH_2PO_4. The ATPase activity was determined in the absence and presence of 200 nM concanamycin A (ConcA) and 10 µM of the protonophore carbonyl cyanide m-chlorophenylhydrazone (CCCP). The V-ATPase activity is defined as the difference in activity in the absence and presence of concanamyin A. The activity was expressed in nmol P_i per mg protein per min.

SDS-PAGE and western blotting

Aliqouts of the total membrane preparations were mixed with 2x SDS sample buffer (200 mM Tris-HCl pH 6.8, 3% (w/v) SDS, 12% (v/v) glycerol, 1 mM EDTA, 0.003% (w/v) bromophenol blue, 1% 2-mercaptoethanol, final concentrations) and boiled for 30 sec at 95°C and subsequently put on ice. Samples were separated by SDS-PAGE on 17% minigels. For western blotting, polyvinylidene fluoride (PVDF) transfers were blocked for 1h with 2% hen egg albumin, 0.01% (w/v) Tween in PBS. Detection was with HRP-conjugated secondary antibodies and enhanced chemiluminescence (Amersham, Rosendaal, The Netherlands).

References

Ancans J, Tobin DJ, Hoogduijn MJ, Smit NP, Wakamatsu K, Thody AJ. Melanosomal pH controls rate of melanogenesis, eumelanin/phaeomelanin ratio and melanosome maturation in melanocytes and melanoma cells. *Exp Cell Res* 2001;268:26-35.

Bhatnagar V, Anjaiah S, Puri N, Darshanam BN, Ramaiah A. pH of melanosomes of B 16 murine melanoma is acidic: its physiological importance in the regulation of melanin biosynthesis. *Arch Biochem Biophys* 1993;307:183-92.

Bligh EG, Dyer WJ. A rapid method of total lipid extraction and purification. *Can J Biochem Physiol* 1959;37:911-7.

Brückner J. Estimation of monosaccharides by the orcinol-sulphuric acid reaction. *Biochem J* 1955;60:200-5.

Coste H, Martel MB, Got R. Topology of glucosylceramide synthesis in Golgi membranes from porcine submaxillary glands. *Biochim Biophys Acta* 1986;858:6-12.

David P, Baron R. The catalytic cycle of the vacuolar H(+)-ATPase. Comparison of proton transport in kidney- and osteoclast-derived vesicles. *J Biol Chem* 1994;269:30158-63.

de Grauw CJ, Gerritsen H. Multiple time-gate module for fluorescence lifetime imaging. *Applied Spectroscopy* 2001:670-8.tant deficient in glycolipids.

Demaurex N, Furuya W, D'Souza S, Bonifacino JS, Grinstein S. Mechanism of acidification of the trans-Golgi network (TGN). In situ measurements of pH using retrieval of TGN38 and furin from the cell surface. *J Biol Chem* 1998;273:2044-51.

Dermine JF, Duclos S, Garin J, et al. Flotillin-1-enriched lipid raft domains accumulate on maturing phagosomes. *J Biol Chem* 2001;276:18507-12.

Dröse S, Bindseil KU, Bowman EJ, Siebers A, Zeeck A, Altendorf K. Inhibitory effect of modified bafilomycins and concanamycins on P- and V-type adenosinetriphosphatases. *Biochemistry* 1993;32:3902-6.

Durham-Pierre D, Gardner JM, Nakatsu Y, et al. African origin of an intragenic deletion of the human P gene in tyrosinase positive oculocutaneous albinism. *Nat Genet* 1994;7:176-9.

Futerman AH, Hannun YA. The complex life of simple sphingolipids. *EMBO Rep* 2004;5:777-82.
Futerman AH, Pagano RE. Determination of the intracellular sites and topology of glucosylceramide synthesis in rat liver. *Biochem J* 1991;280 (Pt 2):295-302.

Gkantiragas I, Brugger B, Stuven E, et al. Sphingomyelin-enriched microdomains at the Golgi complex. *Mol Biol Cell* 2001;12:1819-33.

Grabe M, Oster G. Regulation of organelle acidity. *J Gen Physiol* 2001;117:329-44.

Groux-Degroote S, van Dijk SM, Wolthoorn J, et al. Glycolipid-dependent sorting of melanosomal from lysosomal membrane proteins by lumenal determinants. *Traffic* 2008;9:951-63.

Hakomori S. Inaugural Article: The glycosynapse. *Proc Natl Acad Sci U S A* 2002;99:225-32.

Hakomori S. Carbohydrate-to-carbohydrate interaction, through glycosynapse, as a basis of cell recognition and membrane organization. *Glycoconj J* 2004;21:125-37.

Higuchi K, Kawashima M, Ichikawa Y, Imokawa G. Sphingosylphosphorylcholine is a melanogenic stimulator for human melanocytes. *Pigment Cell Res* 2003;16:670-8.

Hillig I, Leipelt M, Ott C, Zahringer U, Warnecke D, Heinz E. Formation of glucosylceramide and sterol glucoside by a UDP-glucose-dependent glucosylceramide synthase from cotton expressed in Pichia pastoris. *FEBS Lett* 2003;553:365-9.

Hollams EM, Giles KM, Thomson AM, Leedman PJ. mRNA stability and the control of gene expression: implications for human disease. *Neurochem Res* 2002;27:957-80.

Huss M, Ingenhorst G, König S, et al. Concanamycin A, the specific inhibitor of V-ATPases, binds to the V(o) subunit c. *J Biol Chem* 2002;277:40544-8.

Ichikawa S, Nakajo N, Sakiyama H, Hirabayashi Y. A mouse B16 melanoma mutant deficient in glycolipids. *Proc Natl Acad Sci U S A* 1994;91:2703-7.

Ichikawa S, Sakiyama H, Suzuki G, Hidari KI, Hirabayashi Y. Expression cloning of a cDNA for human ceramide glucosyltransferase that catalyzes the first glycosylation step of glycosphingolipid synthesis. *Proc Natl Acad Sci U S A* 1996;93:4638-43.

Janowski BA, Willy PJ, Devi TR, Falck JR, Mangelsdorf DJ. An oxysterol signalling pathway mediated by the nuclear receptor LXR alpha. *Nature* 1996;383:728-31.

Jeckel D, Karrenbauer A, Burger KN, van Meer G, Wieland F. Glucosylceramide is synthesized at the cytosolic surface of various Golgi subfractions. *J Cell Biol* 1992;117:259-67.

Kohyama-Koganeya A, Sasamura T, Oshima E, et al. Drosophila glucosylceramide synthase: a negative regulator of cell death mediated by proapoptotic factors. *J Biol Chem* 2004;279:35995-6002.

Kumar R, Parsad D, Kaul D, Kanwar A. Liver X receptor expression in human melanocytes, does it have a role in the pathogenesis of vitiligo? *Exp Dermatol* 2010;19:62-4.

Kunimoto S, Murofushi W, Kai H, et al. Steryl glucoside is a lipid mediator in stress-responsive signal transduction. *Cell Struct Funct* 2002;27:157-62.

Kunimoto S, Kobayashi T, Kobayashi S, Murakami-Murofushi K. Expression of cholesteryl glucoside by heat shock in human fibroblasts. *Cell Stress Chaperones* 2000;5:3-7.

Lazar MA, Willson TM. Sweet dreams for LXR. *Cell Metab* 2007;5:159-61.

Lee L, Abe A, Shayman JA. Improved inhibitors of glucosylceramide synthase. *J Biol Chem* 1999;274:14662-9.

Lee ST, Nicholls RD, Bundey S, Laxova R, Musarella M, Spritz RA. Mutations of the P gene in oculocutaneous albinism, ocular albinism, and Prader-Willi syndrome plus albinism. *N Engl J Med* 1994;330:529-34.

Lin HJ, Herman P, Lakowicz JR. Fluorescence lifetime-resolved pH imaging of living cells. *Cytometry A* 2003;52:77-89.

Ma HJ, Yue XZ, Wang DG, Li CR, Zhu WY. A modified method for purifying amelanotic melanocytes from human hair follicles. *J Dermatol* 2006;33:239-48.

Michalik L, Wahli W. Peroxisome proliferator-activated receptors (PPARs) in skin health, repair and disease. *Biochim Biophys Acta* 2007;1771:991-8.

Mitchell P. Coupling of phosphorylation to electron and hydrogen transfer by a chemi-

osmotic type of mechanism. *Nature* 1961;191:144-8.

Mitro N, Mak PA, Vargas L, et al. The nuclear receptor LXR is a glucose sensor. *Nature* 2007;445:219-23.

Ni-Komatsu L, Orlow SJ. Heterologous expression of tyrosinase recapitulates the misprocessing and mistrafficking in oculocutaneous albinism type 2: effects of altering intracellular pH and pink-eyed dilution gene expression. *Exp Eye Res* 2006;82:519-28.

Peet DJ, Turley SD, Ma W, et al. Cholesterol and bile acid metabolism are impaired in mice lacking the nuclear oxysterol receptor LXR alpha. *Cell* 1998;93:693-704.

Puri N, Gardner JM, Brilliant MH. Aberrant pH of melanosomes in pink-eyed dilution (p) mutant melanocytes. *J Invest Dermatol* 2000;115:607-13.

Ramsay M, Colman MA, Stevens G, et al. The tyrosinase-positive oculocutaneous albinism locus maps to chromosome 15q11.2-q12. *Am J Hum Genet* 1992;51:879-84.

Raposo G, Marks MS. Melanosomes--dark organelles enlighten endosomal membrane transport. *Nat Rev Mol Cell Biol* 2007;8:786-97.

Rinchik EM, Bultman SJ, Horsthemke B, et al. A gene for the mouse pink-eyed dilution locus and for human type II oculocutaneous albinism. *Nature* 1993;361:72-6.

Rodgers MAJ. Picosecond fluorescence studies of Rose Bengal in aqueous micellar dispersions. *Chem Phys Lett* 1981;78:509-14.

Rosemblat S, Sviderskaya EV, Easty DJ, et al. Melanosomal defects in melanocytes from mice lacking expression of the pink-eyed dilution gene: correction by culture in the presence of excess tyrosine. *Exp Cell Res* 1998;239:344-52.

Rouser G, Fkeischer S, Yamamoto A. Two dimensional then layer chromatographic separation of polar lipids and determination of phospholipids by phosphorus analysis of spots. *Lipids* 1970;5:494-6.

Saha B, Singh SK, Mallick S, et al. Sphingolipid-mediated restoration of Mitf expression and repigmentation in vivo in a mouse model of hair graying. *Pigment Cell Melanoma Res* 2009;22:205-18.

Sanders R, Draaijer A, Gerritsen HC, Houpt PM, Levine YK. Quantitative pH imaging in cells using confocal fluorescence lifetime imaging microscopy. *Anal Biochem* 1995;227:302-8.

Sato K, Toriyama M. Effect of pyrroloquinoline quinone (PQQ) on melanogenic protein expression in murine B16 melanoma. *J Dermatol Sci* 2009;53:140-5.

Schaffner W, Weissmann C. A rapid, sensitive, and specific method for the determination of protein in dilute solution. *Anal Biochem* 1973;56:502-14.

Schultz JR, Tu H, Luk A, et al. Role of LXRs in control of lipogenesis. *Genes Dev* 2000;14:2831-8.

Sharma DK, Choudhury A, Singh RD, Wheatley CL, Marks DL, Pagano RE. Glycosphingolipids internalized via caveolar-related endocytosis rapidly merge with the clathrin pathway in early endosomes and form microdomains for recycling. *J Biol Chem* 2003;278:7564-72.

Simons K, van Meer G. Lipid sorting in epithelial cells. *Biochemistry* 1988;27:6197-202.

Sitaram A, Piccirillo R, Palmisano I, et al. Localization to mature melanosomes by virtue of cytoplasmic dileucine motifs is required for human OCA2 function. *MolBiol Cell* 2009;20:1464-77.

Skulachev VP, Sharaf AA, Liberman EA. Proton conductors in the respiratory chain and artificial membranes. *Nature* 1967;216:718-9.

Sprong H, Degroote S, Claessens T, et al. Glycosphingolipids are required for sorting melanosomal proteins in the Golgi complex. *J Cell Biol* 2001;155:369-80.

Staleva L, Manga P, Orlow SJ. Pink-eyed dilution protein modulates arsenic sensitivity and intracellular glutathione metabolism. *Mol Biol Cell* 2002;13:4206-20.

Steen H, Maring JG, Meijer DK. Differential effects of metabolic inhibitors on cellular and mitochondrial uptake of organic cations in rat liver. *Biochem Pharmacol* 1993;45:809-18.

Sviderskaya EV, Bennett DC, Ho L, Bailin T, Lee ST, Spritz RA. Complementation of hypopigmentation in p-mutant (pink-eyed dilution) mouse melanocytes by normal human P cDNA, and defective complementation by OCA2 mutant sequences. *J Invest Dermatol* 1997;108:30-4.

Thomas JA, Buchsbaum RN, Zimniak A, Racker E. Intracellular pH measurements in Ehrlich ascites tumor cells utilizing spectroscopic probes generated in situ. *Biochemistry* 1979;18:2210-8.

Valiyaveetil FI, Zhou Y, MacKinnon R. Lipids in the structure, folding, and function of the KcsA K^+ channel. *Biochemistry* 2002;41:10771-7.

Van Meer G. Lipid traffic in animal cells. *Annu Rev Cell Biol* 1989;5:247-75.

Weisz OA. Acidification and protein traffic. *Int Rev Cytol* 2003;226:259-319.

Wieczorek H, Cioffi M, Klein U, Harvey WR, Schweikl H, Wolfersberger MG. Isolation of goblet cell apical membrane from tobacco hornworm midgut and purification of its vacuolar-type ATPase. *Methods Enzymol* 1990;192:608-16.

Woo JT, Shinohara C, Sakai K, Hasumi K, Endo A. Isolation, characterization and biological activities of concanamycins as inhibitors of lysosomal acidification. *J Antibiot (Tokyo)* 1992;45:1108-16.

Yamaguchi M, Kasamo K. Modulation in the activity of purified tonoplast H^+-ATPase by tonoplast glycolipids prepared from cultured rice (Oryza sativa L. var. Boro) cells. *Plant Cell Physiol* 2001;42:516-23.

Yamashita T, Wada R, Sasaki T, et al. A vital role for glycosphingolipid synthesis during development and differentiation. *Proc Natl Acad Sci U S A* 1999;96:9142-7.

Yoshinaka K, Kumanogoh H, Nakamura S, Maekawa S. Identification of V-ATPase as a major component in the raft fraction prepared from the synaptic plasma membrane and the synaptic vesicle of rat brain. *Neurosci Lett* 2004;363:168-72.

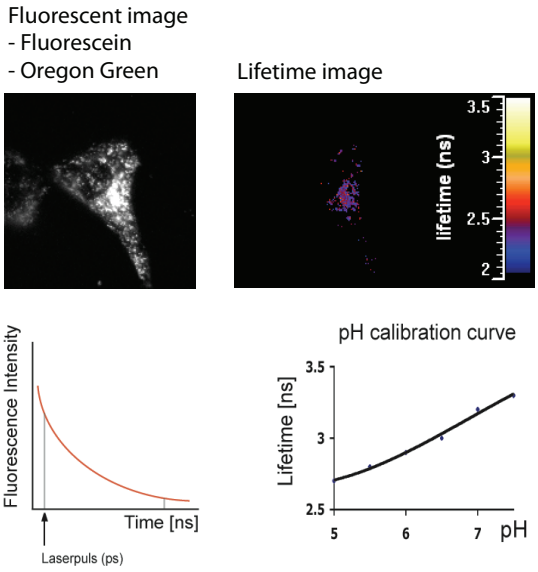

Supplemental Figure S1. Fluorescence lifetime imaging microscopy (FLIM) to measure pH. An intensity threshold was applied to a fluorescent, confocal image (160×160 pixels) of a cell (left) to select the pixels with the highest intensity. The intensity cut-off was set at the point where the fluorescence resembled a punctate signal for lysosomes. For each of these pixels a fluorescence decay curve (bottom left) was measured and the average fluorescence lifetime was calculated. The values are depicted in a false-color lifetime image (right). In this case, MEB4 cells had taken up OG-anti-LAMP-1 for 5 h at 37˚C. The pH could be determined by a calibration curve giving a relation between pH and lifetime values.

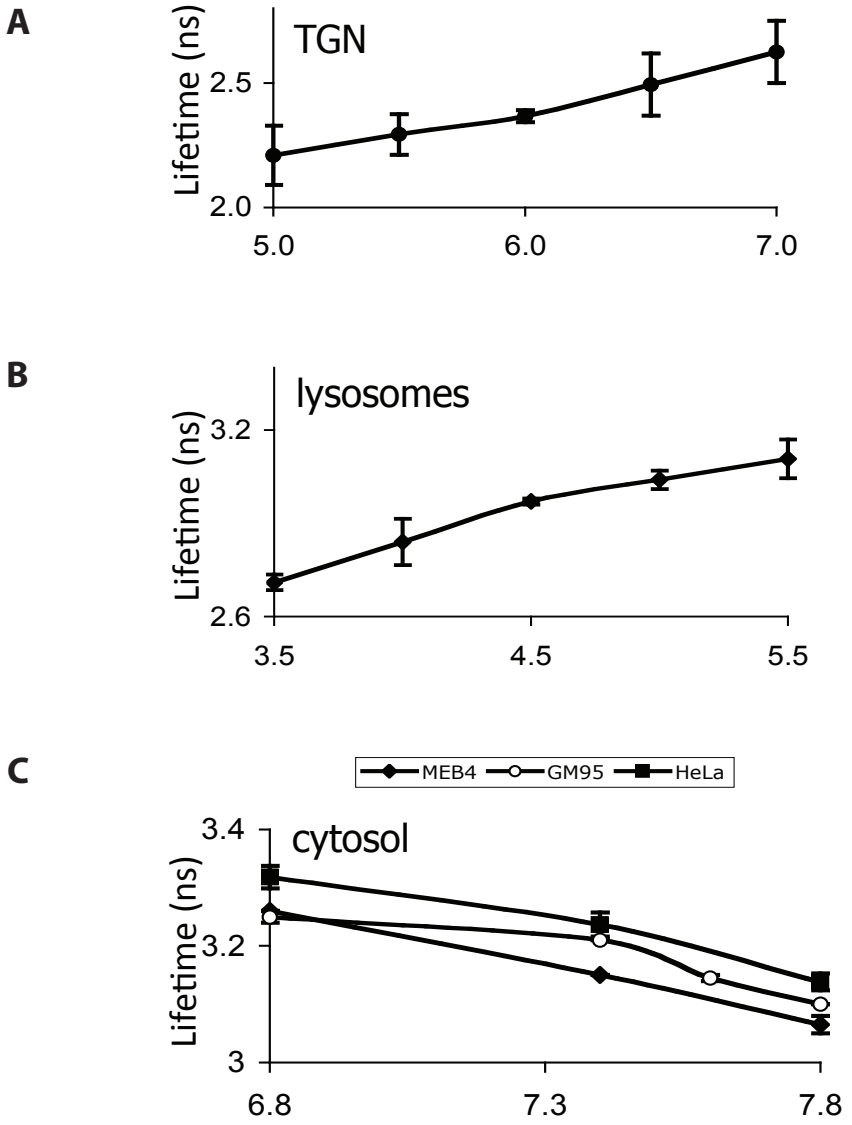

Supplemental Figure S2. Calibration curves of probes in TGN, lysosomes and cytosol using FLIM. (A) pH calibration of anti-CD25-FITC in MEB4 cells using FLIM in the TGN. Calibration measurements on cells were carried out after 10 min incubation in the presence of nigericin (13 μM) in 150 mM K^+ buffers varying in pH between 5.0 and 7.0 at 37°C. Curves measured in MEB4, GM95 and HeLa cells were overlapping (not shown). (B) pH calibration of OG-anti-LAMP-1 in MEB4 cells using FLIM in lysosomes. Calibration curves measured in MEB4, GM95 and MF cells were overlapping (not shown). (C) pH calibration of SNAFL in MEB4, GM95 and HeLa cells in the cytosol. The lines between the data points are intended 'to guide the eye'. For calculations a polynomial fit, degree =2 was used.

Chapter 3

The mammalian vacuolar-type H^+-translocating ATPase is influenced by glycosphingolipids

Seléne van der Poel[1], Jasja Wolthoorn[2], Joep van den Dikkenberg[1], Matthijs Kol[1], Sophie Groux-Degroote[3], Hein Sprong[4] and Gerrit van Meer[1]

[1] Membrane Enzymology, Bijvoet Center and Institute of Membranes, Utrecht University, Utrecht, The Netherlands

[2] Present address: TNO Quality of Life, Zeist, The Netherlands

[3] Present address: Unité de Glycobiologie Structurale et Functionelle, Université des Sciences et Technologies de Lille, France

[4] Present address: National Institute of Public Health and Environment (RIVM), Bilthoven, The Netherlands

Abstract

The V-ATPase is essential and evolutionary conserved in eukaryotes, which also applies to glycosphingolipids. As we had found a less acidic pH in organelles of the glycosphingolipid-deficient cell line GM95, we investigated the activity of the V-ATPase in this cell line compared to the wild-type cell line MEB4. The activity of the V-ATPase was two-fold lower in the GM95 cells and this difference was independent of the proton gradient or membrane potential built up by the proton pump. The apparent K_i of the inhibitors of the V-ATPase, concanamycin A and archazolid A, was higher in the presence of glycosphingolipids. Glycosphingolipids compete with concanamycin A and archazolid A for binding, while inhibitors that bind to other regions of the proton pump, apicularen A and salicylihalamide A, were unaffected by glycosphingolipids. Although the effect of glycosphingolipids on the inhibition of concanamycin A and archazolid A suggests a physical binding of glycosphingolipids to the proton pump, other evidence is lacking. Exogenous addition of glucosylceramide and retransfection of GCS in GM95 cells did not restore V-ATPase activity. Whether there is a direct interaction or an indirect effect on pH, possibly through the melanocytic protein Oca2, remains to be determined.

Introduction

The proton pump, vacuolar-type H^+-ATPase (V-ATPase), is essential for eukaryotic life and maintains an acidic pH in the lumen of a number of cellular organelles (reviewed by Forgac, 2007). Proton pumps are generally found in the Golgi and along the endosomal/lysosomal pathway to acidify the lumen, which serves for example proteolytic cleavage, and the aggregation and sorting of regulated secretory proteins (Tooze et al., 2001; Taupenot et al., 2005). See Figure 1A for a model of the yeast V-ATPase.

The lumenal pH is a carefully regulated parameter. A variety of factors play a role in maintaining the pH and they are part of an intricate system, which is not well understood. Grabe and Oster (2001) devised a model for the effects of different elements in order to further our understanding. The V-ATPase, passive proton leak and ion channels play a role in most organelles to maintain pH. The V-ATPase pumps proton into the lumen and is inhibited by both the proton gradient and membrane potential, which are built up by the enzyme itself (Mitchell, 1961). The passive proton leak counterbalances the build-up of protons. An influx of anions into the lumen balances the charge of protons, thereby counteracting a build-up of an inhibiting electrochemical gradient. As a result, the V-ATPase is able to generate a higher proton concentration and thereby further acidify the lumen.

Previously we found that organelle pH and the transcription of the putative anion channel Oca2 in melanocytes were dependent on glycosphingolipids (Chapter 2). The activity of the V-ATPase was found to be lower in mutant glycosphingolipid-deficient GM95 cells compared to wild-type MEB4 cells (Chapter 2). The lack of an anion channel in the glycosphingolipid-deficient cell line can cause the loss of V-ATPase activity under inhibited conditions. However, the difference in activity was independent of the proton gradient and membrane potential as was established using the protonophore carbonyl cyanide m-chlorophenylhydrazone (CCCP). The protonophore can freely pass the membrane in both its protonated and deprotonated form. It thereby equilibrates the protons and abolishes the proton gradient and the membrane potential built up by the V-ATPase (Skulachev et al., 1967; Steen et al., 1993). Here we addressed the difference in V-ATPase activity between MEB4 and GM95 membranes. We found indications that the glycosphingolipids bind directly to the V-ATPase, however exogenous addition of glucosylceramide did not affect V-ATPase activity.

Results

ATPase activity of the V-ATPase is cell line dependent

The ATP hydrolytic activity of the V-ATPase was determined in total membrane preparations from wild-type melanoma cells MEB4 and the mutant glycosphingolipid-deficient GM95 cells with a colorimetric assay of released inorganic P_i. The V-ATPase activity is defined as the difference in activity in the absence and presence of the specific inhibitor of the V-ATPase, concanamycin A (Woo et al., 1992; Dröse et al., 1993). The background activity of mitochondrial and transport ATPases was decreased by the addition of NaN_3 and vanadate. The total ATPase activity and the activity inhibitable by concanamycin A, NaN_3 and vanadate were determined for total membranes from MEB4 cells (Supplemental Figure S1A).

The V-ATPase in total membranes from the glycosphingolipid-deficient GM95 cells was two-fold lower than that of wild-type MEB4 cells (Figure 1B). The presence of the protonophore CCCP increased the V-ATPase activity three-fold for both cell lines while the difference in V-ATPase activity was maintained. Therefore, the difference in V-ATPase activity in GM95 and MEB4 membranes was independent of the proton gradient and membrane potential while expression levels of subunit B in the cytosolic domain V_1 of the V-ATPase and the transmembrane protein p23, used as a loading control, were similar on western blot (Figure 1C). This shows that the 50% reduction in V-ATPase activity was not due to a decrease in V-ATPase copies.

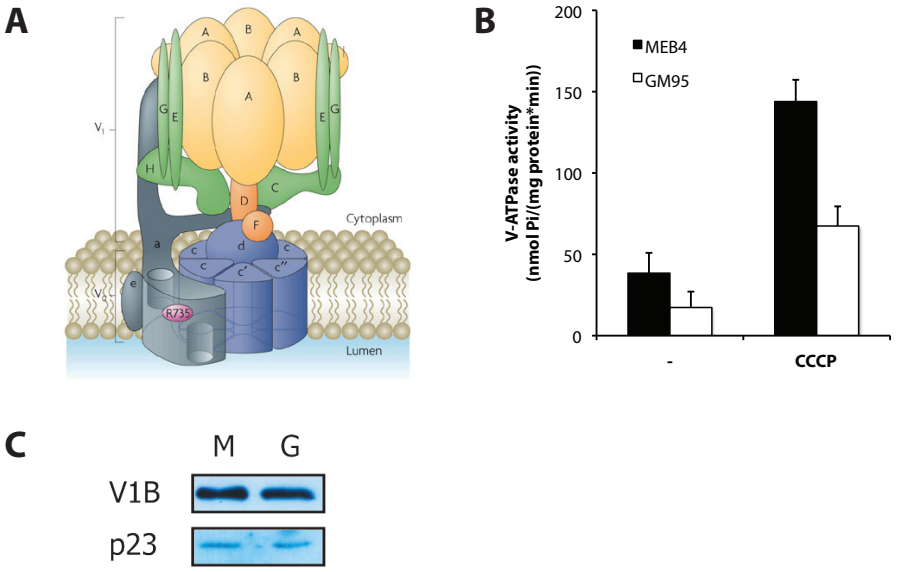

Figure 1. Reduced V-ATPase activity in membranes without glycosphingolipids. (A) A model of the yeast V-ATPase. Subunits in the cytosolic domain V_1 and transmembrane domain V_o are indicated with capital and small letters respectively. The V_1 and V_o domains can separate as part of a regulatory mechanism. Yeast have c" whereas higher eukaryotes have the accessory subunit Ac45 while both have a rotor ring consisting of 6 c-subunits in total (Supek et al., 1994). R735 is an arginine residue important for proton translocation. Picture is from Forgac et al. (2007). (B) V-ATPase activity is reduced in GM95 cells, independent of the proton gradient and membrane potential. Membranes were assayed according to protocol (i) as described in Materials and Methods. The V-ATPase activity is defined as the difference in activity in the absence and presence of 200 nM concanamycin A: the concanamycin-sensitive ATPase activity. The V-ATPase activity is expressed in nmol P_i per mg total protein per min. The maximal, uninhibited V-ATPase activity was determined in the presence of 10 µM of the protonophore CCCP. The average activity is shown of 4 independent experiments in duplicate. (C) Samples were analysed for expression of the B-subunit of the V-ATPase (the cytosolic V_1 domain) and the transmembrane protein p23 as a loading control by western blot.

V-ATPase activity is regulated by the proton gradient and membrane potential

Proton pumping builds up a proton gradient, thereby generating a membrane potential. In order to dissect the influence of both elements on the V-ATPase activity, assays were performed in the presence of the H^+/K^+ exchanger nigericin. By replacing the H^+ with K^+, the proton gradient is abolished while the electrochemical gradient should be unaffected (Pressman, 1976; Reed, 1979).

Removal of the proton gradient alone greatly increased the activity, up to two-thirds of the activity in the presence of CCCP, which abolishes both the proton

gradient and the membrane potential by equilibrating protons over the membrane (Figure 2). The V-ATPase activity was inhibited by both the proton gradient and the membrane potential. However, the influence of the membrane potential was not determined separately.

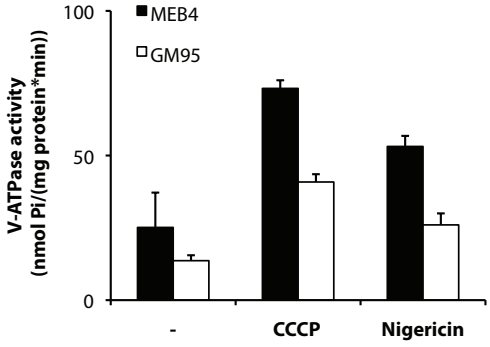

Figure 2. V-ATPase activity is inhibited by the proton gradient and membrane potential. Membranes were isolated and the V-ATPase activity was determined according to protocol (i) as described in the Materials and Methods. The activity assay was performed in the presence of either 10 µM CCCP or 10 µM nigericin (K^+/H^+ exchanger). At least two independent experiments were done in triplicate. A representative experiment is shown.

The apparent K_i of concanamycin A is cell type dependent

Glycosphingolipids increased the ATP hydrolysis rate of the V-ATPase at steady state (Figures 1 and 2), which takes place between subunits A and B in the cytosolic domain V_1. We tested whether these lipids, via an allosteric mechanism, increased ATP binding to the V-ATPase by varying the ATP concentration and calculating the concentration at which half of the maximum ATPase activity was achieved (K_m). The K_m for ATP was similar for both the wild-type cell line MEB4 and mutant GM95 cells (Figure 3).

Concanamycin A binds to the rotor ring of c- subunits in the transmembrane domain V_o (Bowman et al., 2004; Whyteside et al., 2005). Different concentrations of concanamycin A were used in the activity assay to calculate the inhibition constant (K_i) of the drug. The apparent K_i for concanamycin A in MEB4 membranes was much higher (13.6 nM) than in GM95 membranes (3.7 nM) (Figure 4). This implies that in GM95-derived membranes, the V-ATPase is three-fold more sensitive to the drug than in the wild-type MEB4 strain. This suggests that glycosphingolipids bind to the ring of c-subunits and either (i) compete with the inhibitor for the same binding site or (ii) change the binding site of concanamycin A by either an allosteric effect mechanism or by changing the lipid environment.

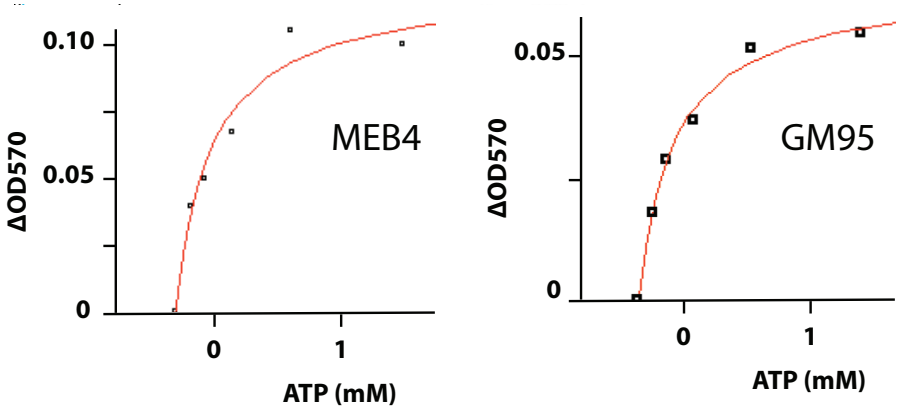

	MEB4	GM95
ΔOD570	0.10 ±0.03	0.05 ±0.01
Apparent K_i (nM)	0.33 ±0.14	0.33 ±0.06

Figure 3. The affinity of the V-ATPase for ATP is independent of glycosphingolipids. Membranes were isolated and the V-ATPase activity assay was performed according to protocol (ii) in Materials and Methods in the presence of 0; 0.1; 0.25; 0.5; 1 or 2 mM ATP. The concanamycin A (ConcA)-sensitive (V-ATPase) activity was determined for each ATP concentration, and the difference in optical density at 570 nm (ΔOD570) in the absence and presence of ConcA, was plotted for MEB4 and GM95. Absolute OD values were -ConcA: 0.59 ±0.024 and +ConcA: 0.49 ±0.02 for MEB4 and -ConcA: 0.40 ±0.01 and +ConcA: 0.35 ±0.0 for GM95. All datapoints were fitted onto the relation for first order kinetics ($V=(V_{max}*S)/(K_m+S)$) and used to calculate the K_m for ATP.

Differences in membrane composition between MEB4 and GM95 cells can influence the partitioning of concanamycin A into the membrane, thereby changing the concentration of concanamycin A available for inhibition and the apparent K_i. In order to test whether MEB4 membranes scavenge a significant fraction of the available concanamycin A, liposomes were made of lipids extracted from MEB4 and GM95 cells and added to isolated total membranes from GM95 cells. Addition of these liposomes to GM95 membranes during the activity assay did not affect the apparent K_i of concanamycin A (3.3 nM and 3.1 nM respectively) (Figure 4B).

In order to test whether the effect of glycosphingolipids on the apparent K_i was specific for concanamycin A, a set of inhibitors was tested with different binding sites, summarised in Table I. Two other inhibitors of the V-ATPase that bind to the transmembrane domain, archazolid A and apicularen A, were investigated. It has been shown that archazolid A (partly) shares the binding site of concanamycin A (Huss et

al., 2005). The apparent K_i of archazolid A was higher in MEB4 membranes (26.3 nM) than in GM95 membranes (8.4 nM), comparable to concanamycin A. The precise binding site of apicularen A has not been identified, but was shown to bind at a different site than concanamycin A and archazolid A (Huss et al., 2005). Recent findings places the binding site between subunits a and c in the transmembrane domain V_o (M. Huss, personal communication). The apparent K_i of apicularen A was similar in membranes from MEB4 cells (0.6 nM) and from GM95 cells (0.8 nM). This suggests that the glycosphingolipids bind the V-ATPase at a specific site.

A

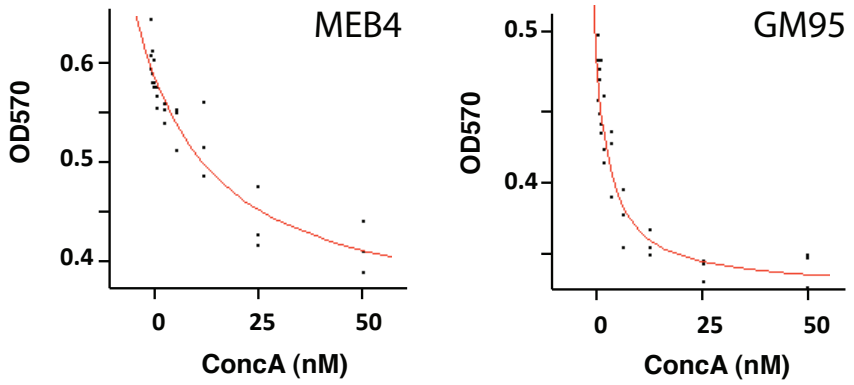

	MEB4	GM95
ΔOD570	0.23 ±0.03	0.17 ±0.02
Apparent K_i (nM)	13.8 ±6.3	3.7 ±1.1

B

	MEB4	GM95	GM95+MEB4$_{lipo}$	GM95+GM95$_{lipo}$
Apparent K_i (nM)	13.8 ±6.3*	3.7 ±1.1*	3.3 ±0.9*	3.1 ±0.8**

Figure 4. The binding site of concanamycin A is altered in the presence of glycosphingolipids. (A) Membranes were isolated and the V-ATPase activity assay was performed according to protocol (ii) in Materials and Methods. The measured OD at 570 nm was plotted for MEB4 (top graph) and GM95 (lower graph). All datapoints were fitted onto the relation for first order kinetics. The maximal ATPase activity, the ConcA-inhibited activity and the apparent K_i were calculated with the first order kinetics relation ($V=(V_{max}*S)/(K_i+S)$). The ΔOD570 is the V-ATPase activity. The table shows the summary of three independent experiments (n=3) while the graphs show a representative experiment. (B) The apparent K_i of concanamyin A was determined in isolated membranes from GM95 in the presence of liposomes derived from MEB4 and GM95 cells as described in Materials and Methods. V-ATPase activity assay was performed according to procedure (ii). *n=3, **n=1.

To find out whether an effect of glycosphingolipids was confined to the transmembrane domain, an inhibitor of the V-ATPase, salicylihalamide A, was investigated that binds the V-ATPase most likely between the transmembrane domain V_o and cytosolic domain V_1 (Huss et al., 2002; Xie et al., 2004). The apparent K_i of salicylhalamide A was slightly higher in GM95 membranes (70.0 nM) compared to MEB4 membranes (56.2 nM), but the difference was not significant (Table I).

Table I. Apparent Ki of different inhibitors. The inhibitors archazolid A (ArcA), apicularen A (ApiA), concanamycin A (ConcA) and salicylihalimide A (SaliA) were tested on membranes isolated from MEB4 and GM95 cells. 'Act.' Is the activity of GM95 membranes expressed in % relative to the activity in MEB4. *n=1, ** n=3

	Activity (%)	MEB4	GM95
ArcA*	96	26.3 ±13.6	8.4 ±2.7
ApiA*	74	0.8 ±0.6	1.2 ±0.6
ConcA**	74	13.6 ±6.3	3.7 ±1.1
SaliA*	56	56.2 ±16.3	70.0 ±13.6

The V-ATPase activity is not restored by addition of glucosylceramide

We investigated whether glucosylceramide (GlcCer), the simplest of the higher glycosphingolipids, influences the V-ATPase directly. Liposomes with increasing amounts of GlcCer were added to the membranes and GlcCer was transferred by means of a GlycoLipid Transfer Protein (GLTP; Mattjus et al., 1999). First, the transfer activity of GLTP was tested using a fluorescent analogue of GlcCer, with a fluorescent pyrene group attached to the acyl chain of GlcCer (pyrGlcCer; Somerharju et al., 1985). Total membranes from GM95 cells were incubated with the liposomes containing traces of pyrGlcCer. The membranes were separated from the liposomes and fluorescence was determined in membranes in the presence of the detergent Triton in order to circumvent fluorescence quenching as described in Materials and Methods. In the absence of GLTP, 5% of the total fluorescence was found in the membrane fraction. The amount of fluorescence found in the membrane fraction relative to total fluorescence, which is defined as transfer activity, was similar for PC/GlcCer of 90/10 and 80/20 mol% (Figure 5A). The transfer activity of GLTP was between 20 and 30%.

Although there was transfer of pyrGlcCer from the liposomes to the membranes by GLTP, addition of liposomes with increasing concentrations of GlcCer did not significantly influence V-ATPase activity in membranes isolated from GM95 cells (Figure 5B).

In order to explore whether the V-ATPase activity is dependent on glycospin-

golipids, GM95 cells were retransfected with the first enzyme in glycosphingolipid synthesis, glucosylceramide synthase (GCS; see also Chapter 2). The V-ATPase activity in isolated membranes from GM95-GCS was not significantly different to the V-ATPase activity found in GM95 cells, while protein levels were similar (data not shown). These results imply that the V-ATPase activity is independent of glycosphingolipids.

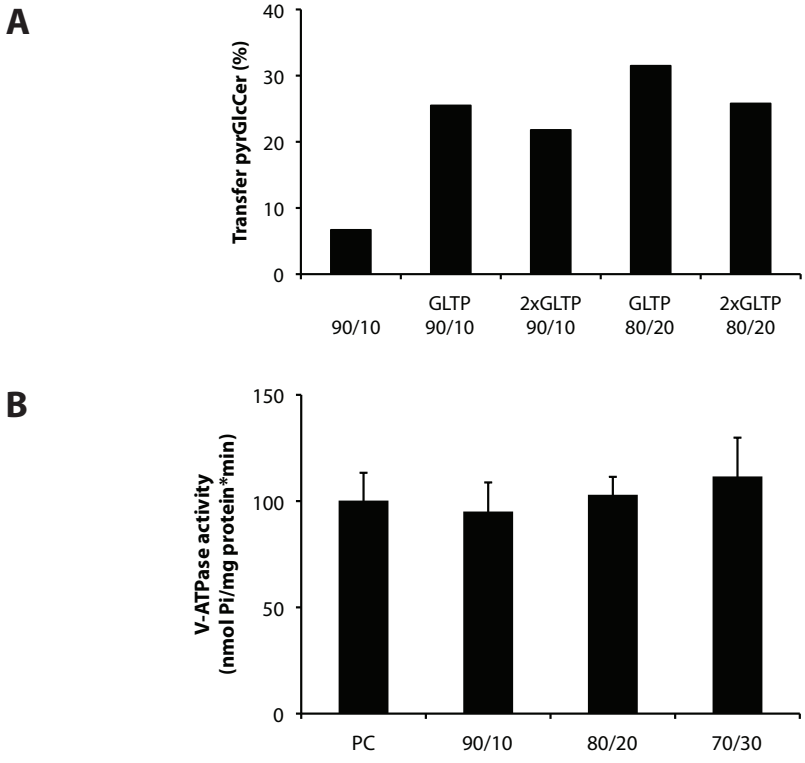

Figure 5. Exogenous GlcCer stimulates the V-ATPase activity in GM95 membranes. (A) Quantitation of the delivery of pyrGlcCer by GLTP to membranes. Total membranes were incubated with PC liposomes, 2 mM total lipid, containing an increasing amount of GlcCer, namely a PC/GlcCer ratio of 90/10 and 80/20 mol%, with 10 and 20 µM pyrene-GlcCer respectively with 4 and 8 µM GLTP (0.13, 0.25 or 0.50 mg/ml). Undelivered pyrGlcCer was removed by centrifugation and the fluorescence was quantified as described. Transfer of pyrGlcCer is expressed as the fluorescence found in the membrane relative to the total fluorescence. (B) GlcCer does not affect V-ATPase activity. Total membranes from GM95 cells were incubated with PC/GlcCer liposomes of 90/10, 80/20 and 70/30 mol% together with 4 µM (0.13 mg/mL) GLTP and analysed for V-ATPase activity according to procedure (i). Controls were incubated with liposomes containing only PC and GLTP. Bars represent the concanamycin A-sensitive ATPase activities expressed in nmol P_i per mg total protein per minute (n=2).

Discussion

We report that the specific activity of the V-ATPase was two-fold higher in total membranes isolated from wild-type MEB4 cells than in membranes from the glycosphingolipid-deficient mutant GM95 cells. The inhibition constant (K_i) of concanamycin A and archazolid A, that both interact with subunit c at a similar binding site in the transmembrane domain V_o, was three-fold higher in wild-type cells. Interestingly, the K_i of apicularen A, that binds subunit c at a different site, was similar for both cell lines. This implies that glycosphingolipids compete with the V-ATPase inhibitors concanamycin A and archazolid A for binding of the V-ATPase. However, exogenous addition of GlcCer to membranes or retransfection of GCS in GM95 cells did not significantly affect the V-ATPase activity.

The V-ATPase activity assays

Variation in absolute activities was observed in the assays, illustrated by Figures 1B and 2. However, the relative difference in V-ATPase activity between MEB4 and GM95 cells was reproducible. Two V-ATPase assays were used because procedure (ii) generally produced larger standard deviations. Procedure (ii) was used for the inhibition studies.

The V-ATPase activity is partially controlled by the proton gradient and by the membrane potential as shown by the effect of the H^+/K^+ exchanger nigericin and the greater effect of CCCP (Figure 2). The notion that a proton motive force (pmf), that is separated in membrane potential ($\Delta\psi$) and proton gradient (ΔpH), delivers the energy needed for ATP synthesis in the case of the mitochondrial F-ATPase, related to the V-ATPase, is the current dogma (Mitchell, 1961). However, Harvey (2009) proposed that the V-ATPase in the midgut of *Manduca sexta* first builds up a membrane potential $\Delta\psi$ and that acidification is restricted by the capacitance. In the latter case, the electrochemical gradient would have a relatively larger impact on the V-ATPase. It has been found that the vacuolar-type H^+-translocating pyrophosphatase (V-PPase) from *Arabidopsis thaliana* and the yeast V-ATPase were not strictly regulated by the proton gradient and that the membrane potential played a role (Hirata et al., 2000). However, the effect of the membrane potential was not dissected in this study.

The results suggest that the activity was largely inhibited by the proton gradient, however as it has been suggested that nigericin also may influence the membrane potential (Achmed and Booth, 1983; Doebler, 2000), this cannot be concluded without determining the contribution of the membrane potential. The data presented here demonstrate that for the mammalian V-ATPase, both the proton gradient and membrane potential play a role in inhibition of V-ATPase activity.

The inhibition studies

The apparent K_i found in this study for the different inhibitors of the V-ATPase were generally higher than reported before (Table I and II), probably due to an overestimation of the active inhibitor concentration because of the chemical instability of the inhibitors (Huss et al., 2002 and 2005; Whyteside et al., 2005). Concanamycin A is a lipophilic compound that preferentially partitions in the membrane (Whyteside et al., 2005). Still, the difference in K_i between MEB4 and GM95 membranes was independent of the presence of bulk lipids, as addition of liposomes from MEB4 and GM95 cells did not influence the K_i, which suggests that the inhibitor was not diluted out by membrane partitioning to a significant extent in the liposomes (Figure 4B). The K_i studies were performed using the V-ATPase assay from procedure (ii) and the assay was performed for 30 min in high KCl buffer. A time course study of the V-ATPase showed that after 30 min, half of the activity was lost but the difference in activity was maintained (Supplemental Figure S1B). It has been shown that high amounts of chloride present in the buffer abolish the membrane potential (Grabe and Oster, 2001) and KCl was replaced by K^+-glutamic acid. The two buffers were compared in Supplemental Figure S1C. The gain of a membrane potential would inhibit the V-ATPase activity in the K^+-glutamic acid buffer. However, the activity was higher in the latter buffer, suggesting there is an unknown additional effect of KCl. Notably, the difference in activity between MEB4 and GM95 was maintained.

Table I shows the inhibitors that were used in this study. The standard deviations in the apparent K_i of apicularen A, salicylhalimide A and archazolid A were substantial. Primarily because the concentrations of inhibitor that were used were higher than the K_i, the inhibition constant could not be determined accurately. In addition, inhibition by archazolid A did not result in a difference in V-ATPase activity between MEB4 and GM95. Since there were variations in absolute activity assays as discussed above, more experiments have to be conducted to conclude that inhibition by archazolid A does not result in a difference in V-ATPase activity. However, the inhibition constant K_i is independent of absolute activity.

Addition of GlcCer

The fact that the apparent K_i of both inhibitors with similar binding sites at the subunit c of the V-ATPase, was dependent on glycosphingolipids (Figure 4), suggests a direct interaction between the glycolipids and the V-ATPase. Addition of glycosphingolipids should then affect the V-ATPase activity. Contrary to our hypothesis, exogenous addition of GlcCer to the membranes did not significantly alter the V-ATPase activity. GlcCer was chosen based on earlier findings that glucosylsphingosine, a precursor of GlcCer, restored pigmentation in GM95 cells (Sprong et al., 2001; Groux-Degroote et al., 2008). However, the effects of higher glycosphingolipids were not explored.

Table II. IC50 values of different inhibitors. The inhibitors archazolid A (ArcA), apicularen A (ApiA), concanamycin A (ConcA), salicylihalimide A (SaliA) were used. [a] Sasse et al., 2003; [b] Huss et al., 2005; [c] Kunze et al., 1998; [d] Xie et al., 2004; [e] Huss et al., 2002. * mdr cell line

Origin	Cell line	ArcA IC50 (nM)	ApiA IC50 (nM)	ConcA IC50 (nM)	SaliA IC50 (nM)
Murine connective tissue	L-929	0.8[a]	4.5[b]	0.2[a]	n.d.
Rat, embryogenic fibroblast cell line	3YI	1.0[b]	3.2[b]	1.4[b]	n.d.
Human cervix carcinoma	KB-VI*	48.0[b]	23.0[b]	28.0[b]	n.d.
Human lung carcinoma	A-594	0.5[b]	0.2[c]	0.2[b]	n.d.
Mouse, embryogenic fibroblast cell line	MI	0.3[b]	1.4[b]	0.6[b]	n.d.
Bovine brain clathrin coated vesicles		n.d.	n.d.	n.d.	<0.1[d]
Manduca sexta V-ATPase in detergent		n.d.	n.d.	n.d.	10[e]

Exogenous addition of glycosphingolipids is experimentally challenging. Since GlcCer is not water-soluble and does not insert into membranes as a monomer, an indirect method had to be used. Although GLTP was shown to have transfer activity (Figure 5A), proper insertion of pyrGlcCer with the total membranes was not assayed. Association is illustrated by the large amount of fluorescent lipid that was found in the membrane fraction without addition of GLTP. Reconstitution of the V-ATPase in a defined lipid environment would circumvent the problems that come with exogenous addition of glycolipids.

The V-ATPase and glycosphingolipids

The retransfection of GCS in GM95 cells also did not restore V-ATPase activity in GM95-derived membranes. The V-ATPase activity may be independent of glycosphingolipids. Previously we noticed that several cellular processes were affected in the glycosphingolipid-deficient cell line GM95. First of all, the cells displayed missorting of tyrosinase, the first rate-limiting enzyme in pigment synthesis (Chapter 2; Sprong et al., 2001). The sorting of the V-ATPase in MEB4 and GM95 was not researched and a different localisation can lead to a shift in the steady state of the enzyme because of a different lumenal pH. However, when the proton gradient and membrane

potential were removed with CCCP, the difference in activity between membranes of MEB4 and GM95 cells was maintained (Figure 1B). Therefore, this cannot explain the difference in activity when no gradients are built up. Another possibility is that the membrane environment is changed by the different localisation. Indeed, the distribution of sphingolipids varies between compartments and there is a gradient of increasing sphingolipids towards the plasma membrane, where sphingolipids are enriched (reviewed by Holthuis and Levine, 2005). The localisation of V-ATPase should be experimentally addressed by for instance immunofluorescence or immuno-electron microscopy. Interestingly, isoforms of subunit a determine the localisation of the V-ATPase, but this is further complicated by the fact that its localisation is not always static (reviewed by Forgac, 2007).

The mutant GM95 cell line was selected using an antibody against α2,3-sialic acid, a component of the GM3 headgroup (Ichikawa et al., 1994). Consequently, it has a glycosylation defect (Supplemental Figure S2), which is only partly restored in GM95-GCS. The selection procedure may also have selected for secondary mutations that directly affect α2-3-sialylation of abundant proteins. Indeed, the glycosylation of the melanocyte-specific protein PMEL17 was affected in GM95 cells and not restored upon GCS transfection (Groux-Degroote et al., 2008). It has been shown that the regulatory subunit Ac45 of the V-ATPase is heavily glycosylated to a protein of about 60 kDa that is subsequently cleaved (Schoonderwoert et al., 2002). When the Ac45 would not be properly glycosylated in GM95 cells, exogenous addition of glycosphingolipids would indeed not restore V-ATPase activity. Interestingly, a heavily glycosylated band of approximately 60 kDa in MEB4 cells was absent in GM95 and did not return in the retransfected GM95-GCS cells (Supplemental Figure S2). We addressed the role of sialylation in the *in vitro* V-ATPase activity in isolated membranes from mutant Chinese Hamster Ovary (CHO) cells that lacked transport of CMP-sialic acid into the Golgi lumen (lec2 cells; Eckhardt et al., 1998). The V-ATPase activity was similar compared to wild-type CHO cells (results not shown). However, these experiments are inconclusive because we have not shown whether Ac45 is expressed in these cells in the first place. Ac45 was initially isolated from chromaffin granules (Supek et al., 1994) and is mostly found in neuroendocrine tissues (Schoonderwoert et al., 2002; Feng et al., 2008). To our knowledge, there is no experimental evidence that other subunits of the mammalian V-ATPase are glycosylated. Interestingly, it has been shown that subunit e in the V_o domain of the *Manduca sexta* V-ATPase has N-linked glycosylations (Merzendorfer et al., 1999).

The V-ATPase activity was not restored by retransfection of GCS, but the lumenal pH in TGN and lysosomes was lowered to the pH found in wild-type MEB4 cells (Chapter 2). The transcription of Oca2 was restored in GM95-GCS and may facilitate the normalisation of lumenal pH in the absence of a fully functional V-ATPase.

Materials and Methods

Materials

Chemicals, unless stated otherwise, were from Sigma-Aldrich (St. Louis, Missouri) and used in the highest purity available. Cell culture media, reagents, antibiotics and fetal bovine serum (FBS "GOLD") were from PAA laboratories (Pasching, Austria). Cell culture plastics were from Costar (Cambridge, MA). All lipids and lipid standards were from Matreya (Pleasant Gap, PA), and were stored as stock solutions in CHCl3/MeOH at -20°C. Phosphatidylcholine (PC) in $CHCl_3$, isolated from egg yolk (Grade I), was from LipidProds (Surrey, England). C10-pyrene-glucosylceramide (pyrGlcCer) was a kind gift from P. Somerharju (University of Helsinki, Finland). Concanamycin A was from Wako Pure Chemical Industries, Ltd. (Osaka).

Cell culture

The glucosylceramide synthase-deficient GM95 and their parental MEB4 cells were from RIKEN Cell Bank (Tsukuba, Japan) and were grown in high glucose Dulbecco's modified Eagle's medium (DMEM) containing 10% FBS at 37°C with 5% CO_2.

Antibodies and lectins

The rabbit polyclonal antibody recognising subunit B of the V-ATPase was a kind gift from M. Forgac (Boston, MA) and the mouse monoclonal anti-p23 (JJ3) antibody was from Abcam (Cambridge, UK). Horseradish peroxidase (HRP)-conjugated secondary goat anti rabbit and mouse IgGs were from Dako (Glostrup, Denmark). Digoxigenin-labeled lectins were from Roche (Nutley, NJ). The lectins were visualised using anti-digoxigenin antibodies (Roche) coupled to alkaline phosphatase followed by diaminobenzidine (DAB) staining.

Membrane preparation for ATPase assays

Cells were grown to 70% confluency on 15 cm dishes for two to three days. Cells were washed, scraped and homogenised through a 23 Gauge needle in buffer (0.25 M sucrose, 20 mM Hepes-KOH, 1 mM EDTA, pH 7.4 with protease inhibitors). Debris and whole cells were removed with a 1,000 x g spin for 5 min at 4°C. Total membranes were isolated from the post-nuclear supernatant (PNS) using 20,000 x g for 30 min at 4°C. The pellet was taken up in 150 µl buffer (20 mM Hepes-KOH, 150 mM K^+-glutamic acid, 5 mM $MgSO_4$, pH 7.4 with protease inhibitors) and protein content was determined with Amidoblack using BSA as a standard (Schaffner and Weissmann, 1973). The samples were diluted to 0.1-0.25 mg/ml total protein.

SDS-PAGE and western blotting

Samples of the total membrane preparations were diluted two times in sample buffer (200 mM Tris-HCl pH 6.8, 3% (w/v) SDS, 12% (v/v) glycerol, 1 mM EDTA, 0.003% (w/v) bromophenol blue, 1% 2-mercaptoethanol, final concentrations) and heated for 30 sec at 95°C and subsequently put on ice.

Samples were separated by SDS-PAGE on 17% minigels. For western blotting, polyvinylidene fluoride (PVDF) transfers were blocked for 1 h with 2% hen egg albumin, 0.01% Tween in PBS. Detection was with HRP-conjugated secondary antibodies and enhanced chemiluminescence (Amersham, Rosendaal, The Netherlands).

ATPase assay

The assay was performed according to one of the following procedures: (i) The method used has been described in Wieczorek et al. (1990) and Huss et al. (2002). Briefly, V-ATPase activity was determined of 4 µg total protein in 20 mM Hepes-KOH pH 7.4, 60 mM K^+-glutamic acid, 2 mM $MgCl_2$, 6.25% DMSO, 2 mM NaN_3 and 0.1 mM vanadate (final concentrations). Addition of 1 mM ATP started the reaction, the sample was incubated for 15 min at 37°C and frozen in liquid N_2 to stop the reaction. The amount of inorganic phosphate (P_i) generated was determined using the malachite green-molybdate-phosphate complex. For the phosphate determination, protein was first precipitated with 5% trichloroacidic acid (TCA) and centrifuged 20,000 x g for 1 min. An aliquot of supernatant (approximately one third) was mixed with 24% H_2SO_4:200 mM Na-molybdate:H_2O (1:3:6 v/v) to final concentrations of 1.5% H_2SO_4 and 37.5 mM Na-molybdate. Then, 1% polyvinyl alcohol with 0.074% malachite green was added and finally 7.8% H_2SO_4. Final concentrations were 4.6% H_2SO_4, 15 mM Na-molybdate, 0.08 % polyvinyl alcohol and 0.006% malachite green. The absorbance was read after 90 min at 625 nm and quantified with a calibration curve of NaH_2PO_4. The ATPase activity was expressed in nmol P_i per mg protein per min. (ii) This protocol was based on David and Baron (1994). V-ATPase activity was determined of 4 µg total protein in 10 mM Hepes-KOH pH 7.4, 75 mM K^+-glutamic acid, 5 mM $MgCl_2$, 2 mM ATP, 2 mM NaN_3 and 0.1 mM vanadate (final concentrations) and incubated at 37°C for 30 min. The reaction was stopped with 35 mM H_2SO_4 (final concentration) on ice. The amount of inorganic phosphate (P_i) generated was determined using the malachite green-molybdate-phosphate complex. Dye solution was added (0.7 M H_2SO_4, 0.03% malachite green and 0.3% ammonium molybdate, final concentrations) and after 20 min the optical density was read at 570 nm. The absorbance of the malachite green-molybdate-phosphate complex at 570 nm was plotted to calculate K_i. The amount of released P_i was quantified with a calibration curve of NaH_2PO_4. Generally, activity measurements were performed in the presence of 5 mM Mg^{2+} and 1-2 mM ATP, concentrations that are 5-fold higher than the respective K_m of the V-ATPase (David & Baron, 1994) and in the presence of 2 mM NaN_3 and 0.1 mM vanadate (final concentrations) to reduce background mitochondrial and transport ATPases. The V-ATPase activity is defined as the difference in activity in the absence and presence of the specific inhibitor concanamycin A, which is the concanamycin A-sensitive activity (Woo et al., 1992; Dröse and Bindseil, 1993). The V-ATPase activity was determined in the absence and presence of 10 µM of the protonophore carbonyl cyanide m-chlorophenylhydrazone (CCCP). For some measurements, nigericin was added (13 µM final concentration) or K^+-glutamic acid was replaced with KCl. In order to determine the K_i, the relation for first order kinetics according to Michaelis-Menten ($V = (V_{max}*S)/(K_i + S)$), was used to fit the datapoints and calculate the absorbance with and without concanamycin A and the apparent K_i.

Addition of MEB4 liposomes to GM95 membranes

Lipids were extracted from MEB4 cells according to Bligh and Dyer (1959). Briefly, cells were washed and scraped in PBS. Lipids were extracted with 3.2 volumes of $CHCl_3$:MeOH (1:2.2 v/v) and occasional vortexing for 30 min at room temperature. Phase separation was achieved with addition of 1 volume 10 mM HAc, 120 mM KCl and 1 volume of $CHCl_3$, vortexing and spinning for 10 min at 3,000 x g. The lower (organic) phase was isolated and dried under a stream of N_2. The waterphase was run over a SepPak C18 cartridge (Waters, Millford, MA) in order to isolate the higher glycosphingolipids. Briefly, the waterphase was run over the column to bind the hydrophobic lipids. The column was washed with water and eluted with MeOH. The eluate was added to the organic phase of the extraction and dried under N_2. Liposomes were formed by hydration of the dried lipids in buffer (20 mM Hepes-KOH, 150 mM KCl, 5 mM $MgCl_2$, pH 7.4), vortexing and sonication to homogenise the suspension. Freeze/thaw cycles with liquid N_2 and a waterbath of 40°C, 10 in total, resulted in larger vesicles. The liposomes were sized passing them 20 times through a 400 nm polycarbonate filter mounted on an Avanti syringe-based extrusion device. An equimolar amount of MEB4 or GM95 liposomes was added to GM95 membranes by phospholipid content as determined according to Rouser et al. (1970).

Quantitation of membrane delivery by GLTP with pyrene-GlcCer

Purification of glycolipid transfer protein (GLTP) was based on West et al. (2004). The protein was eluted in phosphate free buffer and the purity was confirmed by SDS-PAGE analysis. GLTP was concentrated to 1 mg/ml with a protein concentrator (Millipore, Billerica, MA). The transfer activity of GLTP was checked using C10-pyrene-GlcCer (pyrGlcCer) as a donor system (Mattjus et al., 1999). For quantitation of lipid delivery to membranes, total membranes were incubated with PC liposomes, 2 mM total lipid, containing an increasing amount of GlcCer, PC/GlcCer (90/10 mol%) and (80/20 mol%), with trace amounts of pyrGlcCer, namely 10 and 20 µM respectively, for 30 min at 37°C with 4 or 8 µM GLTP (0.125, 0.250 mg/mL). Liposomes were generated by sonication of the lipids in buffer (20 mM Hepes-KOH, 150 mM K^+-glutamic acid, 5 mM $MgCl_2$, pH 7.4). Undelivered pyrGlcCer was separated from the membranes by centrifugation at 20,000 x g for 30 min at 4°C. PyrGlcCer was quantified by measuring fluorescence in the presence of 1% Triton X-100 using a Photon Technology International fluorimeter (λex = 285 nm; λem = 378 nm). The delivery is expressed as the amount of pyrGlcCer found in the membranes as percentage of total pyrGlcCer.

Addition of Glucosylceramide with GLTP

Total membranes from GM95 cells were incubated with PC/GlcCer liposomes (90/10 mol%), (80/20 mol%) and (70/30 mol%) together with 4 µM (0.125 mg/ml) GLTP for 30 min at 37°C, and analysed for V-ATPase activity as described above following procedure (i). Controls were incubated with liposomes containing only PC and GLTP. Bars represent the concanamycin A-sensitive ATPase activities expressed in nmol P_i per mg total protein per minute. Activities were determined in at least three independent experiments and averaged.

References

Ahmed S, Booth IR. The use of valinomycin, nigericin and trichlorocarbanilide in control of the protonmotive force in *Escherichia coli* cells. *Biochem J* 1983;212:105-12.

Bowman BJ, McCall ME, Baertsch R, Bowman EJ. A model for the proteolipid ring and bafilomycin/concanamycin-binding site in the vacuolar ATPase of *Neurospora crassa*. *J Biol Chem* 2006;281:31885-93.

Bowman EJ, Graham LA, Stevens TH, Bowman BJ. The bafilomycin/concanamycin binding site in subunit c of the V-ATPases from *Neurospora crassa* and *Saccharomyces cerevisiae*. *J Biol Chem* 2004;279:33131-8.

Burger KN, van der Bijl P, van Meer G. Topology of sphingolipid galactosyltransferases in ER and Golgi: transbilayer movement of monohexosyl sphingolipids is required for higher glycosphingolipid biosynthesis. *J Cell Biol* 1996;133:15-28.

David P, Baron R. The catalytic cycle of the vacuolar H(+)-ATPase. Comparison of proton transport in kidney- and osteoclast-derived vesicles. *J Biol Chem* 1994;269:30158-63.

Dermine JF, Duclos S, Garin J, et al. Flotillin-1-enriched lipid raft domains accumulate on maturing phagosomes. *J Biol Chem* 2001;276:18507-12.

Doebler JA. Comparative effects of carboxylic ionophores on membrane potential and resistance of NG108-15 cells. *Toxicol In Vitro* 2000;14:235-43.

Dröse S, Bindseil KU, Bowman EJ, Siebers A, Zeeck A, Altendorf K. Inhibitory effect of modified bafilomycins and concanamycins on P- and V-type adenosinetriphosphatases. *Biochemistry* 1993;32:3902-6.

Eckhardt M, Gotza B, Gerardy-Schahn R. Mutants of the CMP-sialic acid transporter causing the Lec2 phenotype. *J Biol Chem* 1998;273:20189-95.

Feng H, Cheng T, Pavlos NJ, et al. Cytoplasmic terminus of vacuolar type proton pump accessory subunit Ac45 is required for proper interaction with V(0) domain subunits and efficient osteoclastic bone resorption. *J Biol Chem* 2008;283:13194-204.

Forgac M. Vacuolar ATPases: rotary proton pumps in physiology and pathophysiology. *Nat Rev Mol Cell Biol* 2007;8:917-29.

Gkantiragas I, Brugger B, Stuven E, et al. Sphingomyelin-enriched microdomains at the Golgi complex. *Mol Biol Cell* 2001;12:1819-33.

Grabe M, Oster G. Regulation of organelle acidity. *J Gen Physiol* 2001;117:329-44.

Halter D, Neumann S, van Dijk SM, et al. Pre- and post-Golgi translocation of glucosylceramide in glycosphingolipid synthesis. *J Cell Biol* 2007;179:101-15.

Harvey WR. Voltage coupling of primary H^+ V-ATPases to secondary Na^+- or K^+-dependent transporters. *J Exp Biol* 2009;212:1620-9.

Hirata T, Nakamura N, Omote H, Wada Y, Futai M. Regulation and reversibility of vacuolar H(+)-ATPase. *J Biol Chem* 2000;275:386-9.

Holthuis JC, Levine TP. Lipid traffic: floppy drives and a superhighway. *Nat Rev Mol Cell Biol*

2005;6:209-20.

Huss M, Ingenhorst G, Konig S, et al. Concanamycin A, the specific inhibitor of V-ATPases, binds to the V(o) subunit c. *J Biol Chem* 2002;277:40544-8.

Huss M, Sasse F, Kunze B, et al. Archazolid and apicularen: novel specific V-ATPase inhibitors. *BMC Biochem* 2005;6:13.

Ichikawa S, Nakajo N, Sakiyama H, Hirabayashi Y. A mouse B16 melanoma mutant deficient in glycolipids. *Proc Natl Acad Sci U S A* 1994;91:2703-7.

Kawasaki-Nishi S, Nishi T, Forgac M. Yeast V-ATPase complexes containing different isoforms of the 100-kDa a-subunit differ in coupling efficiency and *in vivo* dissociation. *J Biol Chem* 2001;276:17941-8.

Lannert H, Bunning C, Jeckel D, Wieland FT. Lactosylceramide is synthesized in the lumen of the Golgi apparatus. *FEBS Lett* 1994;342:91-6.

Mattjus P, Molotkovsky JG, Smaby JM, Brown RE. A fluorescence resonance energy transfer approach for monitoring protein-mediated glycolipid transfer between vesicle membranes. *Anal Biochem* 1999;268:297-304.

Merzendorfer H, Huss M, Schmid R, Harvey WR, Wieczorek H. A novel insect V-ATPase subunit M9.7 is glycosylated extensively. *J Biol Chem* 1999;274:17372-8.

Mitchell P. Coupling of phosphorylation to electron and hydrogen transfer by a chemiosmotic type of mechanism. *Nature* 1961;191:144-8.

Moriyama Y, Nelson N. The vacuolar H^+-ATPase, a proton pump controlled by a slip. *Prog Clin Biol Res* 1988;273:387-94.

Müller M, Irkens-Kiesecker U, Rubinstein B, Taiz L. On the mechanism of hyperacidification in lemon. Comparison of the vacuolar H(+)-ATPase activities of fruits and epicotyls. *J Biol Chem* 1996;271:1916-24.

Nelson N. Evolution of organellar proton-ATPases. *Biochim Biophys Acta* 1992;1100:109-24.

Nelson N, Harvey WR. Vacuolar and plasma membrane proton-adenosinetriphosphatases. *Physiol Rev* 1999;79:361-85.

Nelson N, Perzov N, Cohen A, Hagai K, Padler V, Nelson H. The cellular biology of proton-motive force generation by V-ATPases. *J Exp Biol* 2000;203:89-95.

Pressman BC. Biological applications of ionophores. *Annu Rev Biochem* 1976;45:501-30.

Reed PW. Ionophores. *Methods Enzymol* 1979;55:435-54.

Rouser G, Fkeischer S, Yamamoto A. Two dimensional then layer chromatographic separation of polar lipids and determination of phospholipids by phosphorus analysis of spots. *Lipids* 1970;5:494-6.

Schaffner W, Weissmann C. A rapid, sensitive, and specific method for the determination of protein in dilute solution. *Anal Biochem* 1973;56:502-14.

Schoonderwoert VT, Jansen EJ, Martens GJ. The fate of newly synthesized V-ATPase accessory subunit Ac45 in the secretory pathway. *Eur J Biochem* 2002;269:1844-53.

Skulachev VP, Sharaf AA, Liberman EA. Proton conductors in the respiratory chain and

artificial membranes. *Nature* 1967;216:718-9.

Somerharju PJ, Virtanen JA, Eklund KK, Vainio P, Kinnunen PK. 1-Palmitoyl-2-pyrenedecanoyl glycerophospholipids as membrane probes: evidence for regular distribution in liquid-crystalline phosphatidylcholine bilayers. *Biochemistry* 1985;24:2773-81.

Sprong H, Degroote S, Claessens T, et al. Glycosphingolipids are required for sorting melanosomal proteins in the Golgi complex. *J Cell Biol* 2001;155:369-80.

Steen H, Maring JG, Meijer DK. Differential effects of metabolic inhibitors on cellular and mitochondrial uptake of organic cations in rat liver. *Biochem Pharmacol* 1993;45:809-18.

Supek F, Supekova L, Mandiyan S, Pan YC, Nelson H, Nelson N. A novel accessory subunit for vacuolar H(+)-ATPase from chromaffin granules. *J Biol Chem* 1994;269:24102-6.

Taiz L. The Plant Vacuole. *J Exp Biol* 1992;172:113-22.

Taupenot L, Harper KL, O'Connor DT. Role of H^+-ATPase-mediated acidification in sorting and release of the regulated secretory protein chromogranin A: evidence for a vesiculogenic function. *J Biol Chem* 2005;280:3885-97.

Tooze SA, Martens GJ, Huttner WB. Secretory granule biogenesis: rafting to the SNARE. *Trends Cell Biol* 2001;11:116-22.

Valiyaveetil FI, Zhou Y, MacKinnon R. Lipids in the structure, folding, and function of the KcsA K^+ channel. *Biochemistry* 2002;41:10771-7.

West G, Nymalm Y, Airenne TT, Kidron H, Mattjus P, Salminen TT. Crystallization and X-ray analysis of bovine glycolipid transfer protein. *Acta Crystallogr D Biol Crystallogr* 2004;60:703-5.

Whyteside G, Meek PJ, Ball SK, et al. Concanamycin and indolyl pentadieneamide inhibitors of the vacuolar H^+-ATPase bind with high affinity to the purified proteolipid subunit of the membrane domain. *Biochemistry* 2005;44:15024-31.

Wieczorek H, Cioffi, M., Klein, U., Harvey, W.R., Schweikl, H. & Wolfsberger, MG. Isolation of goblet cell apical membrane from tobacco hornworm midgut and purification of its vacuolar-type ATPase. *Fleischer, S & Fleischer, B eds* 1990:pp. 608-16.

Woo JT, Shinohara C, Sakai K, Hasumi K, Endo A. Isolation, characterization and biological activities of concanamycins as inhibitors of lysosomal acidification. *J Antibiot (Tokyo)* 1992;45:1108-16.

Xie XS, Padron D, Liao X, Wang J, Roth MG, De Brabander JK. Salicylihalamide A inhibits the V0 sector of the V-ATPase through a mechanism distinct from bafilomycin A1. *J Biol Chem* 2004;279:19755-63.

Yamashita T, Wada R, Sasaki T, et al. A vital role for glycosphingolipid synthesis during development and differentiation. *Proc Natl Acad Sci U S A* 1999;96:9142-7.

Yoshinaka K, Kumanogoh H, Nakamura S, Maekawa S. Identification of V-ATPase as a major component in the raft fraction prepared from the synaptic plasma membrane and the synaptic vesicle of rat brain. *Neurosci Lett* 2004;363:168-72.

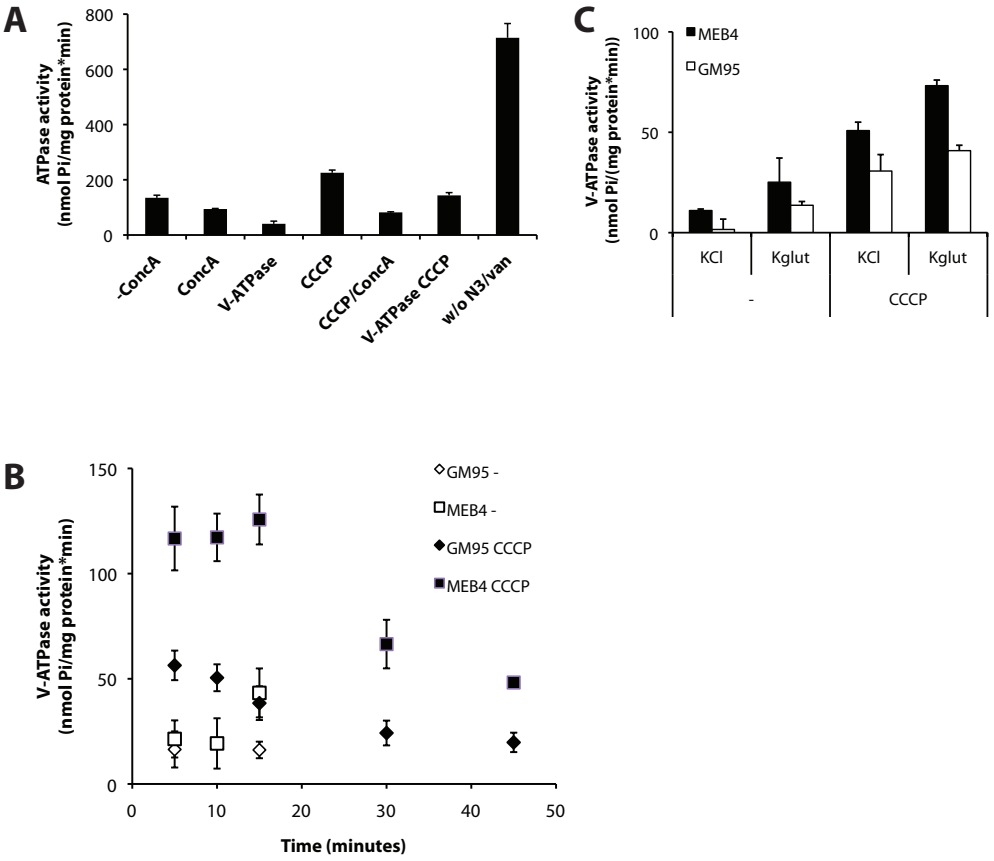

Supplemental Figure S1. Different facets of the V-ATPase assay. (A) The assay dissected. Membranes from MEB4 cells were isolated and the V-ATPase activity assay was performed on 4 µg total protein in the presence of 2 mM NaN_3 and 0.1 mM vanadate following procedure (i) as described in Materials and Methods in the absence and presence of 200 nM concanamycin A (-ConcA, +ConcA), the difference being the V-ATPase activity (V-ATPase), and in the presence of CCCP (CCCP, CCCP/ConcA, V-ATPase CCCP, respectively). The total ATPase activity without NaN_3 and vanadate was determined of 1 µg total protein (w/o N3/van) and subsequently calculated for 4 µg. (B) Time course of the V-ATPase activity on membranes from MEB4 and GM95 cells (diamonds and squares respectively) in the presence of NaN_3 and vanadate following procedure (i) in Materials and Methods. The assay was performed for the indicated time points in the absence and presence of CCCP (white and black point respectively). V-ATPase activity was expressed in nmol P_i per mg protein per min (n=1). (C) V-ATPase activity is optimal in buffer with K^+-glutamic acid. Membranes were isolated from GM95 and MEB4 in two different buffers, with either 150 mM KCl or 150 mM K^+-glutamate. The activity assay was carried out in the presence of the same buffers according to procedure (i) as described in Materials and Methods. V-ATPase activity was expressed in nmol P_i per mg protein per min (n=1).

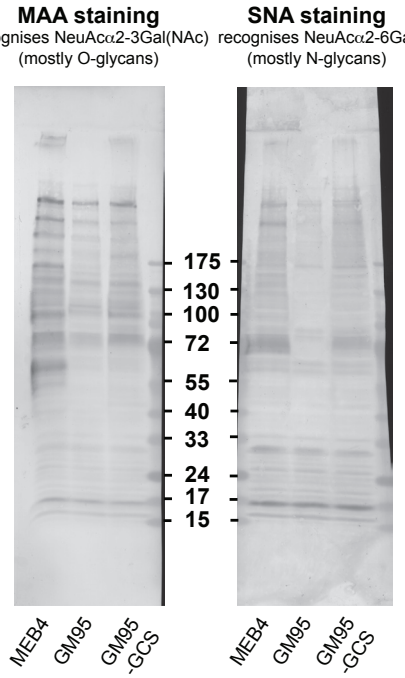

Supplemental Figure S2. Glycosylation in GM95 cells is aberrant. Equal amounts of protein of the different cell lines were resolved by SDS-PAGE and sialic acid was detected on Western blot with digoxigenin conjugated MAA-lectin (against sialic acid-α2,3 galactose) and SNA-lectin (against sialic acid-α2,6 galactose). Lectins were visualised using anti-digoxigenin antibodies coupled to alkaline phosphatase followed by DAB-staining as described in Materials and Methods.

Chapter 4

Reconstitution of the vacuolar-type H^+-translocating ATPase from *Manduca sexta*

Seléne van der Poel[1], Matthijs Kol[1], Markus Huss[2], Martin Dransmann[2], Helmut Wieczorek[2] and Gerrit van Meer[1]

[1] Membrane Enzymology, Bijvoet Center and Institute of Membranes, Utrecht University, Utrecht, The Netherlands

[2] Animal Physiology, Biology Division, University of Osnabrück, Germany

Abstract

The vacuolar H^+-translocating ATPase (V-ATPase) is highly enriched in the midgut of the larvae of the tobacco hornworm *Manduca sexta*. The V-ATPase was isolated and purified from a midgut membrane preparation in a highly pure fraction. The purified protein in 0.01% $C_{12}E_{10}$ was reconstituted in preformed liposomes after destabilisation by CHAPS. The detergent was subsequently removed with Bio-Beads and the resulting proteoliposomes were harvested by centrifugation. The reconstituted V-ATPase displayed ATPase activity in all lipid mixtures and retained native holoenzyme activity in most mixtures. The lipid formulation with phase separating behaviour produced sealed proteoliposomes whereas other lipid mixtures did not significantly result in tight proteoliposomes. The average phospholipid recovery after reconstitution was 50% and recovery of protein varied between 30-60%. Contrary to our hypothesis, the presence of 5 mol% glucosylceramide in any lipid mixture did not significantly influence V-ATPase activity compared to sphingomyelin and did not affect stability of the V-ATPase. Perhaps bovine glucosylceramide cannot influence the insect V-ATPase or the insect V-ATPase in the plasma membrane is distinct from the mammalian V-ATPase in endomembranes. Alternatively, either glycosphingolipids do not regulate the V-ATPase directly or a regulatory mechanism is not conserved in insects.

Introduction

The H^+-translocating ATPase in the vacuolar system of eukaryotes (V-ATPase) is evolutionary conserved and essential (Nelson, 1992; Nelson & Harvey, 1999). The V-ATPase is the main acidifying enzyme in cells and has been extensively studied, as it is such a basic condition for life. The enzyme is a large protein complex that can be separated in two larger domains, namely the domain V_o, which is integral to the membrane, and the cytosolic domain V_1. Both domains consist of multiple subunits. Release of the cytosolic domain V_1 from V_o is one of its many regulatory mechanisms (reviewed by Forgac, 2007). Structural studies of the complex are hampered by its large size of nearly 1 MDa and by possible loss of soluble subunits during purification, but crystal structures of several subunits from different organisms have been published (see legend Figure 1A for examples). Whether or not the structure of the isolated subunit is comparable to the structure it has in the complex, remains to be seen. Recently a cryo-electron microscopy image of the insect V-ATPase was obtained, in which the structures of subunits from other organisms were fitted to generate a high resolution structural model of the holoenzyme (Figure 1A and 1B; Muench et al., 2009).

In Chapter 3 of this thesis, we described the finding that the ATP hydrolytic

activity of the V-ATPase in isolated membranes from melanoma cells depends on glycosphingolipids. Here we set out to devise an *in vitro* set-up to investigate whether glycosylceramide (GlcCer), the precursor of higher glycosphingolipids, influences the activity of the V-ATPase directly. To demonstrate this, we chose to reconstitute the V-ATPase in proteoliposomes with defined lipid compositions. Procedures have been described to reconstitute the V-ATPase from clathrin-coated vesicles (Arai et al., 1987), lysosomes (Okamoto et al., 1996; D'Souza et al., 1987), kidney cortex microsomes (Young et al., 1988), lemon fruits (Müller et al., 1997) and plants (Yamanishi & Kasamo, 1994), but these studies used sources with low natural abundance of the V-ATPase and/or under conditions of suboptimal purification.

The plasma membrane of the goblet cells in the gut of the tobacco hornworm *Manduca sexta* (Figure 1C) contains almost crystalline arrays of the V-ATPase (Beyenbach and Wieczorek, 2006). There, it plays a role in nutrient uptake, fluid secretion and K^+ transport into the gut lumen (reviewed by Beyenbach and Wieczorek, 2006; Castagna et al., 1998). A procedure to obtain the V-ATPase in high quantity and purity from goblet cells was first described by Wieczorek et al. (1990). Thus, we chose it as a protein source for the reconstitution experiments, with the implicit assumption that regulation of the activity of the V-ATPase by glycosphingolipids is a conserved mechanism. Indeed, it has been described for the tonoplast V-ATPase in rice, that the activity of the enzyme is modulated by glycolipids (Yamaguchi and Kasamo, 2001).

This is the first instance that the V-ATPase from the *Manduca sexta* was successfully reconstituted. Although the V-ATPase resides in the plasma membrane of the goblet cells in *Manduca sexta*, the enzyme displayed ATP hydrolytic activity, similar to the holoenzyme in detergent, in a broad range of different lipid mixtures. The presence of GlcCer did not affect the ATP hydrolytic activity or stability of the reconstituted V-ATPase. This suggests there is no regulation of the V-ATPase by GlcCer via a direct interaction. However, the insect V-ATPase is perhaps different than the mammalian variant or the regulatory mechanism is not conserved in insects.

Results

V-ATPase from Manduca sexta is obtained in a highly pure fraction

V-ATPase was isolated from *Manduca sexta* midguts and purified in two subsequent steps as described in Materials and Methods. The last purification step, size exclusion chromatography, yielded the V-ATPase in high quantity (2 mg). The purified fraction showed a typical band pattern of almost exclusively the subunits of the V-ATPase on a Coomassie-stained SDS-PAGE gel (Figure 1D). The identity of the various subunits as they are indicated in Figure 1D has been confirmed previously by mass spectrometric

analysis (Huss and Wieczorek, 2007).

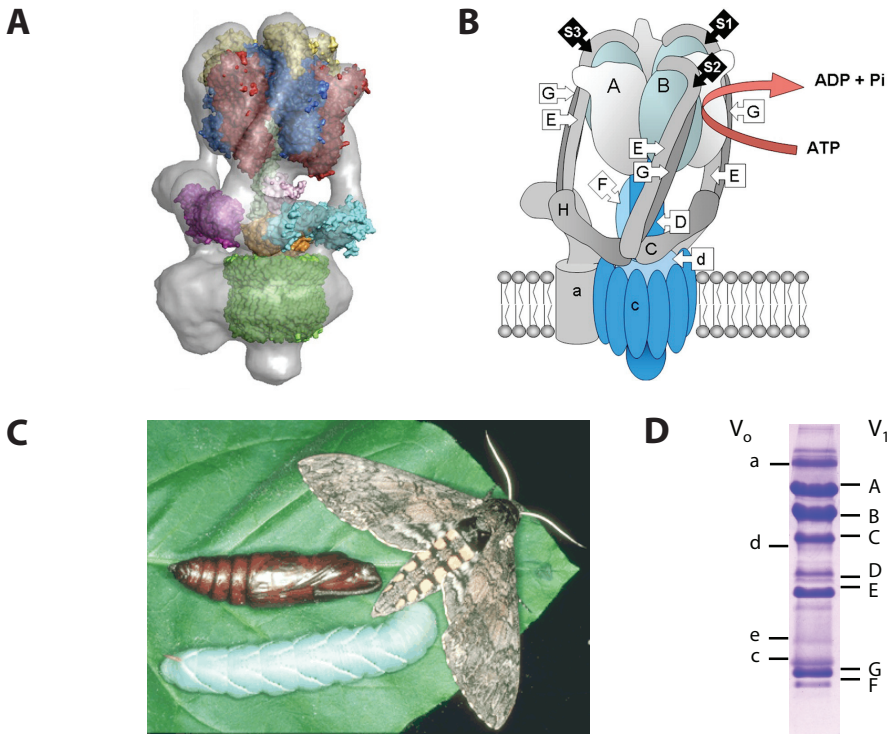

Figure 1. The V-ATPase from *Manduca sexta*. (A) Cryo-electron microscopy structure of the V-ATPase from *Manduca sexta*. V-ATPase reconstruction with subunit crystal structures fitted. Red, *Pyrococcus* subunit A (Maegawa at al., 2006); blue, *Methanosarcina* subunit B (Schäfer et al., 2006); yellow, C-terminal domain of *Pyrococcus* subunit E (Lokanath et al., 2007); cyan, *Saccharomyces* subunit C (Drory et al., 2004); magenta, *Saccharomyces* subunit H (Sagermann et al., 2001); dark green, *Enterococcus* NtpK subunit c-ring (Murata et al., 2005); orange, the *T. thermophilus* homologue of subunit d (Iwata et al., 2004); pink, *T. thermophilus* subunit F (Makyio et al., 2005). The F-ATPase γ-subunit (light green), a presumed functional homologue of subunit D, has been fitted to the central rotor axle in contact with subunit F (*Saccharomyces*; Stock et al., 1999). Picture is from Muench et al. (2009). (B) Model of V-ATPase of *Manduca sexta* based on the cryo-EM structure. Subunits in the cytosolic domain V_1 and membrane-associated domain V_o complex are indicated with capital letters and small letters respectively. Cryo-EM could not distinguish subunit e from subunit a in the V_o domain. Picture is from Muench et al. (2009). (C) Different developmental stages of *Manduca Sexta*; pupa (top left), caterpillar (bottom left) and adult (right) on tobacco leaf. Picture courtesy of prof. dr. Richard Vogt (http://zebra.sc.edu/moth/manduca-l.html). (D) V-ATPase was obtained in a highly pure fraction. V-ATPase was isolated from *Manduca sexta* midguts and purified as described in Materials and Methods. The first picked fraction from a size exclusion chromatography purification is shown here on a Coomassie-stained SDS-PAGE gel. A representative experiment is shown. Subunits in the cytosolic domain (V_1) and integral membrane domain (V_o) are indicated with capital letters and small letters respectively.

Different liposomes have different optimal destabilisation points

The reconstitution protocol was based on the procedure described by Geertsma et al. (2008) for ABC transporters. A schematic representation is included in Figure 2.

The point of optimal destabilisation of liposomes for most efficient reconstitution of ABC transporters was determined to be around 80% residual scattering (Geertsma et al., 2008). The various lipid mixtures used in our study required different CHAPS concentrations to achieve optimal liposome destabilisation (Figure 3).

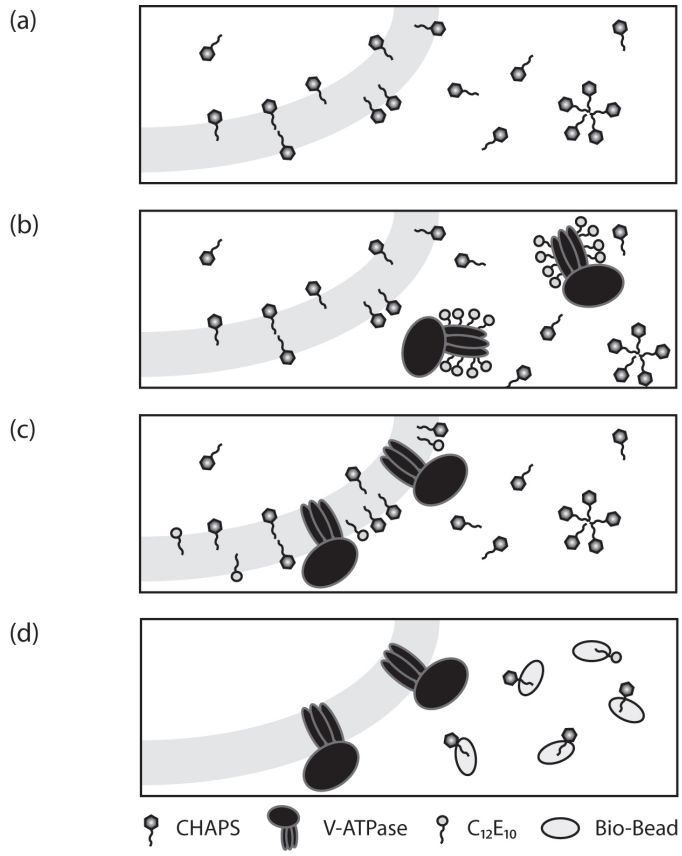

Figure 2. Schematic representation of the reconstitution procedure. Purified V-ATPase, was reconstituted in liposomes of different lipid composition. Liposomes were prepared as described in Materials and Methods. (a) The liposomes were destabilised by CHAPS. (b) Purified V-ATPase in 0.01 % $C_{12}E_{10}$ was added and (c) allowed to insert into the liposomes. (d) Bio-Beads were used to remove detergent.

Destabilisation was easily achieved with liposomes of phosphatidylcholine (PC) only. Liposomes containing PC and cholesterol (Chol) (PC/Chol 55/45 mol%) or PC, phosphatidylethanolamine (PE) and cholesterol (PC/PE/Chol 40/15/45 mol%), required approximately 3 fold higher concentrations of detergent to reach the same extent of destabilisation. The presence of sphingolipids, sphingomyelin (SM) and glucosylceramide (GlcCer) in PC/SM/Chol (40/15/45 mol%) and PC/SM/GlcCer/Chol (40/10/5/45 mol%), made the liposomes more resistant to solubilisation. The lipid mixture consisting of phosphatidylcholine (PC), sphingomyelin (SM) and cholesterol (Chol) in PC/SM/Chol (45/30/25 mol%), a lipid composition that shows phase separation behaviour therefore indicated as 'raft mix' (Baumgart et al., 2003), proved most difficult to destabilise.

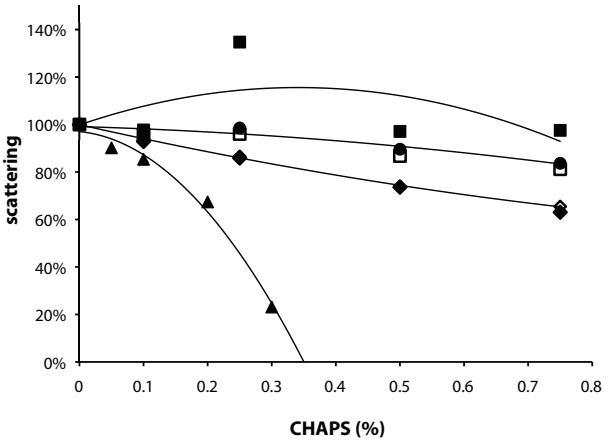

Figure 3. Point of optimal destabilisation depended on liposome formulations. For each composition, the point of optimal destabilisation of the liposomes by CHAPS, leaving 80% scattering at 600 nm, was determined. Liposomes were prepared as described in Materials and Methods. Liposomes were diluted to 3 mM and destabilised by CHAPS with final concentrations between 0-0.8% for 1 h at room temperature while rotating. Scattering was measured in a fluorimeter at 600 nm. Lipid compositions were PC (100 mol%; closed triangles), PC/Chol (55/45 mol%; closed diamonds), PC/PE/Chol (40/15/45 mol%; open diamonds), PC/SM/Chol (40/15/45 mol%; open squares), PC/SM/Chol 'raft' (45/30/25 mol%; closed squares), PC/SM/GlcCer/Chol (40/10/5/45 mol%; closed circles). The black lines are trend lines (second order relation) to describe the relation between scattering and CHAPS concentration in order to calculate the optimal CHAPS concentration.

The V-ATPase is successfully reconstituted in various lipid mixtures

In order to assess the amount of protein lost during the reconstitution and the integrity of the V-ATPase, samples of different steps in the reconstitution were analysed on SDS-PAGE and subunits were visualised using silver stain (Figure 4A). The V-ATPase did

not bind to Bio-Beads (lanes 3-6) and did not aggregate (lane 7). Approximately 20% of the V-ATPase was not reconstituted and therefore not pelleted after high speed centrifugation (lane 8). When the holoenzyme in detergent (lane 1) or the input of the reconstitution (lane 2) were compared with the reconstituted protein in the proteoliposomes (lane 9), all subunits were present after reconstitution in a ratio similar to the input.

The phospholipid recovery was around 50% for all liposomes, but the recovery of protein varied between 30% and 60% (Table I). The protein to lipid ratio was maintained after reconstitution with liposomes resembling the exoplasmic and endoplasmic side of the plasma membrane as well as the liposomes with phase separating behaviour ('raft'). Taking into account the membrane surface area of the headgroup ofdipalmitoyl-PC to be between 70Å^2 (Petrache et al., 2000; Thurmond et al., 1991) and 50Å^2 (Chiu et al., 2002), liposomes with a diameter of 400 nm contain around 1.5 million lipids. Then, at the recovery of 50% of protein and lipid after reconstitution, the average number of V-ATPase molecules was calculated to be about 60 per liposome.

The V-ATPase was reconstituted in different lipid mixtures, which are listed in Table I. ATPase activity assays were performed in the absence or presence of the specific V-ATPase inhibitor concanamycin A (Woo et al., 1992; Dröse et al., 1993), and

Table I. Lipid composition of liposomes and average protein and phospholipid recovery after reconstitution. The different lipid compositions were based on * Baumgart et al. (2003) and ** Van Meer (1989) of which **1 resembles the endoplasmic side of the plasma membrane while **2 resembles the exoplasmic side of the plasma membrane. Protein recovery was calculated from protein determination with Amido Black, phospholipid content was determined according to Rouser (1970).

Lipids	Mol ratio (%)	Average protein recovery (%)	Average phospholipid recovery (%)
PC	100	47	67
PC/Chol	55/45	24	44
PC/PE/Chol	40/15/45	21	64
PC/SM/Chol	40/15/45	32	59
PC/SM/GlcCer/Chol	40/10/5/45	29	51
PC/SM/Chol 'raft-mix'*	45/30/25	32	32
PC/PE/PS/SM/Chol **1	10/20/20/5/45	57	56
PC/PE/PS/GlcCer/Chol **1	10/20/20/5/45	57	59
PC/PE/SM/Chol**2	30/5/20/45	49	42
PC/PE/SM/GlcCer/Chol**2	30/5/15/5/45	42	53

in the presence of the protonophore carbonyl cyanide m-chlorophenylhydrazone (CCCP) (Skulachev et al., 1967; Steen et al., 1993; Figure 4B). The protonophore can pass the membrane and equilibrates protons thereby removing the proton gradient built up by the V-ATPase. This proton gradient is only built up in sealed liposomes, therefore it is used here as a measure for this physical property. In order to ascertain the uninhibited, maximal activity of the V-ATPase in detergent, proteoliposomes were solubilised with 1% $C_{12}E_{10}$.

In all lipid mixtures used here, active, ATP-hydrolysing V-ATPase was reconstituted (Figure 4B). Addition of concanamycin A completely inhibited ATPase activity. Thus, all ATPase activity measured is likely to be attributed exclusively to the V-ATPase. The activity was most likely solely generated by reconstituted V-ATPase as the enzyme was not active in $C_{12}E_{10}$ concentrations below 0.001% (results not shown). The V-ATPase activity in most proteoliposomes was similar to the activity of the holoenzyme and in the presence of CCCP. Therefore, active V-ATPase was reconstituted in permeable liposomes and no proton gradient was built up. The specific activity, per mg protein, of solubilised proteoliposomes was comparable to the activity of the holoenzyme in $C_{12}E_{10}$ (indicated with *). This indicates that the integrity of the V-ATPase was preserved.

The V-ATPase reconstituted in liposomes of PC alone displayed a two-fold decrease in activity compared to other liposomes. This suggests that addition of cholesterol activated or PC inhibited the V-ATPase while the activity of solubilised V-ATPase from PC and PC/Chol liposomes was comparable.

The activity of the V-ATPase reconstituted in PC/SM/Chol (45/30/25 mol%) was lower compared to other lipid mixtures. The 'raft mix' liposomes showed a three-fold decreased activity of the V-ATPase, compared to the solubilised activity. Addition of the protonophore CCCP increased V-ATPase activity towards the activity in solubilised liposomes, therefore the V-ATPase was able to build up a proton gradient. We conclude that these proteoliposomes (PC/SM/Chol, described as the 'raft'-mix) were largely impermeable to protons whereas reconstitution in other liposomes did not result in sealed proteoliposomes.

Addition of GlcCer in proteoliposomes does not affect V-ATPase activity

After we could show functional reconstitution of the V-ATPase in liposomes of various compositions, we proceeded to investigate whether glucosylceramide (GlcCer) affected the activity of the *Manduca sexta* V-ATPase. Two lipid compositions were used, one that resembled the exoplasmic side of the plasma membrane, marked as 'PM-like', and the other mimicked the endoplasmic side of the plasma membrane marked as 'Cytoplasmic-like' (Figure 5). Both these lipid mixtures were doped with 5% GlcCer, or with sphingomyelin (SM) as a control (see Table I for lipid compositions), then lipo-

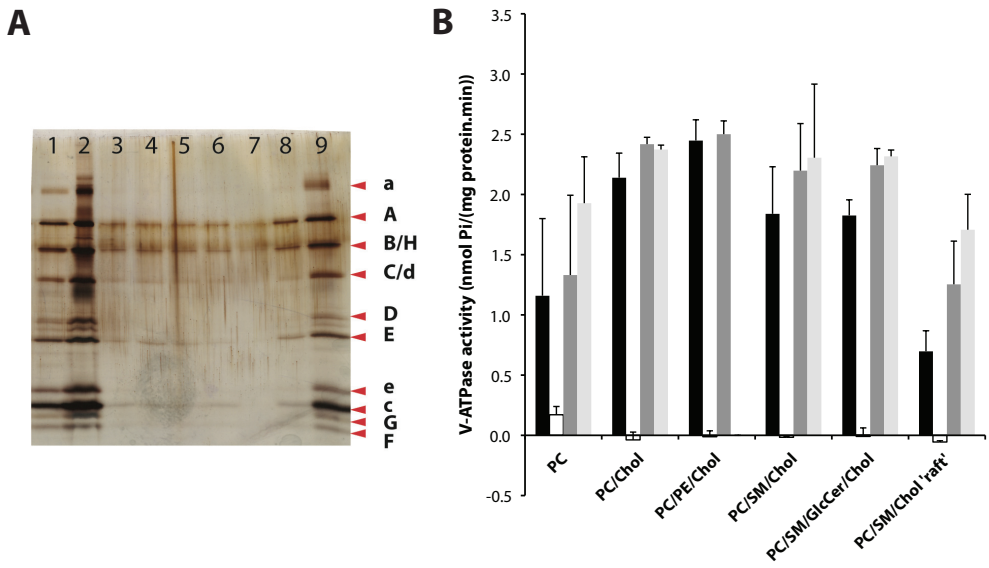

Figure 4. The V-ATPase was successfully reconstituted in different liposomes. (A) Intact V-ATPase was reconstituted in PC/PE/SM/GlcCer/Chol (30/5/15/5/45 mol%). Samples of the holoenzyme (200 ng; lane 1), 1% V-ATPase input (lane 2), Bio-Beads incubations #1-4 (lane 3-6), 1,000 x g spin pellet (lane 7), 100,000 x g supernatant (lane 8), 1% of 100,000 x g pellet (lane 9) were separated on SDS-PAGE and visualised with silver staining. Bio-Beads were incubated with SDS sample buffer for 2 h at room temperature under constant agitation before loading an aliquot of the supernatant on gel. (B) ATPase activity assays of purified V-ATPase reconstituted in different liposomes were performed as described in Materials and Methods. Assays were performed in the absence (black bars) or presence of concanamycin A (white bars), in the presence of CCCP (dark grey bars) or proteoliposomes were solubilised with 1% $C_{12}E_{10}$ (light grey bars). ATPase activity was expressed in nmol P_i per mg protein per min (n=2). The activity of the holoenzyme (2.3 nmol P_i per mg protein per min) in detergent is indicated as a reference (*).

somes were prepared and destabilised as described.

The reconstitutions in plasma membrane-resembling lipid mixture and the cytoplasmic mixture did not result in sealed proteoliposomes (Figure 5). Contrary to our initial hypothesis, there was no significant difference in V-ATPase activity between liposomes with GlcCer or SM in either composition. GlcCer was present in excess as approximately 1200 GlcCer molecules per V-ATPase were expected, calculated using the assumptions mentioned earlier.

In order to exclude that endogenous glycosphingolipids were attached to the V-ATPase masking a stimulatory effect of the GlcCer in liposomes, lipids were isolated

from the holoenzyme in detergent and analysed on Thin Layer Chromatography (TLC) with orcinol staining (Svennerholm, 1956) as described in Materials and Methods. We found no correlation between the absence and presence of glycolipids and the ATP hydrolytic activity of the V-ATPase (results not shown).

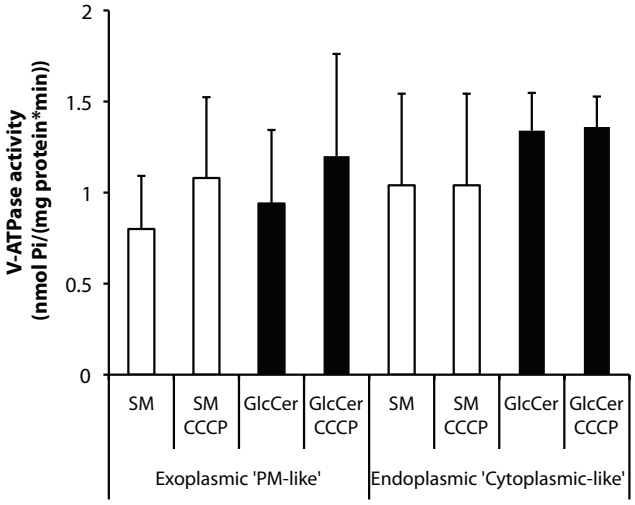

Figure 5. The presence of glucosylceramide did not affect ATPase activity compared to sphingomyelin. Reconstitutions were done in liposomes with GlcCer (black bars) or SM (white bars), resembling either the exoplasmic side of the plasma membrane, PC/PE/SM/GlcCer/Chol (30/5/15/5/45 mol%) on the left, or the endoplasmic side of the plasma membrane, PC/PE/PS/SM or GlcCer/Chol (10/20/20/5/45 mol%) on the right. The ATPase activity assay was performed as described and expressed in nmol P_i per mg protein per min (n=4).

Stability is dependent on lipid composition, but not on GlcCer

Different lipids influence the biophysical properties of the membrane and therefore affect the enzyme activity or stability. As an example, it has been shown that anionic lipids are required for the function of the potassium KcsA channel (Valiyaveetil, Zhou and MacKinnon, 2002). Since we were able to reconstitute the V-ATPase, we had the chance to also assess the stability of its catalytic activity as a function of the lipid membrane composition in which it resides. The enzyme was most stable in $C_{12}E_{10}$ and unstable in proteoliposomes made up of PC only (Figure 6). The presence of sphingolipids and cholesterol stabilised the reconstituted protein. The stability was improved when GlcCer or the phase separating 'raft' mix were used, however the V-ATPase activity was even more stable in PC/SM/Chol liposomes.

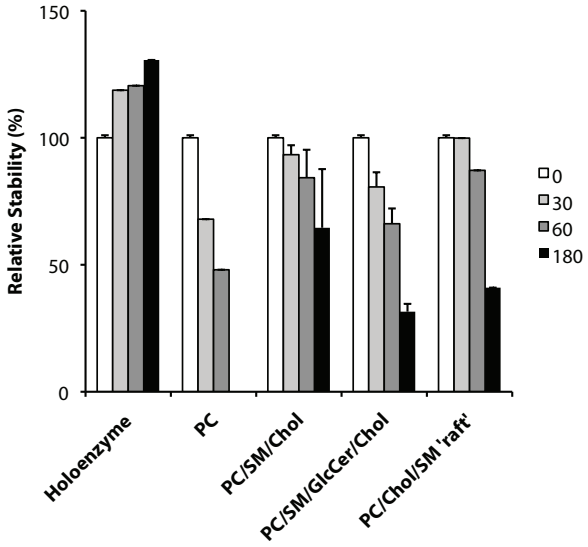

Figure 6. Stability of the V-ATPase reconstituted in different liposomes. Reconstituted V-ATPase or holoenzyme in detergent were incubated at 30°C for 0 (white bars); 30 (light grey bars); 60 (dark grey bars) or 180 min (black bars) before the ATPase activity assay as described in Materials and Methods. The stability is expressed relative to the V-ATPase activity at timepoint 0 (n=2). Investigated lipid compositions were PC (100 mol%), PC/SM/Chol (40/45/15 mol%), PC/SM/GlcCer/Chol (35/15/5/45 mol%) and PC/SM/Chol 'raft' (45/30/45 mol%).

Discussion

Here we report that the proton pump V-ATPase obtained from *Manduca sexta* in a highly pure fraction was, for the first time, successfully reconstituted in a broad variety of defined liposomes. In all liposomal formulations, the reconstituted enzyme showed ATP hydrolytic activity, comparable to activity of the holoenzyme in the detergent $C_{12}E_{10}$. No direct effect of the presence of glucosylceramide (GlcCer) on the V-ATPase activity was observed.

Reconstitution of V-ATPase

The recovery of lipids was comparable for all liposomes, while the protein recovery was variable. Okamoto et al. (1996) and Müller et al. (1997) reported that the protein/lipid ratio of the input was maintained after reconstitution for V-ATPases from lysosomes and lemon fruits respectively. The protein/lipid ratio was similar before and after reconstitution in complex lipid mixtures resembling the two leaflets of the plasma membrane and the raft mixture. Notably, all liposomes with a high PC content (>40 mol%) had a lower protein recovery. Destabilisation was quantified, but insertion of

V-ATPase into the liposomes before removal of detergent probably determines protein recovery and this was perhaps affected in liposomes with high PC content.

The V-ATPase activity was lower in the lipid mixtures resembling the two leaflets of the plasma membrane and in the raft mixture. These membrane compositions were selected, as the enzyme is located at the plasma membrane in *Manduca sexta*. Reconstitution in the raft mixture did not affect integrity of the V-ATPase because the activity of the solubilised protein is comparable to the holoenzyme in detergent. However, the activity was not determined in the presence of 1% $C_{12}E_{10}$ of the V-ATPase reconstituted in the plasma membrane-resembling lipid mixtures. The decrease in activity may constitute a physiological 'brake' by the membrane environment since V-ATPase needs to be tightly controlled (Forgac, 2007).

As the large standard deviations in the activity assays suggest, the reproducibility of the activity assays between reconstitutions was challenging. Whether this was caused by a variation in the quality of the V-ATPase or in the reconstitution remains to be determined. The quality of purified of V-ATPase was constant according to the analysis of SDS-PAGE gels and activity assays of the holoenzyme in detergent. Although there was no correlation between the presence of endogenous glycolipids and the V-ATPase activity, it is a variable that has to be controlled for example with mass spectrometry as the detection by orcinol staining is limiting.

Complex lipid mixtures were used for the reconstitutions and although the protocol for liposome production was constant, the resultant formation of liposomes can be variable. The recovery of glycosphingolipids should be addressed. Most proteoliposomes were not sealed after reconstitution and a proton gradient was not built up. The lipid composition of the liposomes needs to be optimised to improve the sealing of liposomes for instance by replacing PC. The V-ATPase collected after high speed centrifugation is either reconstituted or associated with the proteoliposomes. Although the V-ATPase complex in detergent cannot be pelleted with high speed centrifugation, reconstitution of the V-ATPase should be controlled. In order to distinguish between reconstituted and associated protein complexes, flotation of proteoliposomes on a sucrose gradient can be performed. Addition of CCCP and solubilisation of proteoliposomes gave an indication of functionality, however a functional assay has to be deployed to link ATP hydrolysis activity with actual proton pumping, for instance by measuring acidification of the lumen with acridine orange or oxonol.

Cholesterol as an activating lipid

The presence of cholesterol in liposomes dramatically increased resistance to solubilisation by CHAPS whereas sphingolipids marginally affected destabilisation further. Cholesterol was shown to order lipid acyl chains and inhibited spontaneous peptide flop (Ipsen et al., 1990; Kol et al., 2003). Since almost one in two lipids is cholesterol

(45 mol%), ordering the acyl chains of PC greatly increases impermeability of the membrane. Sphingolipids additionally affected resistance to solubilisation as it has been shown that cholesterol has a high affinity for sphingolipids (Puri et al., 2003; McConnell et al., 2003). Cholesterol and sphingolipids form microdomains, better known as rafts, that also function as the permeability barrier at the apical plasma membrane in epithelial cells (Simons and Van Meer, 1988).

The V-ATPase in PC-liposomes displayed a two-fold decrease in activity, and addition of cholesterol increased activity towards activity that is comparable to the holoenzyme in detergent. The V-ATPase has been found in detergent resistant membranes, which are enriched in cholesterol and sphingolipids (Dermine et al., 2001; Gkantiragas et al., 2001; Yoshinaka et al., 2004). Cholesterol greatly orders the acyl chains of PC as discussed earlier, thereby changing the membrane properties. The membrane will become more ordered and then resembles the preferred membrane environment and this can influence catalytic function.

Glucosylceramide and the V-ATPase

We set out to investigate a direct relation between the activity of the V-ATPase and GlcCer, precursor of higher glycosphingolipids, in an *in vitro* experimental set-up. The V-ATPase from *Manduca sexta* was readily available in high purity and quantity for reconstitution in defined liposomes. GlcCer did not significantly alter the ATP hydrolytic activity or stability of the V-ATPase compared to sphingomyelin (SM). Below, we discuss the implications of this key observation for the proposed hypothesis.

The simplest explanation for this observation is that GlcCer has no regulatory effect on the activity of the V-ATPase. To reconcile this observation with the data obtained with the GM95 and MEB4 cell lines (Chapter 2 and 3), one could conclude that not GlcCer itself, but a higher glycosphingolipid has a regulatory effect on the V-ATPase. However, this would contradict our earlier observations that higher glycosphingolipids are not required to restore pigmentation in GM95 cells (Groux-Degroote et al., 2008). The influence of glycosphingolipids on the ATP hydrolytic activity of the V-ATPase can also be indirect. Other factors that play a role in the complex cellular pH regulatory system, for instance anion channels, were not included in this reconstitution. In Chapter 2 of this thesis, we describe that glycosphingolipids also affect the transcription of the putative anion channel Oca2. In order to address this question, candidate proteins can be included in the reconstitution, but will complicate the interpretation of results.

Alternatively, one could conclude that the V-ATPase from the *Manduca sexta* midgut is not a valid model for the investigation of a direct interaction between a mammalian GlcCer and an insect V-ATPase. The extrapolation of the conservation of a regulatory mechanism from melanoma cells to *Manduca sexta* is an assumption based on the

highly conserved and essential nature of both the V-ATPase and GlcCer in eukaryotes (Nelson, 1992; Nelson & Harvey 1999; Yamashita et al., 1999). However, the V-ATPase, located in the plasma membrane of the goblet cell in the midgut of the *Manduca sexta*, is not comparable with the intracellular V-ATPase in the Golgi and endosomal/lysosomal system in melanoma cells. The *Manduca sexta* V-ATPase is implicated in several ongoing physiological processes, such as nutrient uptake, and perhaps does not require regulation of its activity, but a simple on-off switch suffices (reviewed by Wieczorek et al., 2000; Castagna et al., 1998).

Also other differences between the two organisms can play a role. The commercially available GlcCer used in these reconstitutions was isolated from bovine buttermilk. A recent study by Abeytunga et al. (2008) reported that the sphingolipids in the midgut of the *Manduca sexta* have a different sphingosine backbone. The sphingosine backbone of lipids in mammals is typically 18:1, while lipids in insects have 14:1 or 16:1. The lengths of the acyl chains can vary for insects between 18:0, 20:0 and 22:0 while for mammals mainly 22:0 is found (reviewed by Holthuis et al., 2001). Therefore, the sphingosine backbone and acyl chain are overall shorter in the sphingolipids of insects than of mammals. Based on the fact that the glycosphingolipid-deficient cells were shown to contain sphingomyelin (Sprong et al., 2001), it was anticipated that the headgroup was important and not the lipid backbone. The commercially available GlcCer used in this study was perhaps too large for a spatially limited binding pocket, but insect glycosphingolipids are not commercially available and synthesis of these lipids is laborious. This suggests that the lipid backbone can be important and not the headgroup. The reconstitution should be repeated with glycosphingolipids resembling the endogenous lipids in insects.

The putative glycosphingolipid binding site, the site where the inhibitor concanamycin A binds (see Chapter 3), is possibly different in insects. The binding site is located at the rotor domain of the integral membrane domain V_o, which is a ring of c-subunits. Concanamycin A was shown to bind between two c-subunits in *Neurospora crassa* (Bowman et al., 2006). The rotor domain in *Manduca sexta* consists of 10 similar c-subunits while the mammalian variant contains six copies in total of three isoforms of subunit c (Muench et al., 2009; Forgac, 2007). Therefore, a regulatory mechanism of the V-ATPase by glycosophingolids is perhaps not conserved in the plasma membrane V-ATPase of insects or the glycosphingolipids are not interchangeable between organisms.

Materials and Methods

Materials

Chemicals, unless stated otherwise, were from Sigma-Aldrich (St. Louis, Missouri) and used in the highest purity available. All lipids and lipid standards were from Matreya (Pleasant Gap, PA), and were stored as stock solutions in $CHCl_3$/MeOH at -20°C. Phosphatidylcholine (PC) in $CHCl_3$, isolated from egg yolk (Grade I), was from LipidProds (Surrey, England).

Purification of vacuolar H^+-ATPase from Manduca sexta

The method was based on the purification of the V_1/V_o complex described in Schweikl et al. (1989) and Huss et al. (2002). Midguts were isolated from 32 5th instar larvae, washed and homogenised with an Ultraturax in buffer (0.25 M sucrose, 5 mM Tris-HCl, 5 mM Na2EDTA, pH 8.1, 5 mM Pefabloc SC). The pellet was washed and collected at 150,000 x g for 25 min at 4°C using the 90Ti rotor (Beckman). The pellet was resuspended in 16 mM Tris-HCl, 0.3 mM EDTA, 9.6 mM 2-mercaptoethanol and the V-ATPase was solubilised using 0.1 % $C_{12}E_{10}$ for 10 min while stirring at room temperature. Debris was removed by centrifugation at 100,000 x g at 4°C for 1 h in the 45Ti rotor (Beckman). Supernatant was filtered through a 0.2 µM filter to remove body fat and the sample was concentrated using a protein concentrator tube (Amicon, Millipore, Amsterdam, Netherlands) with a 10 kD cut-off. The sample was loaded onto a discontinuous sucrose gradient (40%; 30%; 20%; 10% sucrose in 16 mM Tris-HCl, 0.3 mM EDTA, 9.6 mM 2-mercaptoethanol 200 mM KCl, 0.01 % $C_{12}E_{10}$) and centrifuged at 300,000 x g at 4°C for 1.5 h in a VTi 65.1 rotor (Beckman). The 30% sucrose fraction was collected and diluted 4 times with 20 mM Tris, 50 mM NaCl, 0.01 % $C_{12}E_{10}$, pH 8.1 before loading the sample onto an ion-exchange column (Resource Q, GE Healthcare). The column was run with a NaCl gradient in 20 mM Tris-HCl, 0.01 % $C_{12}E_{10}$, pH 8.1 and the V-ATPase eluted between 250 and 280 mM NaCl. The eluate was concentrated to 100 µL using a Centricon Plus-20 (Amicon, Millipore, Amsterdam, Netherlands) with 100 kD cut-off and was applied to a gelfiltration column (Superdex 200, GE Healthcare). Samples of fractions were separated on 17% SDS-PAGE and stained with Coomassie Blue. The two purest fractions were pooled and typically contained 2 mg protein in 20 mM Tris-HCl, 50 mM NaCl, pH 8.1, 0.01 % $C_{12}E_{10}$, which was used in subsequent reconstitutions.

Reconstitution procedure

The reconstitution procedure was based on the reconstitution of ABC transporters described, in excellent detail, by Geertsma et al. (2008). For the different lipid compositions used, see Table I. An amount of 10 µmol total lipid was dried under N_2 with agitation to form a lipid film and the film was kept under vacuum for at least 1 h and up to 12 h. The film was hydrated with 20 mM Tris-HCl, 50 mM NaCl, pH 8.1 yielding 10 mM total lipid, and was kept under N_2. The liposomes were sonicated and heated to 60°C to homogenise the liposome suspension. Freeze/thaw cycles with liquid N_2 and a 40°C waterbath, 10 times in total, resulted in larger vesicles. Liposomes were sized by extrusion, passing them 20 times through a 400 nm bicarbonate filter mounted on an Avanti syringe-based

extrusion device. The liposomes were diluted to 3 mM and destabilised / partially solubilised up to 80% residual scattering (see below) with CHAPS (3-[(3-cholamidopropyl)dimethyl-ammonio]-1-propanesulfonate) in final concentrations between 0.1 and 0.5%, for 1 h at room temperature while rotating. The purified V-ATPase was added to the destabilised liposomes at 100 µg/ml, and incubated for 15 min at room temperature while rotating. Final concentrations in the reconstitution mix: 3 mM lipids, 0.1-0.5% CHAPS, 20 mM Tris-HCl, 50 mM NaCl, pH 8.1, 9.6 mM 2-mercaptoethanol and 0.001 % $C_{12}E_{10}$. Detergent was removed from the reconstitution mix by subsequently adding four changes of Bio-Beads (SM-2 adsorbents, Bio-Rad), pretreated according to manufacturer's protocol (Holloway, 1973), incubating for 30 min, 1 h, overnight and 2 h at 4°C while rotating, completely removing the beads after every incubation. A ratio of 1:1 of Bio-Beads (dry weight) to CHAPS was used for all incubations. Debris and precipitated protein was removed by centrifugation at 1,000 x g for 5 min at 4°C, after which the proteoliposomes were collected at 100,000 x g at 4°C for 1 h using the TLA55 rotor. The pellet was resuspended in 20 mM Tris-HCl, 50 mM NaCl, pH 8.1, 9.6 mM 2-mercaptoethanol and the protein content was determined using Amidoblack and BSA as a standard (Schaffner and Weissmann, 1973; Wieczorek et al., 1990). Lipid recovery was calculated from the phospholipid content before and after reconstitution as determined by the inorganic phosphate determination according to Rouser (1970). Analysis of the integrity of the reconstituted protein was done by separating the subunits on SDS-PAGE and staining the gel with silver according to Heukeshoven & Dernick (1988).

Destabilisation by scattering

For each lipid composition (Table I), the point of optimal destabilisation was determined of the liposomes by CHAPS, at which light scattering at 600 nm was reduced to 80%. The liposomes were made as described in 'Reconstitution procedure'. The liposomes were diluted to 3 mM and destabilised by CHAPS with final concentrations between 0-0.8% for 1 h at room temperature while rotating. The extent of destabilisation was determined from the scattering measured in a Varian Cary Eclipse (Varian B.V., Middelburg, Netherlands) fluorimeter at 600 nm.

V-ATPase activity assay

The method used has been described in Wieczorek et al. (1990) and Huss et al. (2002). Briefly, V-ATPase activity was determined of 4 µg total protein in 50 mM Tris-MOPS pH 8.1, 20 mM KCl, 1 mM MgCl2, 6.25% DMSO in the presence of 1.6 mM NaN_3 and 0.1 mM vanadate (final concentrations). Addition of 1 mM ATP started the reaction, the sample was incubated for 2 min at 30°C and frozen in liquid N_2 to stop the reaction. The amount of inorganic phosphate (P_i) generated was determined using the malachite green-phosphate-molybdate complex. For the phosphate determination, protein was first precipitated with 5% trichloroacidic acid (TCA) and centrifuged 20,000 x g for 1 min. Approximately one third of supernatant was mixed with 24% H_2SO_4:200 mM Na-molybdate:H_2O (1:3:6 v/v) to final concentrations of 1.5% H_2SO_4 and 37.5 mM Na-molybdate. Then, 1% polyvinyl alcohol with 0.074% malachite green was added and finally 7.8% H2SO4. Final concentrations were 4.6% H_2SO_4, 15 mM Na-molybdate, 0.08 % polyvinyl alcohol and 0.006% malachite green.

The absorbance was read after 90 min at 625 nm and quantified with a calibration curve of NaH_2PO_4. The ATPase activity was determined in the absence and presence of 1 µM concanamycin A (ConcA) and 10 µM of the protonophore carbonyl cyanide m-chlorophenylhydrazone (CCCP). The V-ATPase activity is defined as the difference in activity in the absence and presence of concanamyin A. The activity was expressed in nmol P_i per mg protein per min.

References

Abeytunga DT, Oland L, Somogyi A, Polt R. Structural studies on the neutral glycosphingolipids of *Manduca sexta*. *Bioorg Chem* 2008;36:70-6.

Arai H, Berne M, Terres G, Terres H, Puopolo K, Forgac M. Subunit composition and ATP site labeling of the coated vesicle proton-translocating adenosinetriphosphatase. *Biochemistry* 1987;26:6632-8.

Baumgart T, Hess ST, Webb WW. Imaging coexisting fluid domains in biomembrane models coupling curvature and line tension. *Nature* 2003;425:821-4.

Beyenbach KW, Wieczorek H. The V-type H^+ ATPase: molecular structure and function, physiological roles and regulation. *J Exp Biol* 2006;209:577-89.

Bowman BJ, McCall ME, Baertsch R, Bowman EJ. A model for the proteolipid ring and bafilomycin/concanamycin-binding site in the vacuolar ATPase of *Neurospora crassa*. *J Biol Chem* 2006;281:31885-93.

Brown D, Breton S. Mitochondria-rich, proton-secreting epithelial cells. *J Exp Biol* 1996;199:2345-58.

Castagna M, Shayakul C, Trotti D, Sacchi VF, Harvey WR, Hediger MA. Cloning and characterization of a potassium-coupled amino acid transporter. *Proc Natl Acad Sci U S A* 1998;95:5395-400.

Chiu SW, Jakobsson E, Mashl RJ, Scott HL. Cholesterol-induced modifications in lipid bilayers: a simulation study. *Biophys J* 2002;83:1842-53.

D'Souza MP, Ambudkar SV, August JT, Maloney PC. Reconstitution of the lysosomal proton pump. *Proc Natl Acad Sci U S A* 1987;84:6980-4.

Dermine JF, Duclos S, Garin J, et al. Flotillin-1-enriched lipid raft domains accumulate on maturing phagosomes. *J Biol Chem* 2001;276:18507-12.

Drory O, Frolow F, Nelson N. Crystal structure of yeast V-ATPase subunit C reveals its stator function. *EMBO Rep* 2004;5:1148-52.

Dröse S, Bindseil KU, Bowman EJ, Siebers A, Zeeck A, Altendorf K. Inhibitory effect of modified bafilomycins and concanamycins on P- and V-type adenosinetriphosphatases. *Biochemistry* 1993;32:3902-6.

Forgac M. Vacuolar ATPases: rotary proton pumps in physiology and pathophysiology. *Nat Rev Mol Cell Biol* 2007;8:917-29.

Geertsma ER, Nik Mahmood NA, Schuurman-Wolters GK, Poolman B. Membrane reconstitution of ABC transporters and assays of translocator function. *Nat Protoc* 2008;3:256-66.

Gkantiragas I, Brügger B, Stuven E, et al. Sphingomyelin-enriched microdomains at the Golgi complex. *Mol Biol Cell* 2001;12:1819-33.

Grabe M, Oster G. Regulation of organelle acidity. *J Gen Physiol* 2001;117:329-44.

Heukeshoven J, Dernick R. Improved silver staining procedure for fast staining in PhastSystem Development Unit. I. Staining of sodium dodecyl sulfate gels. *Electrophoresis* 1988;9:28-32.

Holloway PW. A simple procedure for removal of Triton X-100 from protein samples. *Anal Biochem* 1973;53:304-8.

Holthuis JC, Pomorski T, Raggers RJ, Sprong H, Van Meer G. The organizing potential of sphingolipids in intracellular membrane transport. *Physiol Rev* 2001;81:1689-723.

Huss M, Ingenhorst G, König S, et al. Concanamycin A, the specific inhibitor of V-ATPases, binds to the V(o) subunit c. *J Biol Chem* 2002;277:40544-8.

Huss M, Wieczorek H. Influence of ATP and ADP on dissociation of the V-ATPase into its V(1) and V(O) complexes. *FEBS Lett* 2007;581:5566-72.

Ipsen JH, Mouritsen OG, Bloom M. Relationships between lipid membrane area, hydrophobic thickness, and acyl-chain orientational order. The effects of cholesterol. *Biophys J* 1990;57:405-12.

Iwata M, Imamura H, Stambouli E, et al. Crystal structure of a central stalk subunit C and reversible association/dissociation of vacuole-type ATPase. *Proc Natl Acad Sci U S A* 2004;101:59-64.

Kol MA, van Laak AN, Rijkers DT, Killian JA, de Kroon AI, de Kruijff B. Phospholipid flop induced by transmembrane peptides in model membranes is modulated by lipid composition. *Biochemistry* 2003;42:231-7.

Lokanath NK, Matsuura Y, Kuroishi C, Takahashi N, Kunishima N. Dimeric core structure of modular stator subunit E of archaeal H^+ -ATPase. *J Mol Biol* 2007;366:933-44.

Maegawa Y, Morita H, Iyaguchi D, Yao M, Watanabe N, Tanaka I. Structure of the catalytic nucleotide-binding subunit A of A-type ATP synthase from *Pyrococcus horikoshii* reveals a novel domain related to the peripheral stalk. *Acta Crystallogr D Biol Crystallogr* 2006;62:483-8.

Makyio H, Iino R, Ikeda C, et al. Structure of a central stalk subunit F of prokaryotic V-type ATPase/synthase from *Thermus thermophilus*. *EMBO J* 2005;24:3974-83.

McConnell HM, Vrljic M. Liquid-liquid immiscibility in membranes. *Annu Rev Biophys Biomol Struct* 2003;32:469-92.

Merzendorfer H, Huss M, Schmid R, Harvey WR, Wieczorek H. A novel insect V-ATPase subunit M9.7 is glycosylated extensively. *J Biol Chem* 1999;274:17372-8.

Muench SP, Huss M, Song CF, et al. Cryo-electron microscopy of the vacuolar ATPase motor reveals its mechanical and regulatory complexity. *J Mol Biol* 2009;386:989-99.

Müller ML, Irkens-Kiesecker U, Kramer D, Taiz L. Purification and reconstitution of the vacuolar H^+-ATPases from lemon fruits and epicotyls. *J Biol Chem* 1997;272:12762-70.

Murata T, Yamato I, Kakinuma Y, Leslie AG, Walker JE. Structure of the rotor of the V-Type Na^+-ATPase from *Enterococcus hirae*. *Science* 2005;308:654-9.

Nelson N. Evolution of organellar proton-ATPases. *Biochim Biophys Acta* 1992;1100:109-24.

Nelson N, Harvey WR. Vacuolar and plasma membrane proton-adenosinetriphosphatases. *Physiol Rev* 1999;79:361-85.

Okamoto M, Hiratani N, Arai K, Ohkuma S. Properties of H(+)-ATPase from rat liver lysosomes as revealed by reconstitution into proteoliposomes. *J Biochem* 1996;120:608-15.

Parton RG. Ultrastructural localization of gangliosides; GM1 is concentrated in caveolae. *J Histochem Cytochem* 1994;42:155-66.

Petrache HI, Dodd SW, Brown MF. Area per lipid and acyl length distributions in fluid phosphatidylcholines determined by (2)H NMR spectroscopy. *Biophys J* 2000;79:3172-92.

Puri V, Jefferson JR, Singh RD, Wheatley CL, Marks DL, Pagano RE. Sphingolipid storage induces accumulation of intracellular cholesterol by stimulating SREBP-1 cleavage. *J Biol Chem* 2003;278:20961-70.

Rouser G, Fkeischer S, Yamamoto A. Two dimensional then layer chromatographic separation of polar lipids and determination of phospholipids by phosphorus analysis of spots. *Lipids* 1970;5:494-6.

Sagermann M, Stevens TH, Matthews BW. Crystal structure of the regulatory subunit H of the V-type ATPase of *Saccharomyces cerevisiae*. *Proc Natl Acad Sci U S A* 2001;98:7134-9.

Schafer IB, Bailer SM, Duser MG, et al. Crystal structure of the archaeal A1Ao ATP synthase subunit B from *Methanosarcina mazei* Go1: Implications of nucleotide-binding differences in the major A1Ao subunits A and B. *J Mol Biol* 2006;358:725-40.

Schaffner W, Weissmann C. A rapid, sensitive, and specific method for the determination of protein in dilute solution. *Anal Biochem* 1973;56:502-14.

Schweikl H, Klein U, Schindlbeck M, Wieczorek H. A vacuolar-type ATPase, partially purified from potassium transporting plasma membranes of tobacco hornworm midgut. *J Biol Chem* 1989;264:11136-42.

Simons K, van Meer G. Lipid sorting in epithelial cells. *Biochemistry* 1988;27:6197-202.

Skulachev VP, Sharaf AA, Liberman EA. Proton conductors in the respiratory chain and artificial membranes. *Nature* 1967;216:718-9.

Sprong H, Degroote S, Claessens T, et al. Glycosphingolipids are required for sorting melanosomal proteins in the Golgi complex. *J Cell Biol* 2001;155:369-80.

Steen H, Maring JG, Meijer DK. Differential effects of metabolic inhibitors on cellular and mitochondrial uptake of organic cations in rat liver. *Biochem Pharmacol* 1993;45:809-18.

Svennerholm L. The quantitative estimation of cerebrosides in nervous tissue. *J Neurochem* 1956;1:42-53.

Thurmond RL, Dodd SW, Brown MF. Molecular areas of phospholipids as determined by 2H NMR spectroscopy. Comparison of phosphatidylethanolamines and phosphatidylcholines. *Biophys J* 1991;59:108-13.

Valiyaveetil FI, Zhou Y, MacKinnon R. Lipids in the structure, folding, and function of the KcsA K^+ channel. *Biochemistry* 2002;41:10771-7.

Van Meer G. Lipid traffic in animal cells. *Annu Rev Cell Biol* 1989;5:247-75.

Van Meer G, Voelker DR, Feigenson GW. Membrane lipids: where they are and how they behave. *Nat Rev Mol Cell Biol* 2008;9:112-24.

Wieczorek H. The insect V-ATPase, a plasma membrane proton pump energizing secondary active transport: molecular analysis of electrogenic potassium transport in the tobacco hornworm midgut. *J Exp Biol* 1992;172:335-43.

Wieczorek H, Cioffi M, Klein U, Harvey WR, Schweikl H, Wolfersberger MG. Isolation of goblet cell apical membrane from tobacco hornworm midgut and purification of its vacuolar-type ATPase. *Methods Enzymol* 1990;192:608-16.

Wieczorek H, Grüber G, Harvey WR, Huss M, Merzendorfer H, Zeiske W. Structure and regulation of insect plasma membrane H(+)V-ATPase. *J Exp Biol* 2000;203:127-35.

Woo JT, Shinohara C, Sakai K, Hasumi K, Endo A. Isolation, characterization and biological activities of concanamycins as inhibitors of lysosomal acidification. *J Antibiot (Tokyo)* 1992;45:1108-16.

Yamaguchi M, Kasamo K. Modulation in the activity of purified tonoplast H^+-ATPase by tonoplast glycolipids prepared from cultured rice (*Oryza sativa L.* var. *Boro*) cells. *Plant Cell Physiol* 2001;42:516-23.

Yamanishi HaK, K. Effects of cerebroside and cholesterol on the reconstitution of tonoplast H^+-ATPase purified from mung bean (Vigna radiata L.) hypocotyls in liposomes. *Plant Cell Physiol* 1994;35:9.

Yamashita T, Wada R, Sasaki T, et al. A vital role for glycosphingolipid synthesis during development and differentiation. *Proc Natl Acad Sci U S A* 1999;96:9142-7.

Yoshinaka K, Kumanogoh H, Nakamura S, Maekawa S. Identification of V-ATPase as a major component in the raft fraction prepared from the synaptic plasma membrane and the synaptic vesicle of rat brain. *Neurosci Lett* 2004;363:168-72.

Young GP, Qiao JZ, Al-Awqati Q. Purification and reconstitution of the proton-translocating ATPase of Golgi-enriched membranes. *Proc Natl Acad Sci U S A* 1988;85:9590-4.

Chapter 5

Photoactivatable and clickable glucosylceramide preferentially binds to subunit c of the vacuolar-type H^+-translocating ATPase from *Manduca sexta*

Seléne van der Poel[1], Per Haberkant[1], Matthijs Kol[1], Markus Huss[2], Martin Dransmann[2], Stephan Muench[3], Helmut Wieczorek[2] and Gerrit van Meer[1]

[1] Membrane Enzymology, Bijvoet Center and Institute of Membranes, Utrecht University, Utrecht, The Netherlands

[2] Animal Physiology, Biology Division, University of Osnabrück, Germany

[3] Institute of Membrane and Systems Biology, Faculty of Biological Sciences, University of Leeds, United Kingdom

Abstract

Photoactivatable and clickable sphingolipid analogues of glucosylceramide and ceramide were incorporated into liposomes for reconstitution of the vacuolar-type H^+-translocating ATPase from *Manduca sexta*. Upon photoaffinity labelling, crosslinked products were labelled with Alexa-488 by means of click chemistry and labelled products were visualised by in-gel fluorescence. While bifunctional ceramide gave rise to stoichiometric labelling of the two transmembrane subunits, c and e, bifunctional glucosylceramide preferentially labelled subunit c. Labelling of subunit c in the V_o domain was verified as (i) stripping the V_1 domain did not affect labelling and (ii) the labelled subunit could be isolated by organic solvent extraction. Together with previous findings that pH and V-ATPase activity are affected in glycosphingolipid-deficient GM95 cells, the direct interaction between the glucosylceramide analogue and subunit c suggests a regulatory mechanism of the vacuolar proton pump by glucosylceramide. This control mechanism is of the utmost importance when it is as widely applicable as implied by the fact that both glycosphingolipids and V-ATPase are essential and evolutionary conserved in eukaryotes.

Introduction

Photoaffinity labelling has been successfully used to study a multitude of biological interactions (reviewed by Brunner, 1993). For an overview of photoactivatable groups that has been used to study protein-lipid interactions we would like to refer to a recent review (Haberkant and Van Meer, 2009). Taken the low molecular weight of lipids into consideration, the photoactivatable group should ideally be small and non-perturbing. The photoactivatable diazirine ring is the smallest photoactivatable group. Upon irradiation with ultraviolet light (UV-irradiation), nitrogen is released yielding a highly reactive carbene that then covalently links within nanoseconds to anything that is in close proximity (Ford et al., 1998; Figure 1B). This enables to take 'snap-shots' of protein-lipid interactions. Diazirine containing lipids have been used for the *in vivo* labelling of proteins interacting with phosphatidylcholine (PC), phosphatidylinositol (PI), cholesterol and sphingolipids (Thiele et al., 2000; Haberkant et al., 2008).

Gubbens et al. (2009) demonstrated the use of photoactivatable and clickable PC analogues to screen for peripheral mitochondrial proteins interacting with the headgroup of thus bifunctionalised PC species. Recently, our lab developed photoactivatable and clickable fatty acids that serve as a precursor for the (bio)chemical synthesis of a great number of bifunctionalised lipids (Haberkant et al., manuscript in

preparation). In addition to the diazirine ring, these fatty acids bear a terminal alkyne moiety. The latter serves as a non-native, non-perturbing chemical handle. After photoaffinity labelling, this group can be derivatised by means of click chemistry applying the copper(I)-catalyzed azide-alkyne cycloaddition leading to 1,2,3-triazoles (Figure 1B; bottom panel; Tornøe et al., 2002). A fluorescent label with an azide group can be covalently attached to the pac-lipids via the alkyne moiety. Interference from a bulky fluorescence group during the crosslinking event is therefore circumvented.

Here, we investigated the protein-lipid interactions of the vacuolar-type H^+-translocating ATPase (V-ATPase) isolated from the tobacco hornworm *Manduca sexta* with the bifunctional sphingolipid analogues C15pacCer and C15pacGlcCer (Figure 1A). Earlier we found indications that glycosphingolipids regulate pH, possibly via a direct interaction with the proton pump V-ATPase (Chapter 2 and 3). The reconstitution protocol that was devised utilising the V-ATPase from *Manduca sexta* in Chapter 4, was used to show there is a preferential interaction between the lipid analogue of glucosylceramide, the precursor of higher glycosphingolipids, and the proton pump V-ATPase.

Results

Probing the Protein-Lipid Interactions of the V-ATPase with C15pacCer and C15pacGlcCer

The structure of C15pacGlcCer is illustrated in Figure 1A. In order to probe the protein-lipid interactions of the V-ATPase, liposomes were prepared containing 5 mol% of C15pacCer or C15pacGlcCer as described in Materials and Methods. After reconstitution, proteoliposomes were isolated and interactions of the V-ATPase with bifunctional lipids were captured by irradiation with UV (Figure 1B). The proteoliposomes were subsequently solubilised with 1% SDS to facilitate access of the alkyne group buried in the membrane at the end of the acyl chain. Subsequently, Alexa-488-azide was coupled to crosslinked products to visualise photoaffinity labelled subunits of V-ATPase by in-gel fluorescence (Figure 1B).

C15pacGlcCer preferentially binds subunit c

The V-ATPase consists of a large number of subunits that are organised in a transmembrane domain V_o and a cytosolic domain V_1 (Figure 2A). The stoichiometry of the transmembrane spanning subunits c, a and e is 10:1:1 (c:a:e) according to the model derived from cryo-electron microscopy (cryo-EM) (Muench et al., 2008). Assuming random protein-lipid interactions, the lipid analogues label these subunits in the same molar ratio. C15pacGlcCer labelled one subunit, with similar migration behaviour as subunit c (Figure 2B). The subunits as indicated in Figure 2B were

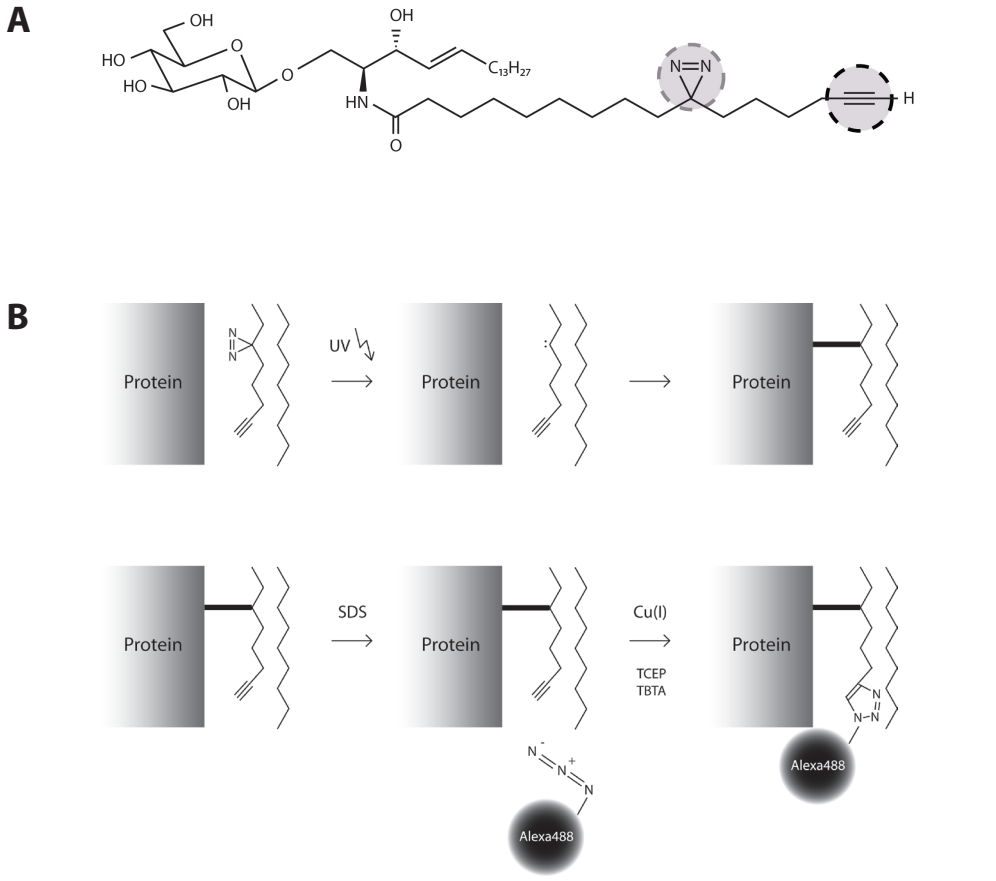

Figure 1. Photo-activatable, clickable glucosylceramide labels proteins and is visualised with fluorescence. (A) Structure of C15pacGlcCer. The overall structure of pac-lipids is built up from a (glucosyl-)sphingosine and incorporated bifunctionalised fatty acid, consisting of 15 carbon atoms (C15) (Haberkant et al., manuscript in prep.). C15pacGlcCer has a diazirine group (circled with grey dashed line) and an alkyne group (circled with black dashed line) located in the acyl chain. (B) Crosslinking of proteins by pac-lipids and fluorescent labelling. Schematic representation of the crosslinking event (top cartoon); upon UV-irradiation (left panel), the photolabile diazirine group disintegrates into N_2 and a highly reactive carbene is left on the acyl chain (center panel). The carbene group can react to anything in close proximity within nanoseconds and a covalent bond is made (right panel). The bottom cartoon shows the click chemistry procedure; the alkyne group buried in the membrane at the end of the acyl chain is made accessible for click chemistry by incubation with SDS (center panel). Then the azide-Alexa-488 was added with copper catalyst (Cu(I)), TCEP and TBTA for a 1,3-dipolar cycloaddition between alkyne and azide to covalently bind the Alexa-488 to the lipid acyl chain (right panel). Procedures are described in more detail in Materials and Methods.

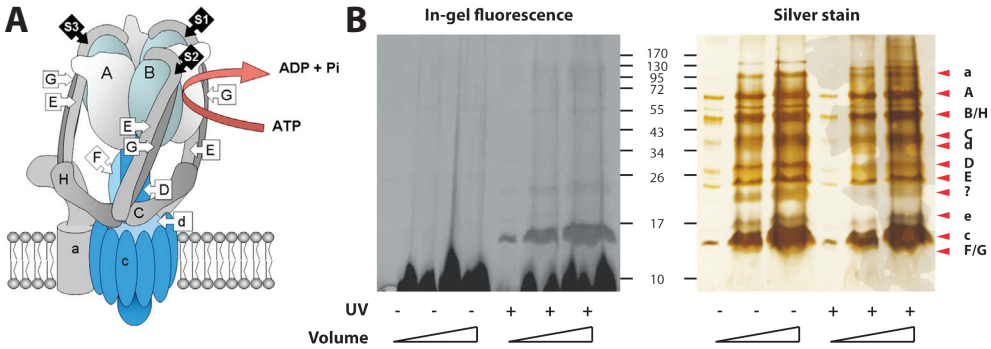

Figure 2. C15pacGlcCer preferentially labels subunit c. (A) Model of V-ATPase of *Manduca sexta* based on the cryo-EM structure. Subunits in the cytosolic domain V_1 and membrane-associated domain V_o complex are indicated with capital letters and small letters respectively. Cryo-EM could not distinguish subunit e from subunit a in the V_o domain. Picture taken from Muench et al. (2009). (B) The purified V-ATPase from *Manduca sexta* was reconstituted in liposomes of PC/SM/pacGlcCer/Chol (35/15/5/45 mol%) according to the protocol in Materials and Methods. Samples were UV-irradiated and labelled with Alexa-488-azide by means of click chemistry. Subunits were separated on a 17% SDS-gel, labelled subunits were visualised with in-gel fluorescence. The gel was subsequently stained with silver as described in Materials and Methods. Subunits of the transmembrane domain V_o and cytosolic domain V_1 are indicated with small and capital letters respectively. Three amounts of sample (1, 5 and 10 µg protein) with and without UV-irradiation were loaded.

previously identified with mass spectrometry (Huss and Wieczorek, 2007). Subunits a and e were not labelled, as no labelling was detected after loading ten-fold of the sample on gel (Figure 2B). The molar ratio 10:1:1 is the number of copies of the subunits present in the membrane, however the protein-lipid interface is the actual determinant for lipid binding. The cryo-EM model data was used to calculate the protein-lipid interface of the transmembrane subunits. As cryo-EM did not allow to distinguish between subunits a and e, the calculated protein-lipid interface of the ring of c subunits and subunits a and e was 5250 Å^2 and 7250 Å^2 respectively. Notably, even though there are more copies of subunit c present, the protein-lipid interface of the rotor of c subunits is smaller than subunits a and e, thereby stressing there is a preferential interaction between subunit c and C15pacGlcCer.

To gain insight into the specificity of the binding of C15pacGlcCer we made use of C15pacCer for comparison. C15pacGlcCer labelled subunit c and C15pacCer labelled subunits c and e while protein levels were similar (Figure 3A). Irradiation with UV affected the integrity of some unlabelled subunits (indicated with *; Figure 3A). The fluorescence intensity was quantified in at least four independent experiments comparing subunits labelled with C15pacCer (grey line) and C15pacGlcCer (black line) (Figure 3B). Histograms of lanes were normalised by setting the highest intensity

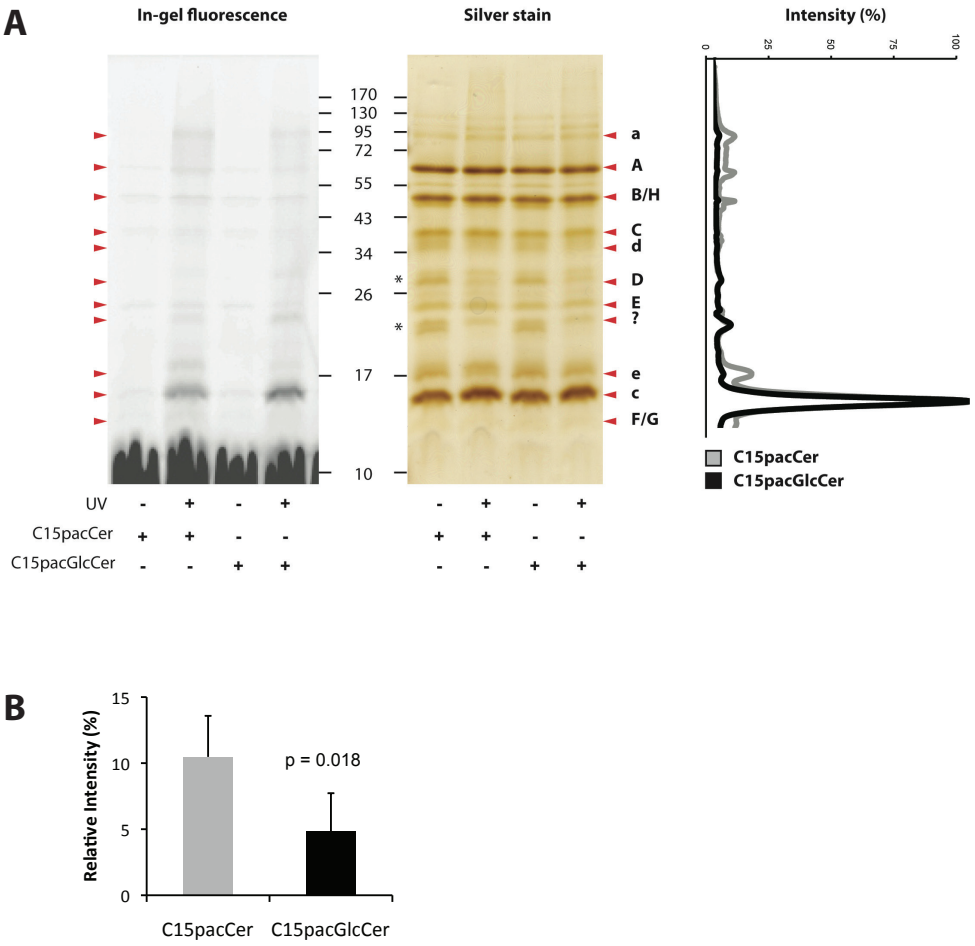

Figure 3. C15pacCer labels subunits c and e. (A) Labelling of subunits from the V-ATPase by C15pacCer and C15pacGlcCer. The V-ATPase was reconstituted in liposomes with either C15pacCer (lanes 1-2) or C15pacGlcCer (lanes 3-4) and samples were UV-irradiated (lanes 2 & 4) or not (lanes 1 & 3). Subunits were separated on 17% SDS-PAGE, labelled subunits were visualised with in-gel fluorescence. The gel was subsequently stained with silver as described in Materials and Methods. Subunits of the transmembrane domain V_o and cytosolic domain V_1 are indicated with small and capital letters respectively. Areas of subunits presumably affected by UV irradiation are indicated by (*). (B) Quantification of the in-gel fluorescence. The quantification was performed for n=4 in which the signal for subunit c was set at 100%. One representative experiment is shown. (C) C15pacCer labels subunit e. The labelling of the subunit e with C15pacCer was expressed relative to the labelling of subunit c. Quantification of the peak of subunit e with C15pacCer and C15pacGlcCer (n=4). The labelling of subunit e by C15pacCer is significantly different compared to the labelling by C15pacGlcCer as determined with Student-T-test.

at 100%. C15pacCer labelling gave rise to a second band with slightly slower migration behaviour than the prominently labelled band. The relative fluorescence intensity of this additional band, which is probably subunit e, was approximately 10% and was significantly different when the labelling with C15pacCer was compared with labelling with C15pacGlcCer (Figure 3C).

The protein-lipid interface of subunit e was estimated using the number of accessible alpha-helices. Subunit e is expected to have one or two alpha-helices (Merzendorfer et al., 1999) while the rotor has fourteen accessible outer helices (Figure 5). Comparison of the number of freely accessible alpha-helices of the ring of c-subunits (14) and subunit e (1 to 2) would result in an accessible protein surface ratio of subunit c against e of 14:1 to 7:1 (c:e). This reflects the difference in relative fluorescence intensity found for subunit e of approximately 10%. Therefore, on basis of the number of freely accessible alpha-helices, C15pacCer labelled subunits c and e stoichiometricly.

V_1 domain stripping and organic solvent extraction

Subunits F and G were not separated from subunit c and showed similar migration behaviour (Figures 2 and 3A). In order to verify the identity of the subunit labelled by C15pacGlcCer, we made use of the architecture of the V-ATPase (reviewed by Forgac, 2007). The subunits F and G are both part of the cytosolic V_1 domain while subunit c is located in the transmembrane V_o domain. The cytosolic V_1 domain was stripped from the transmembrane V_o domain under high pH conditions as described in Materials and Methods. Stripping removed most of the subunits of the V_1 domain and did not affect fluorescent labelling (Figure 4A). The fluorescently labelled band in the UV-irradiated lanes indicated with (*) was not decreased while protein was removed upon stripping. This band is most likely the band of 26 kDa that was identified previously as a dimer of subunit c by N-terminal sequencing (Huss et al., 2002). Subunits F and G were separated from subunit c (Figure 4A) and removed by stripping without affecting fluorescence intensity. Therefore, the prominently labelled band is part of the V_o domain.

Both subunits c and e are located in the V_o domain and have similar migration behaviour (Figures 2, 3 and 4A). In order to distinguish between these subunits, we used a specific characteristic of subunit c. As this subunit is almost exclusively located within the membrane, it is extremely hydrophobic and thus can be extracted with organic solvents (Finbow & Harrison, 1997). Upon photoaffinity labelling and subsequent tagging with Alexa-488, the organic extraction was performed according to procedure (i) in Materials and Methods (Figure 4B). Most of the subunits precipitated in the organic phase. Addition of the waterphase removed remaining subunits A and B as can be seen in the interphase. Washing steps of the precipitate of the organic

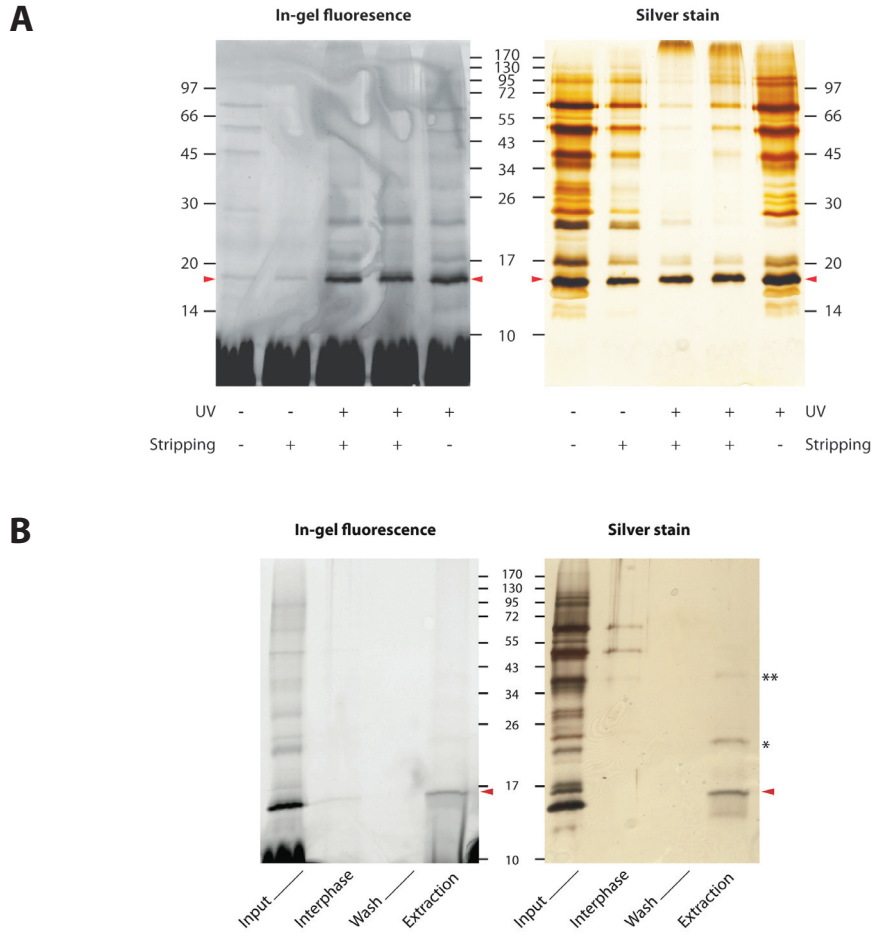

Figure 4. Identification of subunit c. (A) The prominently labelled subunit is a membranous subunit. The cytosolic domain V_1 was stripped from the V_1/V_o complex by incubation at pH 12 before the centrifuge step at high speed. The samples were UV-irradiated (lanes 3-5) or not (lanes 1-2). Stripping was done without UV (lane 2), after UV irradiation (lane 3), before UV irradiation (lane 4) or not (lane 5). Subsequently, labelling with Alexa-488 was done, samples were separated on a 17% SDS-PAGE gel and labelling was visualised with in-gel fluorescence. The gel was stained with silver. Possible dimer of c-subunits is indicated with (*). (B) The prominently labelled subunit is a proteolipid. The reconstituted protein was UV-irradiated, Alexa-488 was attached and the proteolipid was extracted with chloroform/methanol as described in Materials and Methods according to protocol (i). Equal amounts of samples of the Input (lane 1 'I'), Interphase (lane 2, 'In'), Wash (lane 3 'W') and Extraction (lane 4 'E') were separated on a 17% SDS-PAGE gel, visualised with in-gel fluorescence and subsequently silver stained. Possible dimer and trimer of c-subunits are indicated with (*) and (**) respectively.

phase with acetone/ethanol were done to remove lipids. One fluorescently labelled subunit was found in the extract with comparable migration behaviour to the prominently labelled band of the starting material, indicated with the arrow. The bands detected in silver staining (Figure 4B), are possibly the dimer of 26 kDa and a trimer of subunit c (Huss et al., 2002; Lepier, et al., 1996), indicated with (*) and (**) respectively. In conclusion, since the prominently labelled subunit was part of the V_o domain and was extracted with chloroform/methanol, the labelled subunit was identified as subunit c.

Discussion

Here we report that photoactivatable and clickable analogues of glucosylceramide (GlcCer) and ceramide (Cer) labelled the V-ATPase from *Manduca sexta*. The V-ATPase was reconstituted in proteoliposomes with 5 mol% C15pacCer or C15pacGlcCer. C15pacGlcCer preferentially crosslinked subunit c in the transmembrane domain V_o. Labelling of subunit c was verified by (i) stripping the cytosolic V_1 domain did not affect fluorescent labelling and (ii) the labelled subunit was isolated with organic solvent extraction. C15pacCer fluorescently labelled two subunits, subunit c and e in a 10:1 (c:e) ratio reflecting the protein-lipid interface.

The transmembrane domain V_o consists of several subunits, namely subunits a, c and e. Figure 5 shows a model of the organisation of the subunits a, c and e, based on the cryo-electron microscopy study of the V-ATPase from *Manduca sexta* (Muench et al., 2009). The placement of the helices of the c subunits, forming the rotor, was based on the crystal structure of the rotor of the Na^+-V-ATPase from *Enterococcus hirae* (Murata et al., 2005). Compton et al. (2006) modelled subunit e in contact with the rotor and subunit a based on interaction data. Taking the size reports of dipalmitoyl phosphatidylcholine (dipalmitoylPC) (Petrache et al., 2000; Thurmond et al., 1991; Chiu et al., 2002) and rotor dimensions (Murata et al., 2005) into account, 21 lipids were calculated to surround the rotor domain. Assuming protein and lipid recovery of 50 % (Chapter 4), about 60 molecules V-ATPase and 1200 lipid analogues for every V-ATPase is expected per proteoliposome. Even if the number of V-ATPase molecules in proteoliposomes varied greatly, there was a large excess of lipid analogues present.

Without specificity, labelling with the lipid analogues would reflect the protein-lipid interface of the V-ATPase. Notably, even though C15pacCer labelled two of the three subunits, subunit a was not labelled. The cryo-EM study of the V-ATPase from *Manduca sexta* showed that subunit a is accessible in the membrane for lipids (Muench et al., 2009). Either subunit a is lost during reconstitution or perhaps is not in

close proximity of C15pacCer.

UV-irradiation had an effect on the integrity of some unlabeled subunits, as can be seen in Figure 3A indicated by (*), but subunit a stayed largely intact. The recovery of subunits after reconstitution and the ATP hydrolytic activity was comparable to the input holoenzyme, therefore no loss of subunit a is expected (Chapter 4). Possibly the subunit was already lost before reconstitution, but detection of the subunit with silver stain points to the presence of subunit a. Notably, the subunits of the V-ATPase are not stained with silver according to their stoichiometry and especially in the case of subunit a, the staining is minimal (Figure 3A; Huss and Wieczorek, 2007).

The V-ATPase was found in detergent resistant membranes (Dermine et al., 2001; Gkantiragas et al., 2001; Yoshinaka et al., 2004), which are enriched in cholesterol and sphingolipids. Subunit a was not labelled by the sphingolipid analogues,

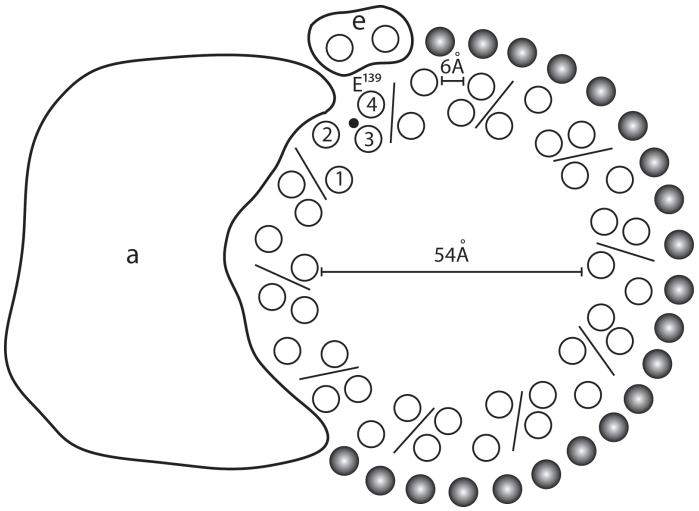

Figure 5. Model of the transmembrane subunits of the Vo domain. The orientation of subunits was derived from the model made by Muench et al. (2009). Location of the α-helices in the rotor ring of c subunits was based on the cytoplasmic projection of the rotor of the Na^+- V-ATPase (Murata et al., 2005), which was also used for the cryo-electron micrograph for *Manduca sexta* V-ATPase. One c subunit comprises of 4 helices, one helix carries the glutamate binding site for protons on the ring (E139) and the location of the sodium atoms is indicated as a black circle. Both the binding sites for the protons and sodium is located in the middle of the membrane. Lines in the rotor indicate the different subunits. The inner and outer diameter of the rotor is 54 and 83 Å respectively. The approximate location and size of subunit a was derived from the cryo-electron micrograph by Muench et al. (2009). Subunit e is placed as described by Compton et al. (2006). The rotor ring is surrounded by 21 lipids (grey circles). Protein-lipid interface was calculated from the cryo-EM data and found to be 5250 $Å^2$ and 7250 $Å^2$ for the rotor of c subunits and subunits a and e respectively.

presumably constituents of the microdomain. This suggests that the subunit is situated outside the microdomain. This would be the first report of a protein that is in two membrane environments simultaneously and has to be investigated further. For instance, by using a phospholipid pac-analogue for phosphatidylcholine (PC) in liposomes for the reconstitution of the V-ATPase one can address the presence of subunit a outside the microdomain.

It was discussed in Chapter 4 that bovine GlcCer does not resemble sphingolipids found in insects (Abeytunga et al., 2008). The lipid analogue of GlcCer used in this study has the same sphingolipid backbone of 18:0, but an acyl chain of 15 carbon atoms in length and thus resembles the endogenous sphingolipids to a greater extent. Activity assays in the presence of the pac-sphingolipids can provide insight whether GlcCer indeed has a regulatory role in the activity of the V-ATPase.

Previous findings that exogenous addition of GlcCer and GCS transfection in GM95 cells did not restore V-ATPase activity lead to the conclusion that the V-ATPase activity is independent of glycosphingolipids (Chapter 3). The finding presented here that there is a direct interaction between GlcCer and subunit c of the V-ATPase contradicts this conclusion. Interestingly, GlcCer binding to subunit c is in agreement with the binding site of the inhibitors concanamycin A and archazolid A used for the competition studies in Chapter 3. The physiological relevance of this interaction is unclear and has to be explored further. The V-ATPase and glycosphingolipids are evolutionary conserved and essential in eukaryotes (Nelson, 1992; Nelson & Harvey, 1999; Yamashita et al., 1999). This suggests that a regulatory mechanism of the V-ATPase by the glycosphingolipids forms a basic condition for life.

Materials and Methods

Materials

Chemicals, unless stated otherwise, were from Sigma-Aldrich (St. Louis, Missouri) and used in the highest purity available. All lipids and lipid standards were from Matreya (Pleasant Gap, PA), and were stored as stock solutions in $CHCl_3$/MeOH at -20°C. Phosphatidylcholine (PC) in $CHCl_3$, isolated from egg yolk (Grade I), was from LipidProds (Surrey, England).

Reconstitution of insect V-ATPase

Purification and reconstitution of the V-ATPase from *Manduca sexta* was performed as described in Chapter 4 using PC/SM/pac-lipid/Chol (35/15/5/45 mol%). The proteoliposome pellet after the 100,000 x g spin was taken up in 100 µL PBS. The sample was divided in samples of at least 20 µL in volume (20-50 µL corresponds with approximately 10-25 µg protein).

Photoaffinity labelling

Samples were irradiated applying a 200 W high pressure mercury lamp (Oriel Photomax) equipped with a pyrex glass filter to remove wavelengths below 350 nm. Samples were placed on ice at a dis tance of 35 cm from the light source and irradiated for 1 min.

Click Reaction

The following stock solutions were prepared and stored at -20°C: 25 mM tris(2-carboxyethyl)phosphine (TCEP)/KOH, pH 7.5 in H_2O (reducing agent), 2.5 mM tris(benzyltriazolylmethyl)amine (TBTA) in DMSO (ligand; stabilises Cu(I) towards disproportion and oxidation), 25 mM $CuSO_4$ in H_2O, 25 mM biotin azide in DMSO, 2 mM Alexa-488-azide in DMSO. Proteoliposomes were solubilised for 5 min at 25°C in PBS containing 1% SDS. The click reaction was performed by the stepwise addition of (i) TCEP (freshly thawed; 1 mM), (ii) TBTA (0.1 mM), (iii) $CuSO_4$ (1 mM) and (iv) Alexa-488-azide (80 µM), respectively. Final concentrations are given in brackets. Samples were vortexed and incubated for 2 h at 25°C. Proteins were separated on a 17% SDS-PAGE gel. SDS-gels were analysed by in-gel fluorescence using the Typhoon Scanner and quantified with Quantity One software (Bio-Rad). Subsequently, the gels were stained with silver according to Heukeshoven & Dernick (1988).

V_1 domain stripping

Bowman et al. (1989) described several stripping procedures for the F-ATPase and this was used as a basis for this protocol. The cytosolic domain V_1 was stripped from the V_1/V_o complex after the 1,000 x g spin, by incubation at pH 12 in 16 mM Tris-HCl, 0.3 mM EDTA, 9.6 mM 2-mercaptoethanol and 50 mM KOH for 1 h on ice. Proteoliposomes were harvested with 100,000 x g at 4°C for 1 h and the pellet was taken up in PBS. The samples were UV-irradiated for 1 min on ice and proteins were separated on a 17% SDS-PAGE gel. Gels were analysed by in-gel fluorescence and subsequently subjected to silver staining.

Organic solvent extraction

The protocol was based on Harrison et al. (1999). The reconstituted protein was UV-irradiated and samples were subjected to click reactions with Alexa-488-azide. The sample was incubated with 15 volumes of chloroform:methanol (2:1) for at least 4 h under constant agitation. An amount of 0.2 volumes of 'waterphase' (10 mM HAc, 150 mM KCl) was added and left overnight at 4°C for phase separation. The chloroform phase was isolated and processed according to one of the following two procedures: (i) the chloroform phase was dried and the precipitated protein was washed twice with acetone:ethanol (1:1). The precipitated protein was taken up in SDS sample buffer (Harrison et al., 1999). (ii) Protein was precipitated with 4 volumes ether and kept at -20°C for 1 h. The precipitated protein was pelleted with 3,300 x g for 2 h at 4°C and taken up in SDS sample buffer (Matthey et al., 1997). Subunits were separated on a 17% SDS-PAGE gel and crosslinked products were visualised by in-gel fluorescence. Subsequently, gels were subjected to silver staining.

References

Abeytunga DT, Oland L, Somogyi A, Polt R. Structural studies on the neutral glycosphingolipids of *Manduca sexta*. *Bioorg Chem* 2008;36:70-6.

Bowman BJ, Dschida WJ, Harris T, Bowman EJ. The vacuolar ATPase of *Neurospora crassa* contains an F1-like structure. *J Biol Chem* 1989;264:15606-12.

Brunner J. New photolabeling and crosslinking methods. *Annu Rev Biochem* 1993;62:483-514.

Chiu SW, Jakobsson E, Mashl RJ, Scott HL. Cholesterol-induced modifications in lipid bilayers: a simulation study. *Biophys J* 2002;83:1842-53.

Compton MA, Graham LA, Stevens TH. Vma9p (subunit e) is an integral membrane V_0 subunit of the yeast V-ATPase. *J Biol Chem* 2006;281:15312-9.

Dermine JF, Duclos S, Garin J, et al. Flotillin-1-enriched lipid raft domains accumulate on maturing phagosomes. *J Biol Chem* 2001;276:18507-12.

Finbow ME, Harrison MA. The vacuolar H+-ATPase: a universal proton pump of eukaryotes. *Biochem J* 1997;324 (Pt 3):697-712.

Ford F, Yuzawa, T., Platz, M., Matzinger, S., and Fulscher, M. Rearrangement of dimethylcarbene to propene: study by laser flash photolysis and ab initio molecular orbital theory. *J Am Chem Soc* 1998;120:4430-8.

Forgac M. Vacuolar ATPases: rotary proton pumps in physiology and pathophysiology. *Nat Rev Mol Cell Biol* 2007;8:917-29.

Gkantiragas I, Brugger B, Stuven E, et al. Sphingomyelin-enriched microdomains at the Golgi complex. *Mol Biol Cell* 2001;12:1819-33.

Gubbens J, Ruijter E, de Fays LE, et al. Photocrosslinking and click chemistry enable the specific detection of proteins interacting with phospholipids at the membrane interface. *Chem Biol* 2009;16:3-14.

Haberkant P, Schmitt O, Contreras FX, et al. Protein-sphingolipid interactions within cellular membranes. *J Lipid Res* 2008;49:251-62.

Haberkant P, van Meer G. Protein-lipid interactions: paparazzi hunting for snap-shots. *Biol Chem* 2009;390:795-803.

Harrison MA, Murray J, Powell B, Kim YI, Finbow ME, Findlay JB. Helical interactions and membrane disposition of the 16-kDa proteolipid subunit of the vacuolar H(+)-ATPase analyzed by cysteine replacement mutagenesis. *J Biol Chem* 1999;274:25461-70.

Heukeshoven J, Dernick R. Improved silver staining procedure for fast staining in PhastSystem Development Unit. I. Staining of sodium dodecyl sulfate gels. *Electrophoresis* 1988;9:28-32.

Huss M, Ingenhorst G, Konig S, et al. Concanamycin A, the specific inhibitor of V-ATPases, binds to the V(o) subunit c. *J Biol Chem* 2002;277:40544-8.

Huss M, Wieczorek H. Influence of ATP and ADP on dissociation of the V-ATPase into its V(1) and V(O) complexes. *FEBS Lett* 2007;581:5566-72.

Lepier A, Graf R, Azuma M, Merzendorfer H, Harvey WR, Wieczorek H. The peripheral complex of the tobacco hornworm V-ATPase contains a novel 13-kDa subunit G. *J Biol Chem* 1996;271:8502-8.

Matthey U, Kaim G, Dimroth P. Subunit c from the sodium-ion-translocating F1F0-ATPase of Propionigenium modestum--production, purification and properties of the protein in dodecylsulfate solution. *Eur J Biochem* 1997;247:820-5.

Merzendorfer H, Huss M, Schmid R, Harvey WR, Wieczorek H. A novel insect V-ATPase subunit M9.7 is glycosylated extensively. *J Biol Chem* 1999;274:17372-8.

Muench SP, Huss M, Song CF, et al. Cryo-electron microscopy of the vacuolar ATPase motor reveals its mechanical and regulatory complexity. *J Mol Biol* 2009;386:989-99.

Murata T, Yamato I, Kakinuma Y, Leslie AG, Walker JE. Structure of the rotor of the V-Type Na^+-ATPase from *Enterococcus hirae*. *Science* 2005;308:654-9.

Nelson N. Evolution of organellar proton-ATPases. *Biochim Biophys Acta* 1992;1100:109-24.

Nelson N, Harvey WR. Vacuolar and plasma membrane proton-adenosinetriphosphatases. *Physiol Rev* 1999;79:361-85.

Petrache HI, Dodd SW, Brown MF. Area per lipid and acyl length distributions in fluid phosphatidylcholines determined by (2)H NMR spectroscopy. *Biophys J* 2000;79:3172-92.

Thiele C, Hannah MJ, Fahrenholz F, Huttner WB. Cholesterol binds to synaptophysin and is required for biogenesis of synaptic vesicles. *Nat Cell Biol* 2000;2:42-9.

Thurmond RL, Dodd SW, Brown MF. Molecular areas of phospholipids as determined by 2H NMR spectroscopy. Comparison of phosphatidylethanolamines and phosphatidylcholines. *Biophys J* 1991;59:108-13.

Tornøe CW, Christensen C, Meldal M. Peptidotriazoles on solid phase: [1,2,3]-triazoles by regiospecific copper(i)-catalyzed 1,3-dipolar cycloadditions of terminal alkynes to azides. *J Org Chem* 2002;67:3057-64.

Yamashita T, Wada R, Sasaki T, et al. A vital role for glycosphingolipid synthesis during development and differentiation. *Proc Natl Acad Sci U S A* 1999;96:9142-7.

Yoshinaka K, Kumanogoh H, Nakamura S, Maekawa S. Identification of V-ATPase as a major component in the raft fraction prepared from the synaptic plasma membrane and the synaptic vesicle of rat brain. *Neurosci Lett* 2004;363:168-72.

Chapter 6

Regulation of organelle pH by glycosphingolipids

Summarising Discussion

Even though only about 5 mol% glycosphingolipids are found in cellular membranes (Van Meer, 1989), glycosphingolipids are essential during development as a lack of these lipids was embryonically lethal in mice (Yamashita et al., 1999). A mutant cell line GM95 deficient in these lipids, was derived from the pigmented mouse melanoma cells MEB4 (Ichikawa et al., 1994). The first observation was that pigmentation is lost in the mutant glycosphingolipid-deficient GM95 cells. This was caused by mislocalisation of tyrosinase, the rate-limiting enzyme in pigment synthesis (Sprong et al., 2001). We were able to locate the sorting signal in the lumenal domain of melanocytic proteins (Groux-Degroote et al., 2008). Subsequently, we found that a lumenal determinant, pH, was less acidic in the TGN and lysosomes of mutant GM95 cells compared to the wild-type MEB4 cell line (Chapter 2). Interestingly, the pH in both organelles of GM95 was comparable to HeLa cells and mouse fibroblasts. Therefore, it is the wild-type MEB4 cell line that has an abnormally low pH in its TGN and lysosomes. A similar low pH was found in a different melanocyte cell line, Melan-a (Chapter 2). As far as we know, this is the first study reporting that melanocytes have an exceptionally low pH in the TGN and lysosomes. The pH in GM95 organelles was lowered to the level of wild-type cells after restoration of the glycosphingolipid content by transfection with the missing glucosylceramide synthase (GCS). In this thesis, we addressed the question how glycosphingolipids regulate the pH.

In the cell line lacking glycosphingolipids, we found that two determinants of lumenal pH were affected: (1) We stumbled upon a novel GCS-dependent pathway for the expression of the putative anion channel Oca2. (2) In addition, the activity of the vacuolar-type H^+-translocating ATPase (V-ATPase) was 2-3 fold reduced in the GM95 cells. Competition studies and labelling with photoactivatable and clickable GlcCer analogues indicate that the V-ATPase may be regulated via a direct interaction with glucosylceramide (GlcCer), the precursor of the higher glycosphingolipids. Glycosphingolipids have been implicated in functions as the impermeability barrier of the plasma membrane, cell-cell interactions and signalling (Simons and Van Meer, 1988; Hakomori, 2002; 2004). The identification of two additional functions of glycosphingolipids, regulation of gene expression and pH, assigns to the glycosphingolipids a versatile and central role in cell physiology.

Lumenal pH regulation by glycosphingolipids

We have shown that two different determinants of pH, Oca2 and the V-ATPase, were affected in GM95 cells (Chapters 2 and 3). This leads to the question whether and how glycosphingolipids regulate the pH at the molecular level.

Oca2

Oca2 is absent in glycosphingolipid-deficient cells and the presence of its mRNA was restored upon placing back the ability to synthesise glycosphingolipids in GM95 by transfection with the GCS (Chapter 2). Either the stability of the mRNA or Oca2 transcription depended on the presence of an active GCS. Because it is unlikely that with a typical half-life of minutes to hours (Hollams et al., 2002) a change in mRNA stability would result in the complete absence of the mRNA in GM95 cells, the question becomes how a product of the GCS could be required for Oca2 transcription. Activation of a number of known lipid-mediated signalling pathways did not induce Oca2 transcription. Interestingly, it has been reported that one signalling pathway using the transcription factor LXR may involve its binding to a glucose (Mitro et al., 2007). The apparent contradiction between the central dogma about the hydrophobic nature of the nuclear receptor-ligand interaction on the one hand, and the hydrophilic nature of glucose and its low affinity for LXR on the other (Lazar and Wilson, 2007), would be resolved if the actual ligand were a glucose-lipid like glucosylceramide, -sphingosine or -sterol. All of these can be produced by the GCS.

The V-ATPase

Under physiological conditions, the V-ATPase builds up a proton gradient and membrane potential by pumping protons into the organelle lumen (Figure 1A). In wild-type melanocytes, Oca2 may decrease the membrane potential by channelling anions into the lumen enabling the V-ATPase to pump in more protons and further acidify the lumen. The rate of pumping would depend on the height of the membrane potential (Chapter 2). The passive proton leak is presumed equal in both cell lines. The membrane permeability is decreased by sphingolipids in the apical membrane of epithelial cells (Simons and Van Meer, 1988). When glycosphingolipids are absent, permeability is increased, therefore increasing proton leak. This would decrease the proton gradient and the V-ATPase would be able to pump more protons in the lumen. However, we see a decrease in activity in the absence of glycosphingolipids. Therefore, proton leak is not likely to generate the observed difference in V-ATPase activity.

The difference in V-ATPase activity between GM95 and MEB4 cells is independent of the presence of a built-up proton gradient and membrane potential. In the absence of gradients, Oca2 and proton leak do not influence V-ATPase activity as no membrane potential is built up (Figure 1B). This leads to the question what causes the difference in specific activity between the two cell lines.

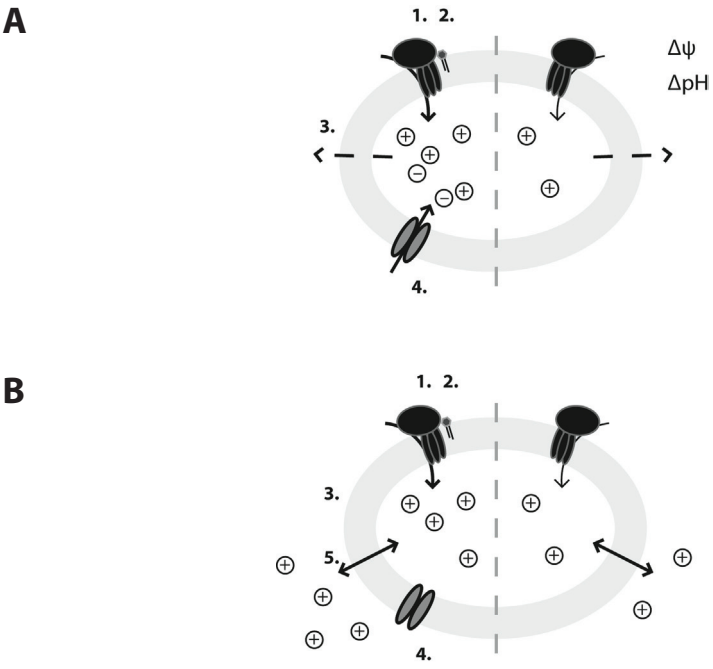

Figure 1. Regulation of lumenal pH in MEB4 and GM95 cells. A model of how lumenal pH is regulated in isolated membranes from MEB4 (left) and GM95 (right), devided by the grey dashed line. (A) The V-ATPase (1.), in MEB4 in the presence of glycosphingolipids (2.), builds up a proton gradient (ΔpH) and membrane potential (Δψ) by pumping protons into the lumen. The passive proton leak (3.) is presumably the same in both cell lines and balances proton pumping. Oca2 (4.) channels anions into the lumen thereby decreasing the membrane potential and the V-ATPase is able to pump in more protons. (B) When the proton gradient and membrane potential are dissipated by the protonophore carbonyl cyanide m-chlorophenylhydrazone (CCCP; 5.), proton leak (3.) is abolished and Oca2 (4.) will not channel anions. The difference in V-ATPase (1.) activity from MEB4 and GM95 membranes is maintained, thereby suggesting there is a difference in V-ATPase functionality, which may depend on glycosphingolipids (2.).

Membrane Environment

The V-ATPase was found in detergent resistant membranes enriched in cholesterol and sphingolipids (Dermine et al., 2001: Gkantiragas et al., 2001; Yoshinaka et al., 2004). The lack of glycosphingolipids can affect the membrane environment, which in turn can influence the function of the V-ATPase. Indeed, in the presence of cholesterol the reconstituted V-ATPase from *Manduca sexta* was more active compared to PC alone presumably because cholesterol greatly orders the acyl chains of PC creating a membrane that resembles more the physical properties of a microdomain (Chapter 4).

Missorting of the V-ATPase can lead to a different membrane environment of the enzyme. Notably, sphingolipids are found in a gradient from the Golgi to the plasma membrane, where they are enriched (reviewed by Holthuis and Levine, 2005). The membrane environment can perhaps affect the integrity of the rotary mechanism or the structure of the rotor of c-subunits in the membrane.

Direct binding

We found indications that there is a direct binding between the glycosphingolipids and the V-ATPase. Inhibition constants (apparent K_i) of concanamycin A and archazolid A with an overlapping binding site on subunit c of the transmembrane domain V_o, were three-fold higher for the V-ATPase in the wild-type MEB4 cells (Chapter 3). Apparently when glycosphingolipids are present, more molecules of inhibitor are required for complete inhibition. Interestingly, the apparent K_i of apicularen A, which has a different binding site on the same subunit c, was independent of glycosphingolipids. This suggests glycosphingolipids and the inhibitors concanamycin A and archazolid A compete for binding. Alternatively, it is due to an allosteric effect.

We explored a possible lipid-protein interaction with the reconstituted V-ATPase from *Manduca sexta* and photoactivatable and clickable lipid analogues of GlcCer and Cer, C15pacGlcCer and C15pacCer (Chapter 5). We found that C15pacGlcCer preferentially binds to subunit c, which is in agreement with the binding site of concanamycin A and archazolid A (Bowman et al., 2004; Huss et al., 2005; Whyteside et al., 2005). This indicates that GlcCer interacts with the V-ATPase and binds subunit c. The binding site of concanamycin A is located at the cytosolic leaflet of the rotor, between two c-subunits in *Neurospora crassa* (Bowman et al., 2006). Interestingly, only GlcCer has excess to the cytosolic leaflet as it is synthesised there and has to flip to the lumenal side of the membrane for conversion to higher glycosphingolipids. The constant synthesis and removal of GlcCer on the cytosolic leaflet can constitute a regulatory mechanism.

This leads to the question how a direct binding can affect the V-ATPase activity. A compelling explanation would be that GlcCer acts as grease in the rotary motor and influence the rate of turning of the rotor ring of c-subunits. The V-ATPase in MEB4 membranes would reach a steady state sooner than GM95 but, given enough time, the activity of V-ATPase in GM95 would eventually reach the activity of MEB4. However, the timecourse experiment of V-ATPase activity in membranes from both cell lines (Chapter 3) shows that the activity in GM95 never reaches an activity comparable to MEB4. Interestingly, a mutagenesis study by Kawasaki-Nishi et al. (2001) of the yeast V-ATPase showed that binding of protons is a rate-limiting step for proton translocation and ATP hydrolytic activity. It is plausible that binding of GlcCer to subunit c can alter the three-dimensional structure and possibly increase the affinity for protons at either

(1) the subunit c or (2) at the hemichannel in subunit a (Figure 2). Binding of GlcCer to subunit c may change the proton-binding site on the rotor thereby increasing affinity for protons. Alternatively, GlcCer may facilitate the transfer of protons from the hemichannel in subunit a on the cytosolic surface to the proton-binding site on the rotor, which is located in the middle of the membrane. Consequently, the presence of GlcCer on the lumenal side of the organelle is required to optimise the proton hopping off the rotor.

Interestingly, a study by Kawasaki-Nishi et al. (2001) of the yeast V-ATPase showed that when proton transport is abolished, the V-ATPase activity is only reduced to 24% compared to wild-type, which is probably due to uncoupling of ATP hydrolysis and proton translocation. This uncoupling mechanism can clarify the seeming contradiction that a 2-fold difference in V-ATPase activity can result in a pH difference of 2 pH units, or 100 fold difference in proton concentration.

V-ATPase regulation independent of glycosphingolipids

The competition studies and direct interaction between subunit c and GlcCer indicate there is a direct effect of glycosphingolipids on the V-ATPase activity (Chapter 3 and 5). We addressed this question with two different methods, (1) exogenous addition of glycolipids to isolated membranes (Chapter 3) and (2) reconstitution of V-ATPase from *Manduca sexta* in defined liposomes (Chapter 4). Since the higher glycosphingolipids LacCer and GM3 were not needed for restoring the pigmentation phenotype in GM95 cells, GlcCer was used (Chapter 3; Groux-Degroote et al., 2008). Contrary to our hypothesis, exogenous addition of GlcCer or the presence of GlcCer in the proteoliposomes did not affect the activity of the V-ATPase. Additionally, the addition of the inhibitor of glycosphingolipid synthesis PDMP, that made the lysosomal pH less acidic in MEB4 cells, did not affect the V-ATPase activity (Chapter 2).

These findings suggest there is no direct effect of the GlcCer on the V-ATPase activity. Alternatively, the glycolipid perhaps affects a process before the V-ATPase ends up in the endosomal system, for example in assembly and processing of the V-ATPase resulting in a less functional enzyme. Therefore, we probed the V-ATPase activity in the GM95 cells retransfected with GCS (Chapter 3). The V-ATPase activity was not restored to wild-type levels in these cells. This implies that the difference in V-ATPase activity is not dependent on glycosphingolipids. Previously, we found that aberrant glycosylation of PMEL17 was not restored in GM95 cells upon retransfection of GCS (Groux-Degroote et al., 2008). GM95 cells were generated using an antibody recognising α2,3-sialic acid and indeed have a glycosylation defect which is only partly restored in GM95-GCS cells as determined with lectin blots (Supplemental Figure S2; Chapter 3). The accessory regulatory subunit of the V-ATPase, Ac45, is heavily glycosylated (Supek et al., 1994; Schoonderwoert et al., 2002). Interestingly, retransfection

of GCS in GM95 cells did not restore a strong signal on the lectin-blot corresponding to the predicted molecular size of Ac45 (Supplemental Figure S2; Chapter 3). Whether Ac45 has an effect on the V-ATPase remains to be determined. This example demonstrates that one should realise that a mutant cell line such as GM95 induced by clonal selection, may harbour other mutated traits induced by the method of selection. Knock-out or knock-down in wild-type cells or retransfected mutant cells are important tools to independently assess the function of a protein or molecule.

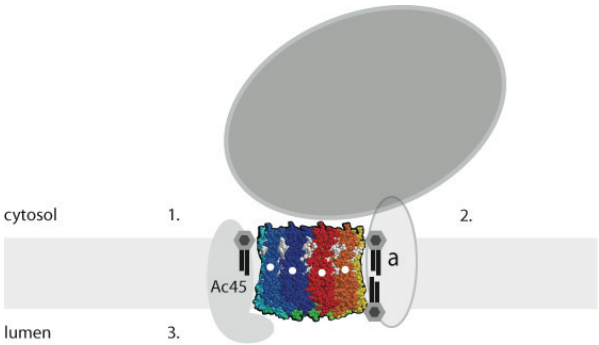

Figure 2. V-ATPase regulation. The rotor of c-subunits is a model based on the rotor in *Neurospora crassa*, picture is modified from Bowman et al. (2006). Colered spheres are individual amino acids and the colours indicate separate c-subunits. The amino acids involved in the concanamycin A binding site are indicated in grey spheres. The location of the proton binding sites on the rotor are indicated with white circles. V-ATPase activity can be influenced by membrane environment (not shown). A direct interaction between glycosphingolipids and the subunit c can lead to changes in the three dimensional structure of the rotor and (1.) increase the affinity for proton binding on subunit c (white circles) or (2.) facilitate efficient proton transfer from the hemichannel in subunit a to subunit c. Alternatively, the heavily glycosylated accessory regulatory subunit Ac45 (3.) is affected in glycosphingolipid-deficient cells.

Outlook

We set out to investigate the role of glycosphingolipids in the regulation of the lumenal pH and found that two determinants of pH, Oca2 and V-ATPase, were affected in the GM95 cells. The transcription of Oca2 is dependent on an active GCS and the products of this enzyme may act as an activator for a novel glycolipid-mediated transcription pathway, which should be investigated further. GlcCer binds to the V-ATPase directly, however the V-ATPase activity could not be restored by exogenous addition of GlcCer or retransfection of GCS in GM95 cells. This suggests that the V-ATPase is

independent of glycosphingolipids. Glycosylation of the regulatory accessory subunit Ac45 is possibly affected in GM95 cells and may result in a decreased V-ATPase activity although this remains to be determined. Although the V-ATPase activity was not restored by retransfection of GCS in GM95 cells, GCS did restore pH in the TGN and lysosomes and Oca2 transcription (Chapter 2). The putative anion channel Oca2 is perhaps able to facilitate lowering of the lumenal pH despite a disabled V-ATPase.

The significance of the binding between the GlcCer and subunit c of the V-ATPase remains unclear and should be investigated further. Since both the V-ATPase and glycosphingolipids are essential and evolutionary conserved in eukaryotes, the two may have co-evolved (Nelson, 1992; Nelson & Harvey, 1999; Yamashita et al., 1999). This would be the first example that glycosphingolipids affect protein function via a direct interaction. If glycosphingolipids regulate pH, two important physiological parameters are interlinked and would constitute an ancient regulatory mechanism essential for eukaryotic life. Unlocking this novel pathway will shed new light on diseases related to pH but also to glycosphingolipids. This encompasses a broad range of diseases such as renal disease, bone disease, tumor metastasis and lysosomal storage diseases.

References

Bowman BJ, McCall ME, Baertsch R, Bowman EJ. A model for the proteolipid ring and bafilomycin/concanamycin-binding site in the vacuolar ATPase of *Neurospora crassa*. *J Biol Chem* 2006;281:31885-93.

Bowman EJ, Graham LA, Stevens TH, Bowman BJ. The bafilomycin/concanamycin binding site in subunit c of the V-ATPases from *Neurospora crassa* and *Saccharomyces cerevisiae*. *J Biol Chem* 2004;279:33131-8.

Dermine JF, Duclos S, Garin J, et al. Flotillin-1-enriched lipid raft domains accumulate on maturing phagosomes. *J Biol Chem* 2001;276:18507-12.

Feng H, Cheng T, Pavlos NJ, et al. Cytoplasmic terminus of vacuolar type proton pump accessory subunit Ac45 is required for proper interaction with V(0) domain subunits and efficient osteoclastic bone resorption. *J Biol Chem* 2008;283:13194-204.

Forgac M. Vacuolar ATPases: rotary proton pumps in physiology and pathophysiology. *Nat Rev Mol Cell Biol* 2007;8:917-29.

Gkantiragas I, Brugger B, Stuven E, et al. Sphingomyelin-enriched microdomains at the Golgi complex. *Mol Biol Cell* 2001;12:1819-33.

Grabe M, Oster G. Regulation of organelle acidity. *J Gen Physiol* 2001;117:329-44.

Groux-Degroote S, van Dijk SM, Wolthoorn J, et al. Glycolipid-dependent sorting of melanosomal from lysosomal membrane proteins by lumenal determinants. *Traffic* 2008;9:951-63.

Hakomori S. Carbohydrate-to-carbohydrate interaction, through glycosynapse, as a basis

of cell recognition and membrane organization. *Glycoconj J* 2004;21:125-37.

Hakomori Si SI. Inaugural Article: The glycosynapse. *Proc Natl Acad Sci U S A* 2002;99:225-32.

Hollams EM, Giles KM, Thomson AM, Leedman PJ. MRNA stability and the control of gene expression: implications for human disease. *Neurochem Res* 2002;27:957-80.

Holthuis JC, Jansen EJ, van Riel MC, Martens GJ. Molecular probing of the secretory pathway in peptide hormone-producing cells. *J Cell Sci* 1995;108 (Pt 10):3295-305.

Holthuis JC, Levine TP. Lipid traffic: floppy drives and a superhighway. *Nat Rev Mol Cell Biol* 2005;6:209-20.

Huss M, Sasse F, Kunze B, et al. Archazolid and apicularen: novel specific V-ATPase inhibitors. *BMC Biochem* 2005;6:13.

Ichikawa S, Nakajo N, Sakiyama H, Hirabayashi Y. A mouse B16 melanoma mutant deficient in glycolipids. *Proc Natl Acad Sci U S A* 1994;91:2703-7.

Kawasaki-Nishi S, Nishi T, Forgac M. Yeast V-ATPase complexes containing different isoforms of the 100-kDa a-subunit differ in coupling efficiency and *in vivo* dissociation. *J Biol Chem* 2001;276:17941-8.

Lazar MA, Willson TM. Sweet dreams for LXR. *Cell Metab* 2007;5:159-61.

Mitro N, Mak PA, Vargas L, et al. The nuclear receptor LXR is a glucose sensor. *Nature* 2007;445:219-23.

Moriyama Y, Nelson N. The vacuolar H^+-ATPase, a proton pump controlled by a slip. *Prog Clin Biol Res* 1988;273:387-94.

Nelson N. Evolution of organellar proton-ATPases. *Biochim Biophys Acta* 1992;1100:109-24.

Nelson N, Harvey WR. Vacuolar and plasma membrane proton-adenosinetriphosphatases. *Physiol Rev* 1999;79:361-85.

Schoonderwoert VT, Jansen EJ, Martens GJ. The fate of newly synthesized V-ATPase accessory subunit Ac45 in the secretory pathway. *Eur J Biochem* 2002;269:1844-53.

Simons K, Van Meer G. Lipid sorting in epithelial cells. *Biochemistry* 1988;27:6197-202.

Sprong H, Degroote S, Claessens T, et al. Glycosphingolipids are required for sorting melanosomal proteins in the Golgi complex. *J Cell Biol* 2001;155:369-80.

Supek F, Supekova L, Mandiyan S, Pan YC, Nelson H, Nelson N. A novel accessory subunit for vacuolar H(+)-ATPase from chromaffin granules. *J Biol Chem* 1994;269:24102-6.

Van Meer G. Lipid traffic in animal cells. *Annu Rev Cell Biol* 1989;5:247-75.

Whyteside G, Meek PJ, Ball SK, et al. Concanamycin and indolyl pentadieneamide inhibitors of the vacuolar H^+-ATPase bind with high affinity to the purified proteolipid subunit of the membrane domain. *Biochemistry* 2005;44:15024-31.

Yamashita T, Wada R, Sasaki T, et al. A vital role for glycosphingolipid synthesis during development and differentiation. *Proc Natl Acad Sci U S A* 1999;96:9142-7.

Yoshinaka K, Kumanogoh H, Nakamura S, Maekawa S. Identification of V-ATPase as a major component in the raft fraction prepared from the synaptic plasma membrane and the synaptic vesicle of rat brain. *Neurosci Lett* 2004;363:168-72.

Regulatie van de zuurgraad in organellen door glycosfingolipiden

Nederlandse Samenvatting

Cellen worden ook wel de 'eenheid van leven' genoemd. Hoe complexer het organisme, hoe meer cellen het heeft. Bacteriën zijn ééncelligen en bestaan dus ook maar uit 1 cel, terwijl mensen wel uit miljarden cellen bestaan. Een cel bestaat uit verschillende kleinere onderdelen, organellen genoemd. De algemene topografie van de cel is bijgevoegd in Figuur 1. In de kern of nucleus zit het erfelijke materiaal, het DNA, opgeborgen. Het DNA wordt afgelezen in de kern en het afschrift gaat naar het cytosol waar het in het endoplasmatisch reticulum omgezet wordt naar eiwitten. Dan gaan de eiwitten naar het distributie centrum van de cel, het Golgi systeem, voor de laatste kleine veranderingen en verder naar het *trans*-Golgi netwerk voor sortering naar de juiste locatie. Het transport door de cel wordt verzorgd door de endosomen. Wanneer een eiwit niet meer goed functioneert, wordt het in de lysosomen afgebroken. Mitochondrieën zijn de energiecentrales van de cel, waar de energie wordt genereert om fysiologische processen mogelijk te maken. De verschillende onderdelen worden bij elkaar gehouden door een speciaal laagje moleculen, het plasmamembraan, wat de cel beschermt voor invloeden van buitenaf.

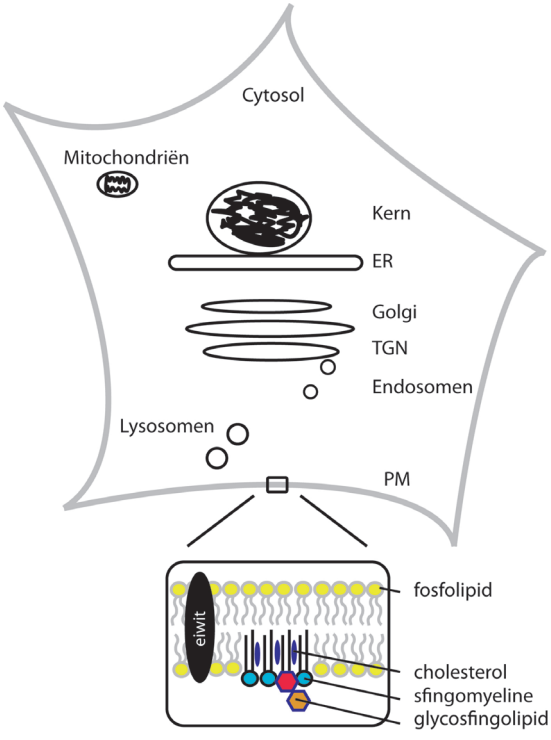

Figuur 1. Schematische weergave van een dierlijke cel. DNA wordt afgelezen in de kern, waarna het transcript in het cytosol terecht komt en in het endoplasmatisch reticulum (ER) wordt omgezet naar een eiwit. Het eiwit wordt in het ER gevouwen en vervolgens gebracht naar het Golgi, het distributie centrum van de cel. Daar aangekomen worden kleine veranderingen gemaakt, zoals suikers toegevoegd aan de buitenkant van het eiwit op gespecificeerde plekken. Dan wordt de 'postcode' afgelezen door sorteer eiwitten in het *trans*-Golgi Netwerk (TGN) en verpakt in endosomes voor transport door de hele cel. Bepaalde transmembraan eiwitten gaan bijvoorbeeld naar het plasma membraan (PM). Het PM bestaat uit verschillende lipiden, waar ook eiwitten in zitten. De lipiden hebben een bepaalde organisatie, waarbij sfingolipiden dicht bijeen pakken met cholesterol daartussen voor een optimale barrière functie van het plasma membraan.

Het celmembraan

Het plasma membraan is hoofdzakelijk gemaakt van twee ingrediënten, namelijk eiwitten die in het membraan zitten, de zogeheten transmembraan eiwitten, en de vetten ofwel de lipiden. Lipiden kunnen grofweg in drie groepen worden verdeeld, namelijk de fosfolipiden, de sfingolipiden en sterolen. Met sterolen wordt cholesterol bedoelt en is ongelooflijk belangrijk voor de mens. Problemen zoals hoge cholesterol ontstaan als er een groot overschot aan vetten is. Lipiden zijn bijzonder omdat zij zichzelf spontaan kunnen organiseren in een membraan structuur. Dat komt doordat de ene helft van een lipid van water houdt ofwel hydrofiel is en de andere helft juist water afstoot ofwel hydrofoob. In Figuur 2 worden de moleculaire structuren van de lipiden vergeleken.

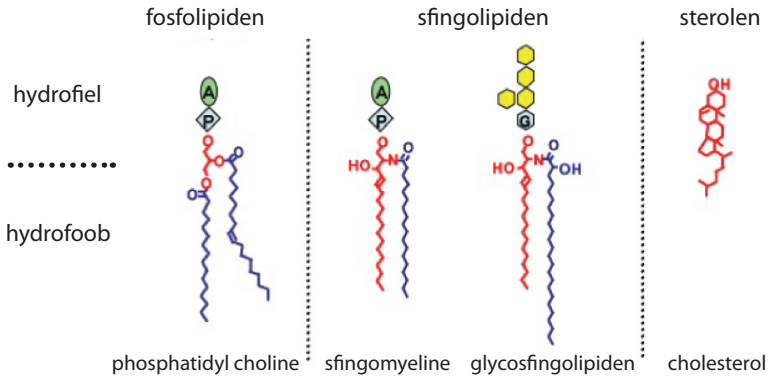

Figuur 2. Moleculaire structuren van lipiden. Lipiden kunnen grofweg in drie groepen worden verdeeld, namelijk de fosfolipiden, de sfingolipiden en sterolen. Boven de streep is het hydrofiele gedeelte van de lipiden en daarboven het hydrofobe gedeelte terwijl cholesterol voornamelijk hydrofoob is. Fosfolipiden hebben een gekromd hydrofoob gedeelte, en sfingolipiden juist een recht hydrofoob gedeelte waardoor de sfingolipiden zich dicht bijeen gepakt kunnen rangschikken. Daartussen past het cholesterol, waardoor het membraan optimaal waterdicht wordt afgesloten. P=fosfaat, G=glucose, A=choline, gele hexagon=verschillende suikers.

Het grote verschil tussen fosfolipiden en sfingolipiden is dat het hydrofobe gedeelte van fosfolipiden een gekromde structuur heeft en de sfingolipiden zijn juist recht. Dit heeft invloed op de flexibiliteot en doorlaadbaarheid van het membraan. Cholesterol is een heel erg hydrofoob molecuul en vind je geheel in het membraan. Het past precies in de ruimte tussen de hydrofobe staarten van sfingolipiden en vormt daardoor een bijzonder waterdicht geheel en hierdoor wordt de barrière functie van het plasma membraan versterkt (dit is ook geïllustreerd in Figuur 1). Lipid moleculen zullen in een waterige oplossing zich spontaan in structuren rangschikken, zodat de hydrofiele delen naar het water gericht zijn en de hydrofobe

gedeelten naar elkaar, zodat water er niet bij kan komen. Dit is ook het werkingsprincipe van zeep, als het hydrofobe vuil en vet wordt ingesloten door de zeepmoleculen en zo wordt opgelost in het afwaswater zodat de vaat weer schoon wordt.

Glycosfingolipiden
Een heel klein gedeelte van het plasma membraan, doorgaans zo'n 5%, bestaat uit glycosfingolipiden (Figuur 2). Glycosfingolipiden zijn heel speciaal omdat ze essentieel zijn voor het leven. Je kunt niet leven zonder glycosfingolipiden ook al komen ze relatief weinig voor. Deze lipiden hebben een dus speciale taak en uit onderzoek komt steeds meer naar voren dat het een uitgebreid takenpakket is. Glycosfingolipiden hebben een hydrofiel gedeelte wat bestaat uit verschillende suikers, altijd beginnend met glucose, vandaar de naam 'glycosfingolipiden'. De lipiden zijn belangrijk voor communicatie tussen cellen en spelen een rol in het correct sorteren van eiwitten, maar zijn ook belangrijk voor de kwaliteit van de barrière functie van het plasma membraan. Het onderzoek beschreven in dit boekje is gericht op een mogelijke andere belangrijke taak voor de glycosfingolipiden, namelijk het reguleren van de zuurgraad of pH in de cel.

De cellulaire pH
De zuurgraad is belangrijk voor verschillende belangrijke fysiologische processen zoals de sortering van eiwitten en de afvalverwerking van producten die in de cel overbodig zijn geworden in de lysosomen. De zuurgraad wordt gereguleerd door een grotendeels onbekend en ingewikkeld proces, wat een samenspel is van de protonen pomp en andere eiwitten. Protonen worden in organellen (zoals lysosomen) naar binnen gepompt door de vacuolaire protonen pomp (V-ATPase), waardoor het organel verzuurt. De correcte pH wordt bereikt doordat er een balans is tussen het pompen van protonen door de V-ATPase, het passief weglekken van protonen en het doorlaten van andere ionen naar binnen of naar buiten door andere eiwitten zoals bijvoorbeeld het OCA2 eiwit. Protonen zijn ook positief geladen deeltjes, waardoor het organel ook geladen wordt. Deze lading over een membraan wordt een membraan potentiaal genoemd terwijl er ook een gradiënt is van de protonen, omdat de concentratie protonen veel hoger wordt in het organel door het pompen. Andere eiwitten zorgen ervoor dat de ladingsbalans weer wordt herstelt met het doorlaten van andere ionen, die geen rol spelen in het bepalen van de zuurgraad, maar wel lading hebben.

Glycosfingolipid-deficiënte GM95 cellen
Glycosfingolipiden zijn essentieel voor het leven, maar er zijn cellen die geen glycosfingolipiden kunnen synthetiseren doordat zij het enzym missen voor de eerste stap in glycosfingolipid synthese, de GM95 cellen. Hieruit blijkt dat de lipiden belangrijk

zijn voor de ontwikkeling van een organisme.

De glycosfingolipid-deficiënte GM95 cellen worden gebruikt voor onderzoek naar de functie van deze speciale lipiden. De mutante GM95 cellen komen voort uit MEB4 cellen, het wild-type, welke zijn geïsoleerd uit de huid van een muis. Net zoals de cellen in onze huid, maken deze huidcellen pigment aan en zijn daardoor zwart (zie Hoofdstuk 2). Pigment producerende cellen worden ook wel melanocyten genoemd, waar ook melanoma, te weten huidkanker, van is afgeleid.

De eerste conclusie aangaande de functie van de glycosfingolipiden was gemakkelijk aangezien de GM95 cellen wit waren en dus geen pigment aanmaken. Hieruit is op te maken dat glycosfingolipiden nodig zijn voor pigment productie en dat GM95 cellen een pigmentatieziekte hebben. In Hoofdstuk 1 van dit boekje worden verschillende pigmentatieziekten besproken en uiteen gezet wat de oorzaken zijn. Pigmentatieziekten komen veelvuldig voor, waarvan de oculocutaneous albinisme type 2, afgekort OCA2, het meest voorkomt. Deze ziekte wordt veroorzaakt door een gebrek aan het eiwit OCA2, ook bekend als p-eiwit, waardoor geen pigment in het haar, de huid en het oog voorkomt.

De pH is afhankelijk van glycosfingolipiden

Onderzoek wees uit dat eiwitten benodigd voor pigment synthese, niet op de juiste locatie aankwamen in GM95. De informatie voor de juiste sortering (de 'postcode') werd gevonden aan de binnenkant van het eiwit, dus aan de binnenkant van een organel, terwijl normaliter dit soort informatie aan de buitenkant wordt gevonden zodat het makkelijk kan worden afgelezen. Blijkbaar werkt het signaal niet naar behoren, aangezien de eiwitten niet op de juiste locatie aankomen. We hebben we naar verschillende parameters gekeken die het milieu van een organel kan beïnvloeden, waaronder pH. In Hoofdstuk 2 hebben we de zuurgraad in de mutante GM95 cellen en het wild-type MEB4 gemeten door gebruik te maken van een fluorescent molecuul wat ook gevoelig is voor pH. Fluorescentie is een bijzondere eigenschap van moleculen, welke energie uit licht opnemen en dan in de 'aangeslagen toestand' raken om daarna weer 'terug te vallen' en dat gaat gepaard met het uitzenden van licht wat je kunt meten. Voorbeelden zijn de verkeersborden die lijken op te lichten als de autokoplamp daarop schijnt en hebben dan ook een laagje fluorescente moleculen.

Het uitgezenden van licht is eindig en de tijdspanne waarin dit gebeurt wordt 'lifetime' genoemd. Hier zijn bijzondere moleculen gebruikt, waarvan de 'lifetime', afhankelijk is van de pH. Hierdoor is het mogelijk is om pH te meten in levende cellen. De fluorescente moleculen worden gekoppeld aan antilichamen, die aan bepaalde eiwitten binden aan de buitenkant van de cel. Die eiwitten waren constant heen en weer getransporteerd en daardoor komt het fluorescente molecuul in de cel terecht (Figuur 3). Normaal worden dit soort 'vreemde' stoffen afgebroken in de cel, maar we

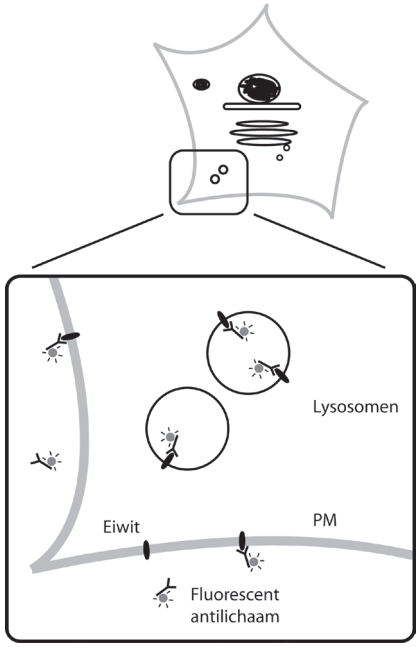

Figuur 3. Schematische weergave van antilichaam opname in levende cellen voor FLIM. Fluorescence Lifetime Imaging Microscopy (FLIM) is een techniek waarbij het verval (de lifetime) van het uitgezonden licht (fluorescentie) van een fluorescent molecuul wordt bepaald gebruik makend van een microscoop. In dit geval is dat fluorescente molecuul (grijze cirkel) gekoppeld aan een antilichaam (zwarte λ-vorm). Het antilichaam kan de levende cel niet penetreren, maar herkent een specifiek eiwit aan het plasma membraan en bindt daaraan. Vervolgens wordt het geheel de cel in gebracht en komt het fluorescent molecuul in het organel terecht waar de pH gemeten moet worden, in dit geval zijn dat de lysosomen.
Er zijn bepaalde eiwitten die van nature constant over het plasma membraan gaan, die worden 'recycled'. Normaal worden vreemde deeltjes afgebroken, maar je kunt dit voorkomen door de cellen te groeien in de aanwezigheid van een speciaal stofje.

kunnen dit voorkomen door een stofje toe te voegen aan de cellen.

De meting van de pH wees uit dat de cellen zonder glycosfingolipiden (GM95) een hogere pH hadden dan de wild-type MEB4 cellen in het TGN en de lysosomen. Ook als we de synthese van glycosfingolipiden in de wild-type cellen remden, zagen we een verandering van pH in de lysosomen, dus concludeerden we dat het gebrek aan glycosfingolipiden de oorzaak is van de hogere pH in GM95 cellen.

Oca2 expressie is glycosfingolipid-afhankelijk

Om te bepalen of dit pH effect veroorzaakt wordt door het gebrek aan glycosfingolipiden, werd de lysosomale pH gemeten in Melan cellen. Als deze melanocyten (pigment cellen uit de huid) het eiwit Oca2 of p-eiwit missen, veroorzaakt dit de pigmentatieziekte OCA2 terwijl de glycosfingolipiden niet aangetast wordt. De pH in de lysosomen was hoger in de cellen zonder Oca2 eiwit expressie. Ook de glycosfingolipid-deficiënte GM95 cellen had geen Oca2 expressie en dit werd weer herstelt door de synthese van glycosfingolipiden in GM95 cellen. Hieruit kunnen we concluderen dat de glyco-sfingolipiden de expressie van Oca2 reguleert en dat wellicht niet de lipiden, maar Oca2 de pH beïnvloed. Om dit te bewijzen, werd Oca2 terug geplaatst in GM95 cellen, maar dit repareerde niet de pigmentatie. De glycosfingolipiden spelen dus wel degelijk een rol naast Oca2 in pigmentatie en waarschijnlijk pH.

De activiteit van de V-ATPase is afhankelijk van glycosfingolipiden

De pH wordt grotendeels gereguleerd door de protonen pomp V-ATPase en al in Hoofdstuk 2 bleek dat de pomp twee keer minder actief is in GM95 vergeleken met de wild-type cellen. Dat zou de hogere pH kunnen verklaren, want als de pomp twee keer minder werkt, komen er ook minder protonen in het organel en wordt het minder zuur dus wordt een hogere pH gevonden. In Hoofdstuk 3 werd de activiteit van de V-ATPase in detail onderzocht.

In het onderzoek werd gebruik gemaakt van een specifieke remmer van de V-ATPase, concanamycine A. Dit molecuul remt alleen de V-ATPase waardoor alleen gekeken kan worden naar de V-ATPase. In de mutante GM95 cellen was minder remmer nodig voor het volledig stilzetten van de pomp. Het lijkt alsof de lipiden in de weg zitten van binding van concanamycine A, waardoor een hogere concentratie van de remmer nodig is. Andere remmers met verschillende bindingsplekken aan de V-ATPase, resulteerden in een vergelijkbare benodigde concentratie voor beide cellijnen. Dit suggereert een binding van de glycosfingolipiden aan de pomp met ofwel een direct effect door competitie te vertonen met de remmer voor dezelfde bindingsplek, of indirect door de drie-dimensionale structuur van de V-ATPase te veranderen, dus ook de bindingsplek van de remmer. Bovendien is de bindingsplaats van de remmer gelokaliseerd in het membraan, waar ook de glycosfingolipiden te vinden zijn.

Glycosfingolipiden binden direct aan de V-ATPase

Om een direct effect te laten zien van de glycosfingolipiden op de activiteit van de V-ATPase, werd de V-ATPase geïsoleerd om zo andere interfererende factoren te verwijderen en om het eiwit te plaatsen in een gedefinieerde lipiden omgeving. Dit wordt reconstitutie genoemd. Aangezien veel eiwit benodigd is, is gekozen voor V-ATPase afkomstig van een tabaksworm, *Manduca sexta*. Deze wormen leven op tabaksbladeren om dan later te metamorfoseren tot motten. In Hoofdstuk 4 zijn de reconstitutie en de activiteitsmetingen van de V-ATPase beschreven. Het effect van glucosylceramide, het meest simpele glycosfingolipid, werd bepaald. Glucosylceramide was gekozen op basis van eerdere onderzoeken waarin het, in tegenstelling tot andere glycosfingolipiden, essentieel was om de GM95 cellen te herstellen. De reconstitutie was succesvol, want de V-ATPase was behield zijn activiteit na reconstitutie, maar er was geen effect van het toevoegen van glucosylceramide. Er zijn verschillen tussen glycosfingolipiden in insecten en de glucosylceramide, geïsoleerd uit runderen, die gebruikt is voor de reconstitutie. Aangezien glycosfingolipiden en V-ATPase voorkomen in bijna elk hoger organisme en behouden zijn gebleven tijdens de evolutie, was de aanname dat hoogstens kleine verschillen zijn opgetreden en dat de V-ATPase in insecten zou reageren op glucosylceramide uit runderen. Glycosfingolipids afkomstig uit insekten zijn momenteel niet commercieel verkrijgbaar en bemoeilijkt het testen van de

hypothese.

In Hoofdstuk 5 werd gebruik gemaakt van een andere techniek om te testen of er een directe binding is tussen het lipid en de V-ATPase. Wederom werd de V-ATPase van de *Manduca sexta* gereconstituteerd in liposomen met een speciaal ingebouwd lipid. Het lipid bindt alles binnen 5.10^{-10} m (een halve miljoenste meter) onder invloed van sterk UV licht, ook wel een foto-activeerbaar lipid genoemd. Hierna wordt het lipid gemarkeerd met een fluorescent molecuul. De V-ATPase is een eiwit wat bestaat uit verschillende kleinere eiwit onderdelen van een bekende grootte. Deze eiwit onderdelen worden gescheiden op grootte in een gel met behulp van electriciteit en eiwitten kunnen zichtbaar gemaakt worden door ze met zilver te kleuren. Vervolgens kan het lipid zichtbaar gemaakt worden door te kijken naar fluorescentie en wordt duidelijk welk eiwitten gebonden zijn aan het foto-activeerbare lipid.

Het foto-activeerbare glucosylceramide bond specifiek één eiwit, subunit c. Hier bevindt zich ook de bindingsplaats van concanamycine A, de remmer waarvan de concentratie voor volledige remming afhankelijk was van de aanwezigheid van glycosfingolipiden.

Conclusie

Dit is de eerste beschrijving dat glycosfingolipiden de expressie van een eiwit, Oca2, reguleren. Tevens is het de eerste keer dat er een interactie is aangetoond tussen een glycosfingolipid, glucosylceramide, en een eiwit, de V-ATPase. Verder onderzoek moet uitwijzen hoe glucosylceramide de activiteit van de V-ATPase kan beïnvloeden en in Hoofdstuk 6 worden een aantal aanbevelingen gedaan. De rol van glycosfingolipiden in de regulatie van de zuurgraad kan tweedelig zijn, namelijk de regulatie van de eiwit expressie van Oca2 en de activiteit van de protonen pomp V-ATPase.

De glycosfingolipiden en de V-ATPase zijn beiden essentieel voor het leven en behouden gebleven tijdens de evolutie. De connectie tussen glycosfingolipiden en de V-ATPase zou dus kunnen duiden op een fysiologisch belangrijk en onmisbaar mechanisme, een basis voorwaarde voor het leven.

Dankwoord

Hier ligt ie dan...een geweldig stukje werk (al zeg ik het zelf) ! Dit was allemaal niet mogelijk geweest zonder de steun en medeleven van vele mensen ! Ik zal proberen jullie allemaal te bedanken, en nu maar hopen dat ik niemand vergeet...

Allereerst Gerrit, ik ben blij dat we het toch voor elkaar hebben ! Ik waardeerde het enorm dat je altijd ruim de tijd nam om presentaties door te nemen en dat ik altijd kon binnenlopen om je 'even snel' wat data te laten zien. Het was fijn om bewegingsvrijheid te krijgen, daar heb ik veel van geleerd. Congressen en vrijdagmiddag borrels waren altijd erg gezellig en vooral informatief. Je enthousiasme voor onderzoek werkt aanstekelijk en hopelijk zul je dat niet verliezen of worden getemperd nu je een spin bent in het politieke web van de Universiteit Utrecht.

Maarten, onze discussies over het wel en wee van de V-ATPase en de wereld heb ik erg gewaardeerd. Bedankt voor al het advies ! Hein, de eerste 1,5 jaar hebben we fijn samen gewerkt en ik wens je veel succes bij de RIVM. Erik, mijn mentor, we hebben al een tijdje geen update gedaan, of heel even op het Bijvoet Symposium, maar jouw advies was zeer belangrijk ten tijde van een belangrijke verandering in mijn PhD-leven, bedankt.

I would like to thank the people without whom this booklet would have been completely different and would not have had this colourful cover ! A big 'Danke schön' to the all the members of the Wieczorek group at the University of Osnabrück where I was a guest for five months for making me feel at home in the group. I especially want to thank Helmut and Markus for the warm welcome and professional input I enjoyed at the Tierfysiologie group and for the ongoing tremendous support I received. Martin, Danke schön für die viele(n) Preps !! Katja and Johanna, thanks for helping me with the seemingly endless phosphate determinations ! Andrea, Christin, Derek, Felix, Gunnar, Jothi, Katharina and Svenja, thanks for showing me Osnabrück and good luck with finishing your PhD and beyond ! Andrea and Jothi, I hope I have actually helped to improve your English ? Katharina, every time I see my t-shirt of the space invaders or pac-man I will think of you. Svenja, our frequent visits to the Ratskeller and Pizzeria were really fun ! This made the stay in Germany so much easier, however not for the wallet ! Hopefully we will meet again.

Natuurlijk een geweldig luide 'bedankt' aan al die mensen die hebben bij gedragen aan het tot stand komen van dit boekje. Hans en Dave van Moleculaire Biofysica, jullie zijn heel belangrijk geweest voor de basis van dit proefschrift ! Hans, bedankt voor al het advies, onafhankelijk met wat voor project ik dan ook weer mee aankwam, en alle goede zorgen. Dave, ik realiseer me dat je de dupe was van mijn ijzige vastberadenheid om alle metingen het liefst op 1 dag, maar dan toch op zijn minst binnen een paar dagen te willen doen ! Bedankt dat je altijd de deur voor me open hebt gehouden. Ik heb erg genoten van al die uren in het donker met Peter Gabriel ! Matthijs, ik vond het erg gezellig die paar weken samen proefjes doen in

Osnabrück ! Ik weet nu zelfs dat je toonladders doet onder de douche of is dat teveel info ?! Sorry dat ik geen rekening hield met je eet patroon, men raakt namelijk zo gewend aan het leven op Magnum-ijsjes… Bedankt voor al je hulp en advies over liposomen en beyond ! Per, wij hebben ook proefjes gedaan, waar Hoofdstuk 5 het resultaat van is. Er ligt zelfs nog een weekje werk wat dit boekje niet heeft gehaald. Bedankt dat jij en Bettina mij 'jullie' Heidelberg wilden laten zien tijdens die enerverende week ! Ik denk dat je wel kennis hebt gemaakt met de Nederlandse levercapaciteit…Veel succes met de PAC® lipids !

Joep & Ruud, met z'n tweeën de motor van Membraanenzymologie. Zonder jullie is het maar leeg en kaal op het lab en in de kantoren, zeker op vrijdagmiddag ! Geen warmte, geen geluid, geen bier…bedankt dat ik altijd mijn verhaal kwijt kon. Joep, heel erg bedankt voor alle hulp met de assays !! Ik hoop dat je het toch echt een keertje de stoute schoenen aantrekt en dat ik je misschien als buur kan verwelkomen in NZ ! Ook natuurlijk bedankt dat jij en Ruud mijn paranimfen willen zijn, ik vertrouw erop dat we er een feestje van gaan maken ! Sandra, mijn afleiding in N611. Als wij gingen babbelen hielden we niet meer op ! Na jouw vertrek werd het wel erg stil naast mij, maar ik kon je altijd lastig vallen met vragen op de chat ! We kwamen elkaar weer tegen toen ik ging werken met David bij Philips. Ik hoop dat je snel weer nieuwe mogelijkheden ziet na die ellende bij MSD. En hopelijk heb je binnenkort je levensweg gevonden, succes ! David, bedankt dat je mij bezig hebt willen houden in Eindhoven voor de afgelopen drie maanden bij Philips. Ik hoop dat ik een footprint heb achtergelaten zodat de roadmap van het OHC project je genoeg challenges brengt ! (even de vertaling voor de normale mens: ik hoop dat ik nuttig was). Ik wil graag ook Golo, de projectleider, bedanken voor het geven van positieve feedback over mijn kleine bijdrage.

Mijn kamergenoten over de jaren: Sophie, Jasja, Sylvia en Rob. Sophie, you were at the ME only for a short period of time while I was there, but that did not stop you from helping me during my PhD from Lille, thanks a lot for that ! In Chapter 3 you can find your lectin blots ! Jasja, jij hebt het project opgestart en ik wil je bedanken voor al je steun door de jaren heen. Sylvia, gelukkig hoor ik goede geluiden komen uit San Diego. All the best ! Rob, het was kort maar krachtig zal ik maar zeggen, bedankt voor de gezelligheid !

Joost, bedankt voor de discussies aan de lunchtafel en dat je me altijd het gevoel gaf dat ik een erg gewilde PhD-student was. Dirk en Toon, jullie bleven toch soms stiekem nog even voor de vrijdag-borrel, gezellig ! Klaartje, van jou kwamen altijd de mailtjes over vrouwen in de wetenschap, girl-power ! Veel succes met het werk en je gezinnetje ! Guillaume en Philippe, you were an inspiration. KD Lee, thank you for the inspiring lunch stories. Cécile, bedankt voor alle morele en professionele ondersteuning ! Dick, sorry dat ik altijd zoveel stuk maakte, maar jij kon het gelukkig altijd weer maken, veel plezier met overal onze afgedankte apparaten

brengen en golfen ! Catheleyne, mijn eeuwige slaapkamergenoot. Geen congres ging voorbij of we werden òf ingedeeld òf de andere kamergenoot was zo eng…ik heb erg genoten van ons nachtelijke geneuzel. Fikadu, I was always jealous of the collaboration you had with Ana, it must be so nice to have a sparring partner. All the best in Boston ! Ana, I am sorry I made you feel so bad for not joining the 'Maliebaanloop'. I will definitely invite you to the 'Saint Clair Vineyard Run' in the near future ! Good luck in New York with Andre ! Susanne, my professional matchmaker. Sense and simplicity isn't it ? Thanks for the support during the last weeks of my PhD when I was running around like a headless chicken on the lab. Good luck at Sanquin and as a groupleader at a distance ! Hanneke en Patricia; ik vind het geweldig dat er zo nu en dan een berichtje van jullie binnenkomt. Ik heb alle koffie/thee-breaks heel erg gewaardeerd en ik wens jullie alle geluk van de wereld ! I also want to thank the relatively 'new kids on the block', RK and Cedric, for the 'gezelligheid' at ME. Hanka, it is FANTASTIC that I could borrow your computer and crash it for the printing of my thesis ! Also thank you for the FANTASTIC movie moments ! Ramon, het was jammer dat je er zo kort was, maar het ga je goed ! Bedankt voor je peptalk rond kerst. Antoinette, de allernieuwste aanwinst van ME, veel succes met je spannende project.

Ik wil Adri, Ed en Martje bedanken voor het realiseren van de Masterclass. Het voelde een beetje als mijn kindje. Ook de studenten Elleke, Guus, Markus, Hilde waren hier onmisbaar !

Ook zou ik graag al onze vrienden willen bedanken; de feestjes waren altijd een goede afleiding. Voor de omslag werd ik geïnspireerd door jullie fascinatie met wormen. Na het wormenavontuur (worm-kebab) in Nottingham ben ik niet meer van het imago van wormen-wetenschapper afgekomen, maar gelukkig kwam het op het laatst toch goed in Osnabrück met de *Manduca sexta* ! Chris, heel veel succes met alles. Slumpie, sorry dat Koek je baan heeft ingepikt in NZ ! Wie weet, Niels, misschien moet je weer een huurwoning voor ons afbellen over 3 jaar ! Mike & Anne, dit keer doen we de grote oversteek zonder jullie ! Erik & Nomvuyo, we are sorry we cannot attend your wedding next year, I guess Erik has his revenge now for missing our wedding after his departure to South Africa...?! Have fun at your wedding ! Nomvuyo, I wish you the best of luck with your Biomedical Sciences studies in Leuven and hope you will become the scientist you want to be. Eveline & Flip, dat concert was grandioos, sorry voor de brakheid. Guido & Lenny, Mireille & Mark, geniet van de bank 'waar je zo lekker op kan hangen' ! Nathan, hopelijk laat je nu wel alles heel op 4 september !? En Jürgen, ik zal onze ellenlange gesprekken missen over ons werk. Maaike & Josh, hopelijk is Josh over 3 jaar geannexeerd, want het bewijs is geleverd van zijn integratie…hij was echt boos over het verlies van Nederland in de WK finale ! Ron & Bonnie, niet gaan trouwen als wij weg zijn ! Edwin & Pascalle, op naar het volgende olie-zuinige VW-busje ! Leden van het prille shopclubje (eigenlijk meer eet- en drink-clubje), dat al snel is uitge-

groeid tot een traditie, Anne, Charlene en Marita; het is jammer dat ik dit niet door kan zetten. Ik hoop dat er nog een plekje is voor mij over 3 jaar. Hugo & Marita, al die etentjes ! Oud & Nieuw in april…niets is ons te gek ! Heel erg bedankt voor de afleiding en Marita ook voor het rennen, het was gezellig ! Hopelijk gaan we niet teveel missen in drie jaar (gaan we even voor het gemak vanuit dat we weer terugkomen), maar we vinden het geweldig dat jullie langs willen komen ! Klazien, ik vind het geweldig dat we nog steeds contact hebben al is het sporadisch, het is nooit awkward ! Ik vind het jammer dat ik je nooit de kans heb gegeven om je Master-actie te kunnen goedmaken, maar daar vinden we nog wel wat op ! Heel veel plezier en geluk met Frank, Lieske en Henkie !

Paps & mams, jullie hebben niet alleen de afgelopen 4 jaar, maar mij mijn hele leven al gestimuleerd om door te zetten en verder te kijken dan mijn neus lang is. Ik bewonder de ongelooflijke energie waarmee jullie alles aanpakken (voornamelijk katten en verhuisdozen) om ons, de kinderen, zo goed mogelijk te helpen. Frits & Renée, de schoonouders, jullie hebben ons liefdevol opgenomen nadat we dakloos waren geworden na de verkoop van ons huisje in Utrecht. Ook jullie hebben ons op alle fronten kunnen en vooral willen helpen. Bedankt daarvoor ! Alex & Jennifer, er komt zoveel op jullie af nu...jullie laten er geen gras over groeien ! Heel veel plezier en we hopen er toch een beetje deel van kunnen uitmaken ook al zitten we best ver weg. Vicky-lee & Arne, heel veel geluk samen ! Ook wil ik twee kleine mannetjes bedanken, Jamie en Duncan, die altijd een lach op mijn gezicht brengen. Niet teveel groeien hè in die drie jaar ! Mario & Heleen, onze 'mobiel-verschaffende eenheid', bedankt voor het meedenken. En dan Koek niet te vergeten. Het is vrij stressvol om te promoveren en dan is het nog een graadje erger om de partner te zijn van iemand die aan het promoveren is (denk ik…). Soms waren de pieken en dalen extreem, maar je hebt mij altijd geholpen om alles flink te relativeren. We hebben wel een waardevolle les geleerd; als er maar iets dreigt goed te gaan, vieren die handel !

En dan nu…op naar het Nieuw-Zeelandse avontuur !

Curriculum vitae

Seléne van der Poel was born on 28 July 1981 in Gorinchem, The Netherlands. She graduated from grammar school (Utrechts Stedelijk Gymnasium in Utrecht, The Netherlands) in 1999. After a gap year she went on to study Chemistry at Utrecht University in September 2000. Her interest in biochemical research was ignited during an internship at the Bio-Organic Chemistry group supervised by prof. Dr. Hans Kamerling and Dr. Koen Halkes in 2003, for the Bachelor Chemical Sciences. In order to obtain the Master degree in Biomolecular Sciences, she researched the physiological function of the sphingomyelin synthases under supervision of M.Sc. Klazien Huitema in the group of Dr. Joost Holthuis at the Researchgroup Membrane Enzymology in 2004. For an external internship at the Molecular Toxicology Group, Nottingham University, she investigated the neurobiology of the model organism *Caenorhabditis elegans* with Dr. David Bell in Nottingham, England in 2005. Seléne graduated cum laude as Master of Biomolecular Sciences in September 2005 and immediately started her PhD on the role of glycosphingolipids in maintaining organelle pH with prof. Dr. Gerrit van Meer and Dr. Hein Sprong at the Researchgroup Membrane Enzymology at Utrecht University. During her PhD she conducted research into the reconstitution of the proton pump V-ATPase isolated from *Manduca sexta* at the Animal Physiology group, University of Osnabrück, Germany, in collaboration with prof. Dr. Helmut Wieczorek en Dr. Markus Huss.